British Geological Survey
NATURAL ENVIRONMENT RESEARCH COUNCIL

Preliminary assessment of the environmental baseline in the Fylde, Lancashire

Groundwater Programme

Open Report OR/18/020

BRITISH GEOLOGICAL SURVEY

GROUNDWATER PROGRAMME

OPEN REPORT OR/18/020

Preliminary assessment of the environmental baseline in the Fylde, Lancashire

R.S. Ward (1), G. Allen (2), B.J. Baptie (1), L. Bateson (1), R A Bell (1), A.S. Butcher (1), Z. Daraktchieva (3), R. Dunmore (4), R.E. Fisher (5), A. Horleston (6), C.H. Howarth (3), D.G. Jones (1), C.J. Jordan (1), M. Kendall (6), A. Lewis (4), D. Lowry (5), C.A. Miller (3), C.J. Milne (1), A. Novellino (1), J. Pitt (2), R.M. Purvis (4), P.L. Smedley (1) and J. M. Wasikiewicz (3)

(1): British Geological Survey
(2): University of Manchester
(3): Public Health England
(4): University of York (National Centres for Atmospheric Science)
(5): Royal Holloway University of London
(6): University of Bristol

Keywords

baseline, groundwater, atmospheric composition, ground motion, seismicity, water quality, shale gas, hydraulic fracturing, soil gas, radon.

Bibliographical reference

WARD, R.S. ET AL. 2018. Preliminary assessment of the environmental baseline in the Fylde, Lancashire. *British Geological Survey Open Report*, OR/18/020. 104 pp.

Keyworth, Nottingham British Geological Survey 2018

BRITISH GEOLOGICAL SURVEY

The full range of our publications is available from BGS shops at Nottingham, Edinburgh, London and Cardiff (Welsh publications only) see contact details below or shop online at www.geologyshop.com

The London Information Office also maintains a reference collection of BGS publications, including maps, for consultation.

We publish an annual catalogue of our maps and other publications; this catalogue is available online or from any of the BGS shops.

The British Geological Survey carries out the geological survey of Great Britain and Northern Ireland (the latter as an agency service for the government of Northern Ireland), and of the surrounding continental shelf, as well as basic research projects. It also undertakes programmes of technical aid in geology in developing countries.

The British Geological Survey is a component body of the Natural Environment Research Council.

British Geological Survey offices

BGS Central Enquiries Desk

Tel 0115 936 3143 Fax 0115 936 3276
email enquiries@bgs.ac.uk

Environmental Science Centre, Keyworth, Nottingham NG12 5GG

Tel 0115 936 3241 Fax 0115 936 3488
email sales@bgs.ac.uk

The Lyell Centre, Research Avenue South, Edinburgh EH14 4AP

Tel 0131 667 1000 Fax 0131 668 2683
email scotsales@bgs.ac.uk

Natural History Museum, Cromwell Road, London SW7 5BD

Tel 020 7589 4090 Fax 020 7584 8270
Tel 020 7942 5344/45 email bgslondon@bgs.ac.uk

Cardiff University, Main Building, Park Place, Cardiff CF10 3AT

Tel 029 2167 4280 Fax 029 2052 1963

Maclean Building, Crowmarsh Gifford, Wallingford OX10 8BB

Tel 01491 838800 Fax 01491 692345

Geological Survey of Northern Ireland, Department of Enterprise, Trade & Investment, Dundonald House, Upper Newtownards Road, Ballymiscaw, Belfast, BT4 3SB

Tel 028 9038 8462 Fax 028 9038 8461
www.bgs.ac.uk/gsni/

Parent Body

Natural Environment Research Council, Polaris House, North Star Avenue, Swindon SN2 1EU

Tel 01793 411500 Fax 01793 411501
www.nerc.ac.uk

Website www.bgs.ac.uk
Shop online at www.geologyshop.com

Foreword

This report presents the collated preliminary results from the British Geological Survey (BGS) led project *Science-based environmental baseline monitoring associated with shale gas development in the Fylde, Lancashire.* The project has been funded by a combination of BGS National Capability funding, in-kind contributions from project partners and a grant awarded by the Department of Business Energy and Investment Strategy (BEIS). It complements an on-going project, in which similar activities are being carried out, in the Vale of Pickering, North Yorkshire. Further information on the projects can be found on the BGS website: www.bgs.ac.uk.

The project has initiated a wide-ranging environmental baseline monitoring programme that includes water quality (groundwater and surface water), seismicity, ground motion, atmospheric composition (greenhouse gases and air quality), soil gas and radon in air (indoors and outdoors). The motivation behind the project(s) was to establish independent monitoring in the area around the proposed shale gas hydraulic fracturing sites in the Fylde, Lancashire (Cuadrilla Resources Ltd) before any shale gas operations take place.

As part of the project, instrumentation has been deployed to measure, in real-time or near real-time, a range of environmental variables (water quality, seismicity, atmospheric composition). These data are being displayed on the project's web site (www.bgs.ac.uk/lancashire). Additional survey, sampling and monitoring has also been carried out through a co-ordinated programme of fieldwork and laboratory analysis, which has included installation of new monitoring infrastructure, to allow compilation of one of the most comprehensive environmental datasets in the UK.

The monitoring programme is continuing. However, there are already some very important findings emerging from the limited datasets which should be taken into account when developing future monitoring strategy, policy and regulation. The information is not only relevant to Lancashire but will be applicable more widely in the UK and internationally. Although shale gas operations in other parts of the world are well-established, there is a paucity of good baseline data and effective guidance on monitoring. The project will also allow the experience gained, and the scientifically-robust findings to be used, to develop and establish effective environmental monitoring strategies for shale gas and similar industrial activities.

Acknowledgements

A large number of individuals in BGS and the partner organisations have contributed to the project. This assistance has been received at all stages of the study. In addition to the collection of data, many individuals have freely given their advice, and provided the local knowledge so important to the ongoing programme of work. Of the many individuals who have contributed to the project we would particularly like to thank the following: Andy Newell, Kay Green, Tom Barlow, Andy Marriott, Elliott Hamilton, Charles Gowing, Jenny Bearcock, Mike Bowes, Sean Burke, Sarah Collins, Leanne Hughes, Ian Mounteney, Dan Parkes, Johanna Scheidegger, Barry Townsend and Debbie White.

Contents

FIGURES

TABLES

1 Introduction

This report presents the initial results of the environmental baseline monitoring in the Fylde, Lancashire, carried out by the British Geological Survey (BGS) and its partners. The objective of this monitoring is to acquire a comprehensive set of data in order to establish baseline environmental conditions ahead of Cuadrilla's proposed shale-gas exploration activities in the area. Cuadrilla submitted two applications to explore for shale gas in 2014, one at Preston New Road (PNR) and one at Roseacre Wood (Figure 1). In 2016 and following an appeal and public enquiry, the Cuadrilla application for the PNR site was approved by Secretary of State for the Department for Communities and Local Government. A decision on the appeal in respect of the Roseacre Wood site was delayed pending a reopening of the public enquiry in order to examine outstanding questions over highways management.

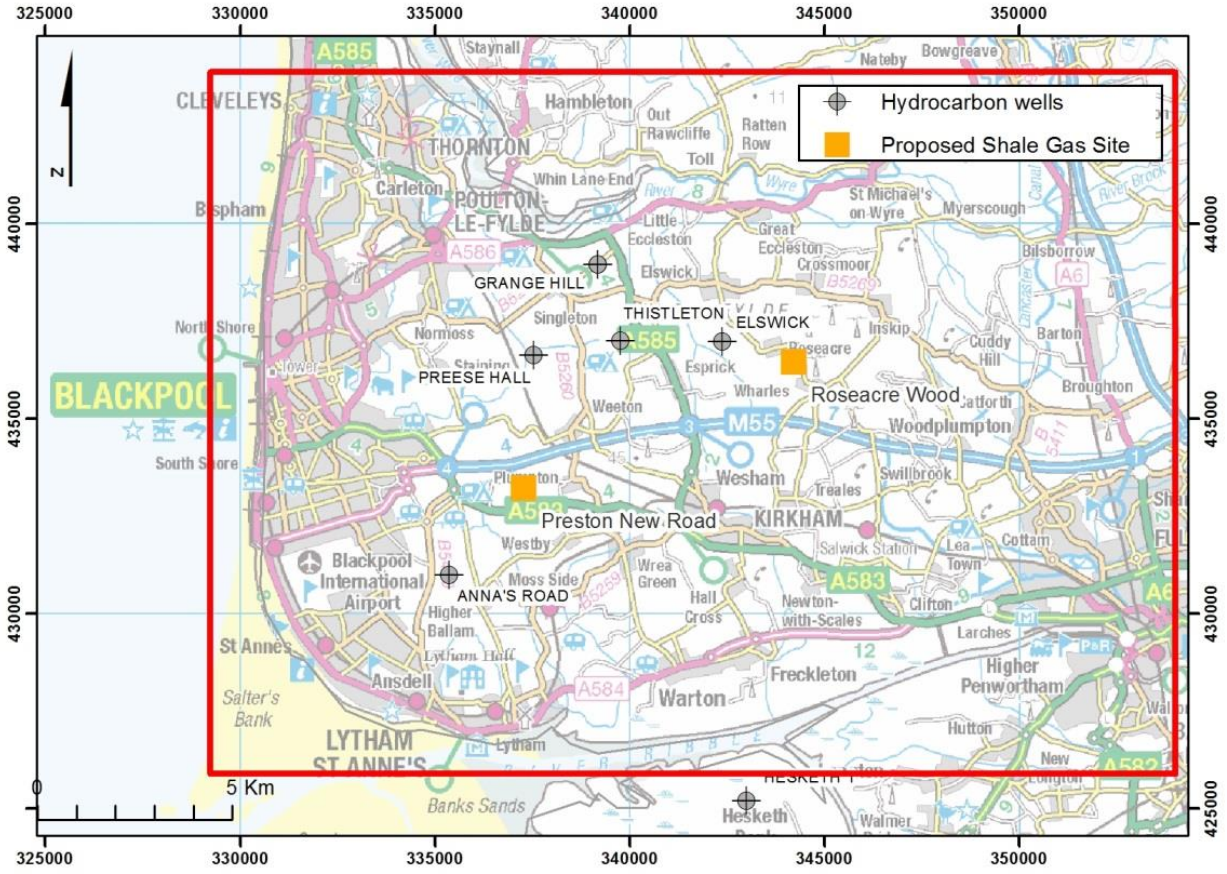

Figure 1. Location of the Fylde, Cuadrilla sites subject to planning permission and hydrocarbon wells. © Crown Copyright and/or database right 2018. Licence number 100021290 EUL

Public concerns over shale-gas exploration and development have included the potential pollution of surface waters and groundwater (drinking water), triggering of earthquakes and impacts on air quality (health related and greenhouse gases). Concerns particularly relate to hydraulic fracturing ('fracking') activities but risks are associated with other stages of the shale gas operation throughout its lifetime. Environmental safeguards need to be in place to ensure the risks are minimised and environmental monitoring throughout the life cycle of the operation provides assurance of those safeguards.

Although a number of studies in countries where shale gas is a developed industry have inferred a link between groundwater quality, seismicity, health impacts and hydrocarbon extraction (Jackson et al., 2013; Llewellyn et al., 2015; Osborn et al., 2011), establishing a causal

relationship is difficult without evidence of the pre-development baseline conditions. This can provide a more robust basis for establishing whether any environmental change(s) or events are related to the shale gas exploration and development.

This report outlines the preliminary results of investigations carried out so far to establish the pre-development environmental baseline in the Fylde and covers key diagnostic analyses for water, air, seismicity, ground motion, soil gas and radon.

It is important to note that the baseline assessed here relates to the conditions pertaining currently under pre-development (pre-fracking) environmental conditions and does not imply a pre-modern 'pristine' condition. The baseline conditions are therefore subject to inputs such as contamination from pre-existing agricultural, domestic and industrial sources.

The Operator (Cuadrilla) has a requirement to monitor as part of its environmental permit conditions. BGS's monitoring activities have been additional to and independent of this monitoring.

2 Study area

2.1 GEOGRAPHY

The Fylde is a flat, low lying area, forming part of the West Lancashire Plain. It is dominated by the urban centres of Lytham St Annes and Blackpool, but surrounded by agricultural land, both pasture and arable (Figure 2). The topography is mostly flat, ranging from 0–47 mOD, with the Kirkham Moraine forming a subtle topographic high towards the east (Cripps et al., 2017). Two major rivers bound the Fylde: the River Wyre to the north and the River Ribble to the south. Another slight topographic high separates the valleys occupied by these two rivers (Newell et al., 2016). In the area close to PNR, surface drainage comprises mostly small ditches, often with very low flows in the summer months. Marton Mere is the only glacial lake in the area, thought to occupy a kettle hole, and is designated as an SSSI. Across the Fylde are multiple flooded brick pits; small hollows or depressions where clay has previously been extracted and have now formed ponds. These legacy man-made features are now of ecological importance.

The area has a previous history of hydrocarbon exploration/development and five hydrocarbon wells have been drilled previously across the Fylde (Figure 1). One (Elswick) is classed as a production well, while three are fully abandoned (Preese Hall, Thistleton and Anna's Road) and plans are in place for abandonment of the fourth (Grange Hill).

Figure 2. Topography of the Fylde and clay hollows found commonly in the area

2.2 REGIONAL GEOLOGY

Background information on the Quaternary and bedrock geology of the Fylde is given by Cripps et al. (2017) and Newell et al.(2016), but a brief overview is provided here.

2.2.1 Quaternary geology

The Fylde is dominated by Quaternary-age glacigenic deposits (Figure 3), comprising mostly till (clay-rich), glaciofluvial deposits (sand and gravel) and some glaciolacustrine deposits (clays and silts). These tills, sands and gravels are of variable thickness and lateral extent due to the varying character of depositional environments and physical processes (Cripps et al., 2017). The most widespread unit at the surface is till, with the associated glaciofluvial deposits forming linear outcrops. In general, the sequence broadly comprises a basal till overlain by glaciofluvial sand and gravel, which is in turn overlain by an upper till. There are major local variations to this succession and the units are both laterally and vertically variable, making interpolation of units very difficult.

Holocene deposits occur around Blackpool and in both the River Wyre and River Ribble estuaries. These consist mostly of clays, silts and sands of alluvium and tidal-flat origin. A large area of wind-blown cover sand is present around Blackpool and Lytham St Annes. Areas of peat are also present: at surface occupying a roughly north-south channel east of Blackpool, with some sub-surface layers (2–3 m thick) around Lytham St Annes and Blackpool.

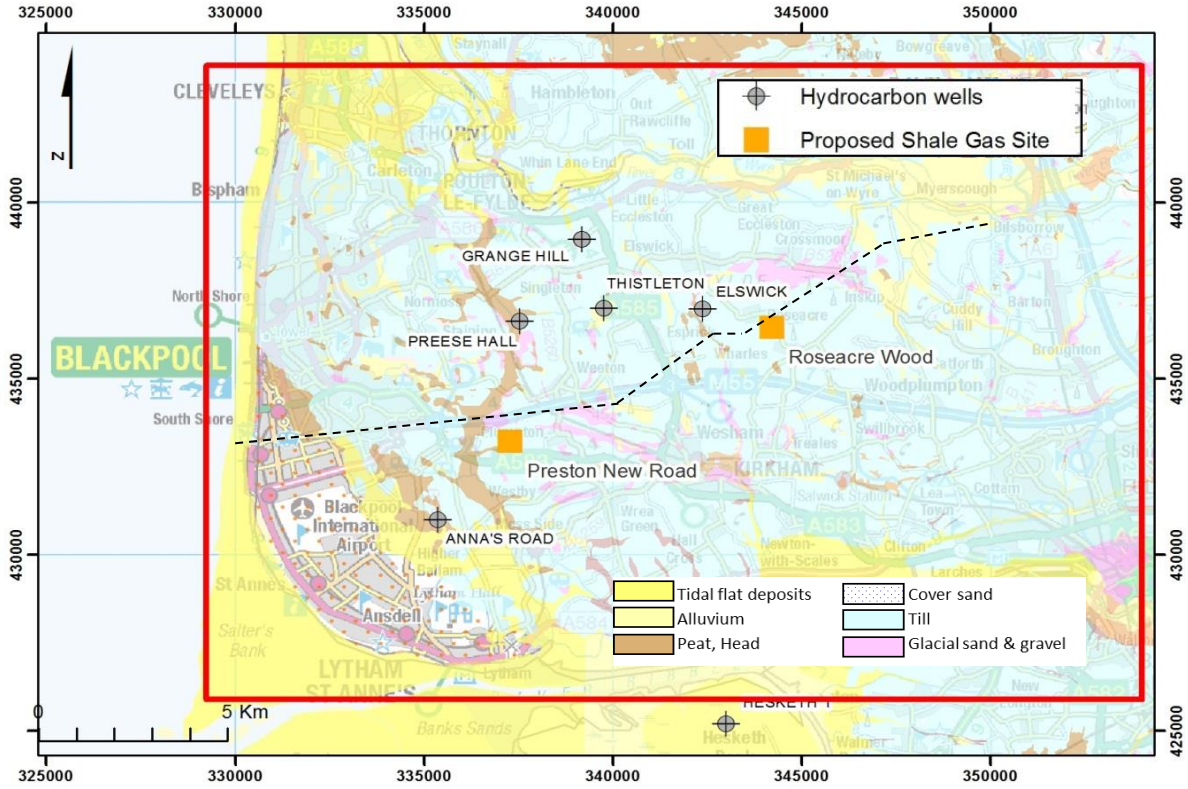

Figure 3. Regional Quaternary geology of the Fylde. Dashed line refers to cross section in Figure 4. © Crown Copyright and/or database right 2018. Licence number 100021290 EUL

Figure 4. Quaternary geology cross section (from Cripps et al., 2017)

Borehole records show that the thickness of the Quaternary deposits is variable, between 1–86 m, and the sediments thin to the east of the area where the rockhead is closer to surface. The Kirkham Moraine is present between the two Cuadrilla sites. The glaciofluvial deposits are the main aquifer unit in these Quaternary deposits and have also been known as the 'Middle Sands' (Worthington, 1972) and defined by the Environment Agency for the purposes of the Water Framework Directive (WFD) as the 'West Lancashire Quaternary Sand and Gravel Aquifers'.

Close to PNR, borehole records report a confining upper boulder clay ca. 10 m thick, comprising alternating sand/gravel and clay layers (forming a shallow aquifer) and then ca. 15 m of glacial sands and gravels, forming the main Quaternary aquifer. At Roseacre Wood, the lower boulder clay unit is missing. Instead, ca. 15 m of glaciofluvial deposits sit directly on the Mercia Mudstone Group (MMG), and are overlain by an upper unit of boulder clay.

2.2.2 Bedrock geology

In the Fylde, the Quaternary deposits overlie a thick (up to ca. 350 m) sequence of Triassic MMG deposits, the latter dominated by mudstone with thin layers of halite and sandstone (Aitkenhead et al., 1992; Wilson and Evans, 1990). These are thickest within the deep graben structure of the Kirkham Basin (Figure 5). The SW–NE-trending Woodsfold Fault is a normal fault with downthrow to the west. To the west of the fault, BGS geological mapping indicates that MMG occurs everywhere at rockhead, although modelling undertaken for this study (see below) suggests that MMG thins or is absent in a section to the north of the Thistleton 1 borehole (Figure 6) (Newell et al., 2016). Below the MMG, the Permo-Triassic Sherwood Sandstone Group (SSG) reaches a thickness of some 750 m.

The Woodsfold Fault forms the eastern margin of the West Lancashire Basin. To the east of the fault, the MMG is missing and the SSG forms the top of the bedrock, underlying Quaternary deposits directly.

The SSG rests on Carboniferous strata, the eroded top of which define the Variscan unconformity. The top of the Carboniferous has considerable relief created by differential movement of fault-bounded blocks. The Kirkham Basin is bounded to the west by a faulted structural high (including the Elswick Dome), where the deep hydrocarbon exploration boreholes Elswick 1 and Thistleton 1 were drilled (Figure 6). Westwards from this high, the top Carboniferous surface dips toward the west under Blackpool and toward the Formby Point Fault which forms the boundary of the East Irish Sea Basin (Newell et al., 2016).

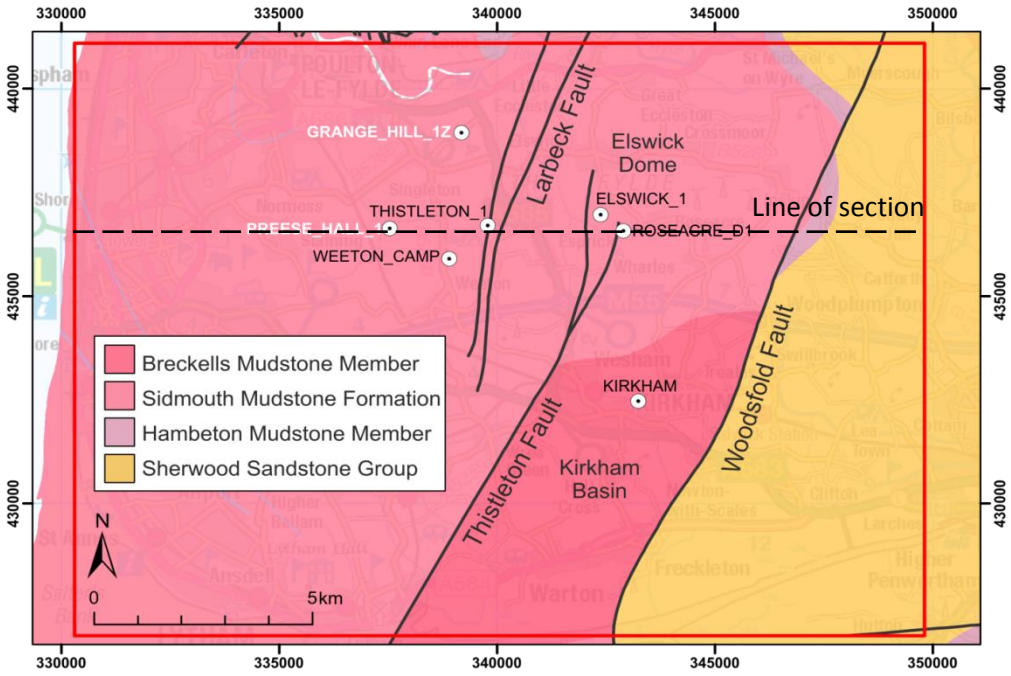

Figure 5. Bedrock geology of the Fylde. © Crown Copyright and/or database right 2018. Licence number 100021290 EUL

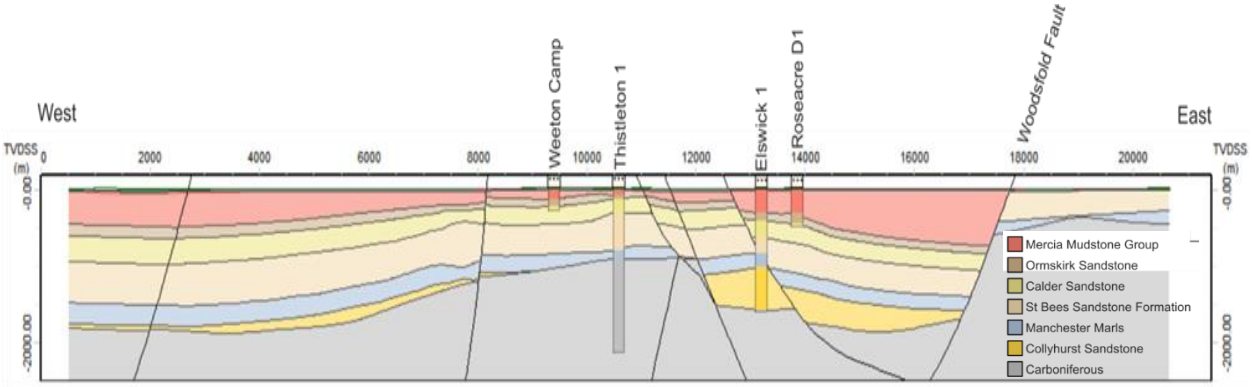

Figure 6. E–W geological cross section across the Fylde

2.3 REGIONAL HYDROGEOLOGY

2.3.1 Quaternary deposits

The glacial sands and gravels are the main aquifer in the Fylde, although they do not form one laterally continuous aquifer unit. In general, the sand and gravel units occur as discontinuous lenses interbedded with clays, and are confined by the upper boulder clay. In areas such as PNR, shallower lenses of sand may be water-bearing, but are separated from the main glaciofluvial ('Middle Sands') aquifer by thin clay layers. The variability in the thickness (or presence) of the upper boulder clay will affect the degree of confinement and hence the hydrogeological conditions within the shallow aquifer.

Historically, few investigations have been undertaken on the Quaternary aquifer in this area. The deposit is mostly defined as a Secondary (undifferentiated) Aquifer by the Environment Agency (Figure 7). Where peat or tidal-flat deposits are present, the shallow sediments are defined as Unproductive and the alluvium, blown sands and glacial sands/gravels are classed as Secondary A. These glaciofluvial deposits are used locally by small businesses, farms and golf courses but problems with water quality (mostly iron) and groundwater yields are not uncommon.

Groundwater levels are generally shallow (1–2 m below ground surface) and are artesian in parts, especially in topographic lows located near to surface drainage.

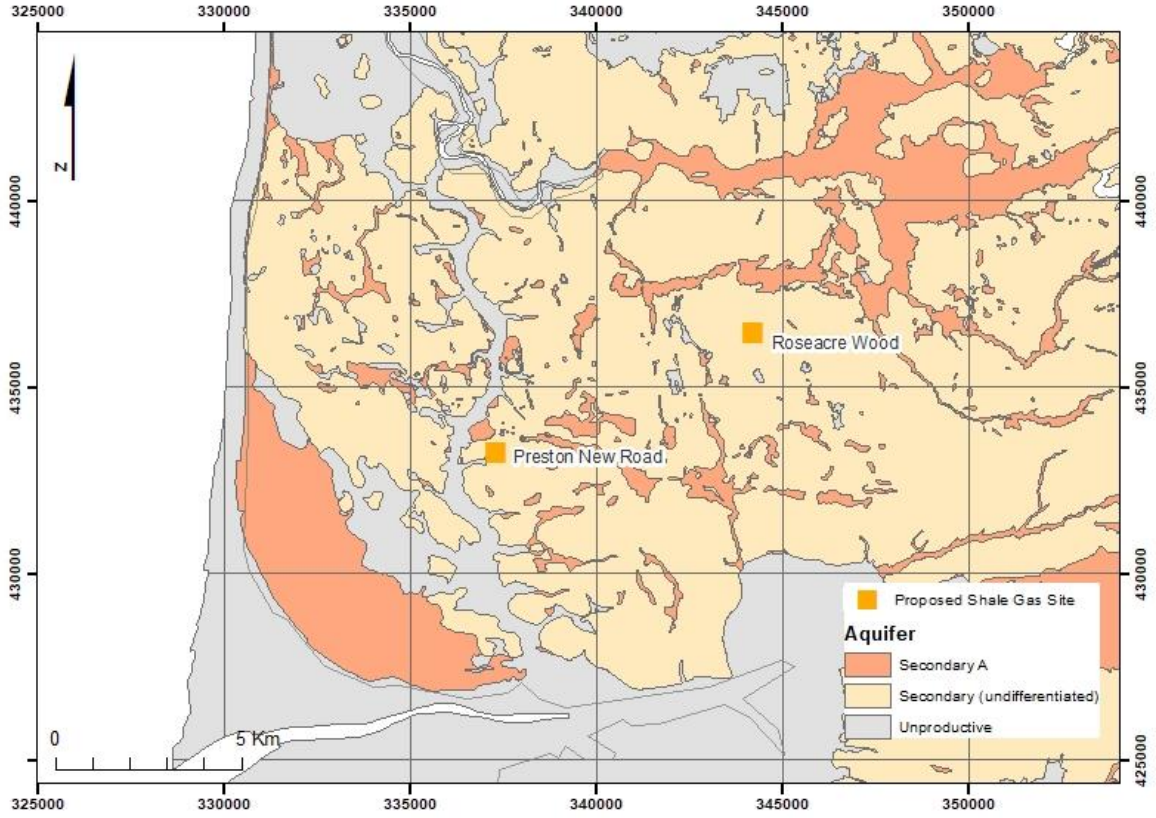

Figure 7. Environment Agency designation of the Quaternary aquifer across the Fylde, showing locations of the proposed shale-gas sites. Geological information, BGS © NERC

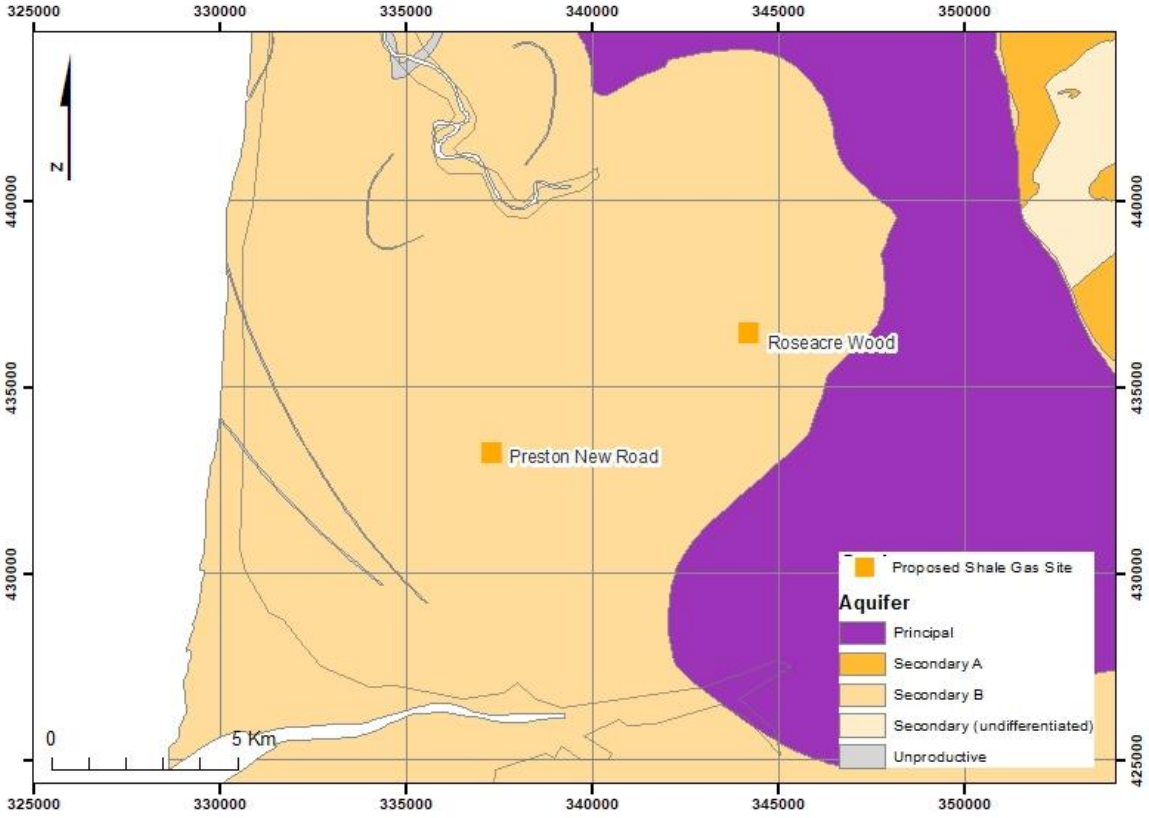

Figure 8. Environment Agency designation of the bedrock aquifer across the Fylde, showing locations of the proposed shale-gas sites. Geological information, BGS © NERC

2.3.2 Sherwood Sandstone Group

In the area of the Fylde peninsula (west of the Woodsfold Fault), the top of the Sherwood Sandstone Group occurs at some 370 m depth below surface. This is at too great a depth to be of practical use for water supply. To the east of the Woodsfold Fault, as the SSG is at rockhead (shallow), it is classed by the Environment Agency as a Principal Aquifer (Figure 8) and is used for public water supply.

To the east of the Woodsfold Fault, Quaternary deposits cover the SSG, the boulder clay again acting as a confining layer. In areas where the Quaternary deposits comprise sand and gravel, these are in hydraulic continuity with the SSG.

Recharge to the SSG primarily occurs through the Quaternary deposits (Sage and Lloyd, 1978) but also from permeable sandstone and limestone layers in the Carboniferous sequence (Bowland Fells), across the Bilsborrow Fault (Figure 9). Investigations to remap the Fylde SSG aquifer by the Environment Agency in the 1990s identified that the regional groundwater flow direction is from east to west, following the line of topography (Seymour et al., 2006). Main groundwater discharge points are thought to be the River Ribble to the south and River Wyre in the north. However, this is complicated by the occurrence of marl bands within the SSG and N–S faulting, especially near Preston, which can isolate parts of the sandstone and cause local anisotropy. The SSG in this area has a lower porosity and hydraulic conductivity compared to equivalent units in the Midlands as the sandstones of the Fylde tend to be more consolidated and cemented (Seymour et al., 2006).

As part of their groundwater models, the Environment Agency have historically taken the Woodsfold Fault as a regional barrier to groundwater flow, based on the conclusion that there is no juxtaposition along the fault of the deep and shallow SSG aquifer. The contact with the shallow SSG along the fault line is taken to be the MMG (Figure 9). Investigations by Sage and Lloyd (1978) identified that groundwater from the SSG to the east of the Woodsfold Fault discharged through the Quaternary deposits.

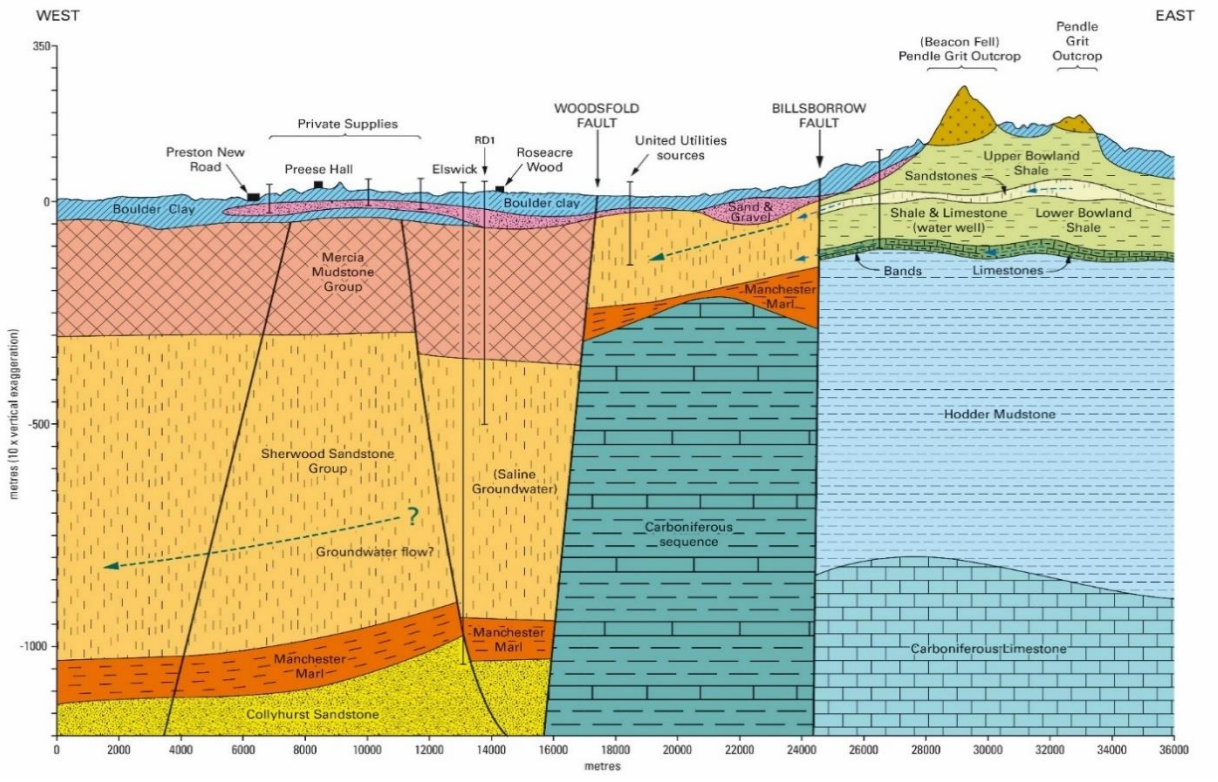

Figure 9. Hydrogeological conceptual model of groundwater in an E–W section across the Fylde, Lancashire.

3 Water monitoring

3.1 WATER MONITORING NETWORK

A monitoring network of groundwater and surface water sites has been established across the Fylde, including areas proximal to PNR and Roseacre Wood, in order to evaluate baseline water quality and allow for evaluating any future changes in conditions should shale-gas operations take place. The constructed hydrogeological model (Figure 9) was used to inform the selection of sites suitable for monitoring and further investigation. Sites for surface water and groundwater monitoring were chosen within approximately 10 km of the proposed shale-gas exploration sites, with effective barriers imposed by the Rivers Wyre and Ribble and the Fylde west coast. An inventory of groundwater sites was collated from information in available well databases augmented by field visits. Groundwater sources are mainly boreholes owned by local small businesses and households, although some public water supplies exist in the area of interest. First-order stream sites were sought for surface-water monitoring to limit the size of the influencing catchment area.

A shortlist of suitable sites was drawn up on the combined basis of site access, source condition (status and representativeness) and site safety. Investigations established that availability of suitable groundwater sites was limited in the area of interest and so all groundwater sites deemed to be suitable, accessible and representative for sampling have been included in the resulting water monitoring network. The established monitoring network comprises 19 groundwater sources and 11 surface waters, the latter all streams (Figure 10 and Table 1). Groundwater sources include 9 sites from the Superficial (Quaternary) aquifer and 10 sites from the Sherwood Sandstone to the east of the Woodsfold Fault. All groundwater sites in the initial water monitoring network are owned by third parties.

3.2 BGS BOREHOLES

As the water monitoring network relied on pre-existing groundwater sources which were in some cases not located ideally, a decision was made to purpose-drill a number of water boreholes closer to the proposed Cuadrilla sites for the purposes of detailed investigation and monitoring, with a view to final reinstatement for private water supply pending further investigations. These were located within ca. 1 km of the PNR or Roseacre Wood proposed sites (Figure 10 and Table 1). Shallow boreholes completed within the Quaternary (Superficial) aquifer were installed in pairs, one ‘deep’ and one ‘shallow’ (though all <50 m below ground level. Completions were according to site conditions, favouring screens within sandy horizons to provide best-available groundwater yields.

A single borehole was also completed within the Sherwood Sandstone at 500 m depth, at some 2 km distance west of the Roseacre Wood site. This borehole was cased off from surface to 350 m depth with an open-hole section, wholly within the Sherwood Sandstone, thereafter.

Table 1. Water monitoring sites and purpose

Site Number	Site Type	Monitoring Type
Site 1–24	Groundwater	Initial network
Site 25–35	Surface water	Initial network
Site 36–48	Groundwater	BGS borehole
Site 49–53	Groundwater	Cuadrilla borehole

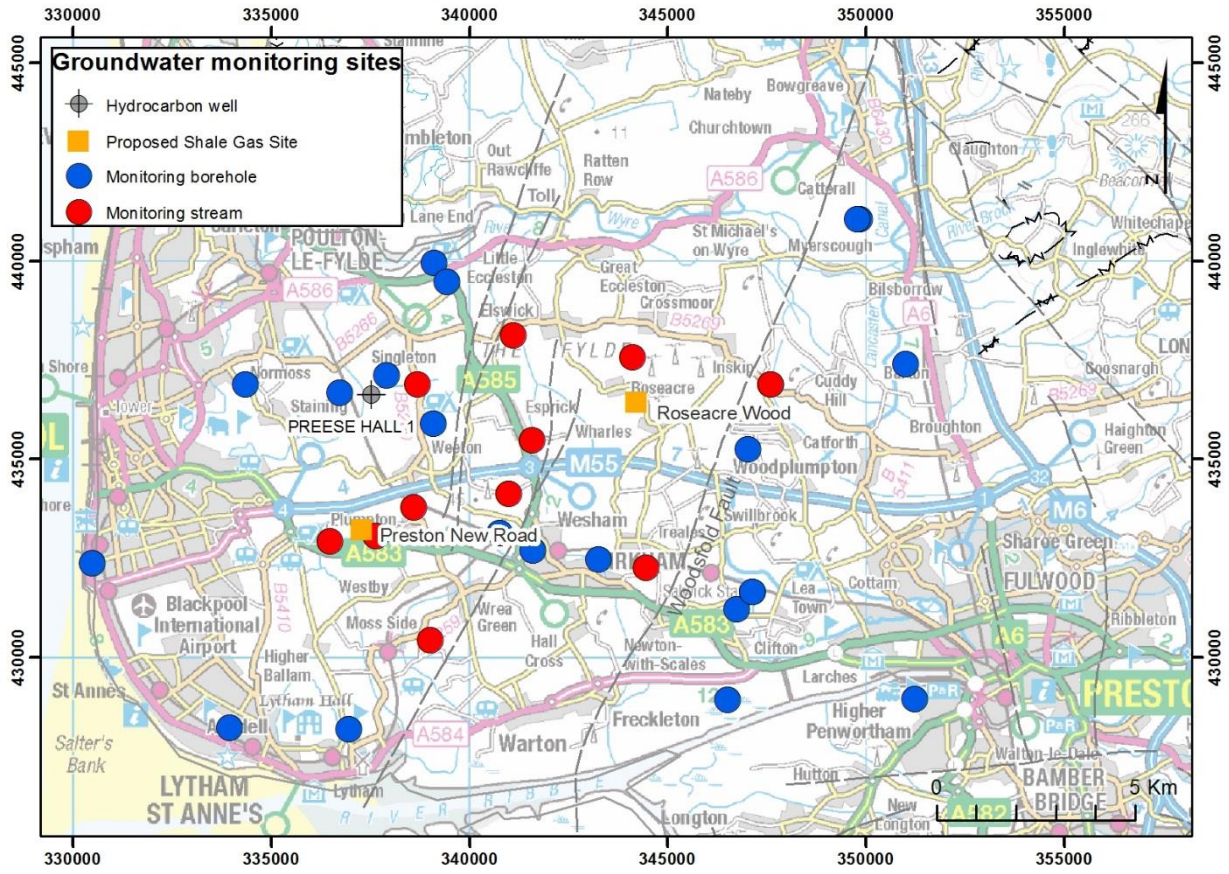

Figure 10. Location of groundwater and stream sites in the water monitoring network. © Crown Copyright and/or database right 2018. Licence number 100021290 EUL

3.3 SAMPLING AND ANALYSIS

Sampling of groundwater and surface water in the monitoring network began in February 2015. Sites have been sampled quarterly in accordance with BS ISO 5667-11 (2009). Groundwater sources were purged before sampling and where possible, flow cells were set up inline to monitor redox characteristics. These, along with pH, temperature and specific electrical conductance (SEC), were monitored until stable readings were obtained, at which point, total alkalinity was determined onsite by titration and samples were collected for subsequent laboratory analysis. Samples for analysis of major cations, anions and trace metals were filtered (0.22 µm) and collected in factory-new LDPE bottles, pre-rinsed with filtered sample. Aliquots for determination of major-cation and trace-metal concentrations were acidified (1% v/v) with pure HNO_3 (and subsequently in the laboratory with 0.5% v/v pure HCl). Samples for determination of non-purgeable organic carbon (NPOC) were filtered (0.45 µm) using Ag-impregnated filters and collected in acid-washed glass bottles. Samples for dissolved gases were collected inline at pump pressure in steel bombs. Samples were also collected periodically for organic compounds (total petroleum hydrocarbons, TPH; polycyclic aromatic hydrocarbons, PAH; volatile (and semi-volatile) organic compounds, VOC/SVOC).

Major cations and trace elements were analysed by ICP-MS and anions by ion chromatography. The analysing laboratory holds ISO 17025:2005 certification for analysis of environmental materials (including water) using these methods. The laboratory operates an AQC regime including use of International Standard Reference Materials and operates an Aquacheck proficiency testing scheme.

Samples for TPH were solvent-extracted and analysed using a modified USEPA 8015B method. Solvent-extractable petroleum hydrocarbons with carbon banding in the range C8-C40 were determined by GC-FID. Gasoline Range Organics (GRO) in the carbon chain range of C4-12

were determined by headspace GC-FID. Samples for SVOC were solvent-extracted and analysed using a modified USEPA 8270 method, by GC-MS. The testing laboratory holds ISO 17025 certification for TPH CWG and SVOC in surface water. VOC determinations were by direct aqueous injection using purge-and-trap GC-MS and PAH determination by solvent extraction, GC-MS. The testing laboratory for VOC, PAH determinations holds ISO 17025:2005 certification for these methods in water.

In addition, a non-accredited (semi-quantitative) analysis of water samples by target-based screening has also been determined using GC-MS and LC-MS.

3.3.1 Real-time monitoring

Real-time monitoring for a restricted number of water-quality parameters has been carried out within six of the shallow BGS boreholes located around the PNR and Roseacre Wood sites. Monitoring includes water temperature, water level, pH and electrical conductivity. These are monitored hourly to obtain high-resolution data for characterisation of the groundwater baseline conditions and to act as early-warning indicators of any future environmental change. Data are telemetered to BGS and displayed on the BGS website (www.bgs/ac/uk/lancashire).

3.4 WATER QUALITY RESULTS

3.4.1 Superficial aquifer

Water-quality data for groundwater from the Quaternary (Superficial) aquifer indicate an overwhelmingly anoxic condition (lacking dissolved oxygen), with pH values near neutral. Dominant ions are Ca, Na and HCO_3, though SO_4 concentrations are relatively high in some samples (Figure 11). Most have low conductivity although some groundwater samples have values more than 1000 µS/cm (Figure 11).

As a result of the anoxic condition of the groundwater, concentrations of nitrate (NO_3) are low and concentrations of dissolved iron (Fe) and manganese (Mn) are high (Figure 12). Concentrations of arsenic (As) and ammonium (NH_4) are relatively high in some. Methane (CH_4) is also often detected, though rarely at high concentrations. The site in the Superficial aquifer with the highest observed concentrations of CH_4 (of the order of 3 mg/L) has a depleted $\delta^{13}C_{CH4}$ isotopic signature (-73.1 ‰ VPDB) consistent with a biogenic methane origin, possibly linked to degradation of peat within the superficial deposits present at the site.

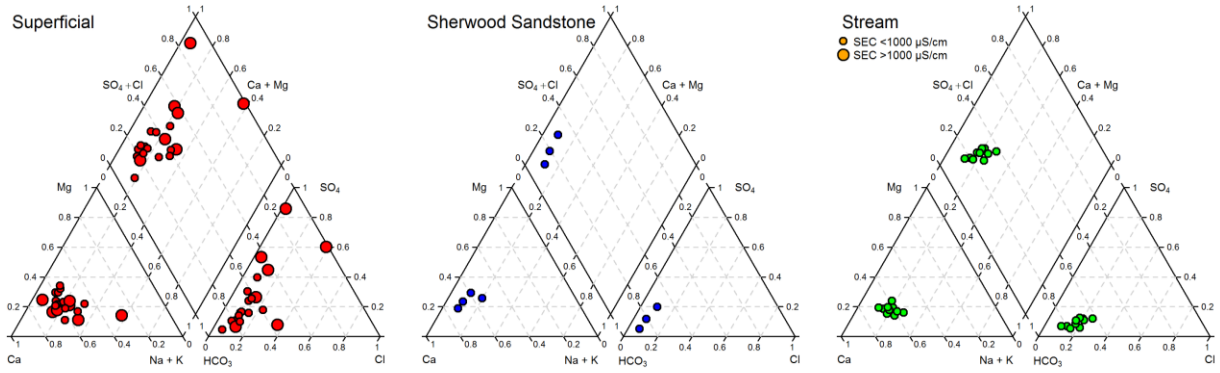

Figure 11. Piper diagrams showing the major-ion chemistry of groundwater (Superficial and Sherwood Sandstone aquifers) and stream water samples from the monitoring network (sampling February 2016). Symbol sizes are distinguished by electrical conductivity (SEC)

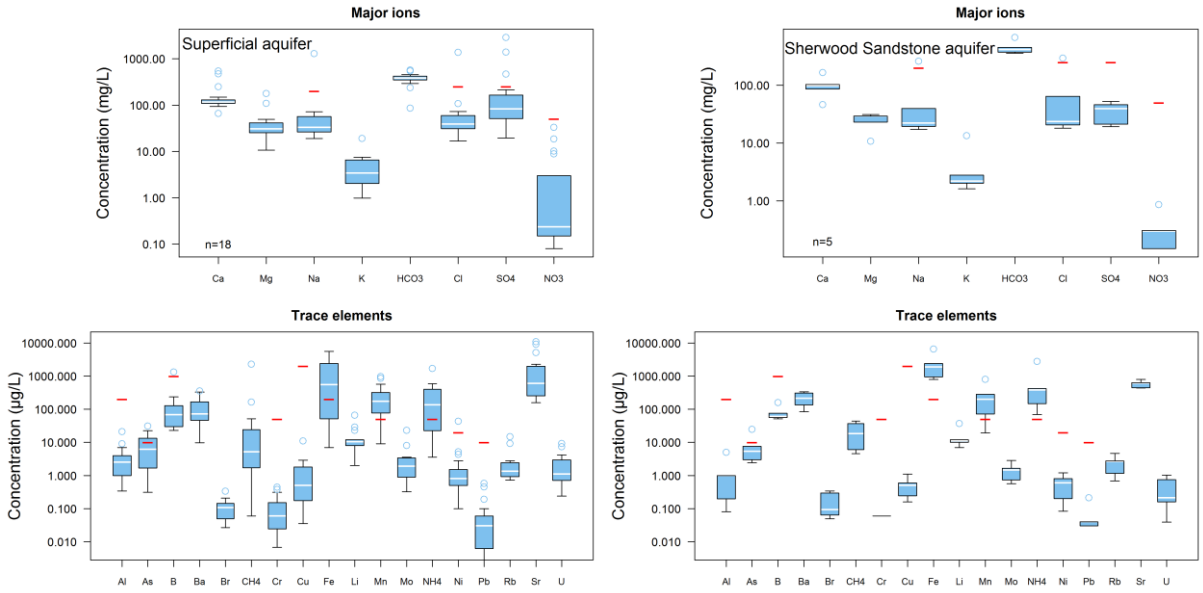

Figure 12. Box plots showing summary chemical data for groundwater samples collected from the Superficial (left) and Sherwood Sandstone (right) aquifers. Red lines indicate European drinking-water limits for relevant analytes.

Monitoring of groundwater in the Superficial aquifer (Figure 13) has shown that the chemical characteristics have been broadly consistent over time, although variations are greater at some sites (e.g. Site 3) than others. Monitoring at Site 4 ceased in Summer 2016 due to the installation of water-treatment equipment at the site, negating access to raw groundwater for sampling.

Monitoring of groundwater from the BGS boreholes in the Superficial aquifer (Figure 14) shows a greater heterogeneity of water types. Two sites show relatively high concentrations of Ca and SO_4 (greater than 500 mg/L and 1500 g/L respectively); one of these shows high concentrations of Na and Cl (ca. 1400 mg/L) relative to samples from the other BGS sites. Variability is likely due to spatial variability in mineral-dissolution and ion-exchange reactions.

Spatial variation in dissolved methane concentration in the Superficial groundwater is sporadic (Figure 15). One of the samples with the highest observed concentration occurs in the south-western part of the Fylde. This roughly coincides with occurrences of peat deposits in the shallow Quaternary sediments (Figure 3). One of the Cuadrilla boreholes on the PNR well pad also has groundwater with comparatively high CH_4 concentrations.

Activities of dissolved radon gas are low in the groundwaters, typically <10 Bq/L (Figure 16). This is consistent with clay-dominated superficial deposits in the UK, and with the Public Health England/BGS map of radon potential in the Fylde: http://www.ukradon.org/information/ukmaps.

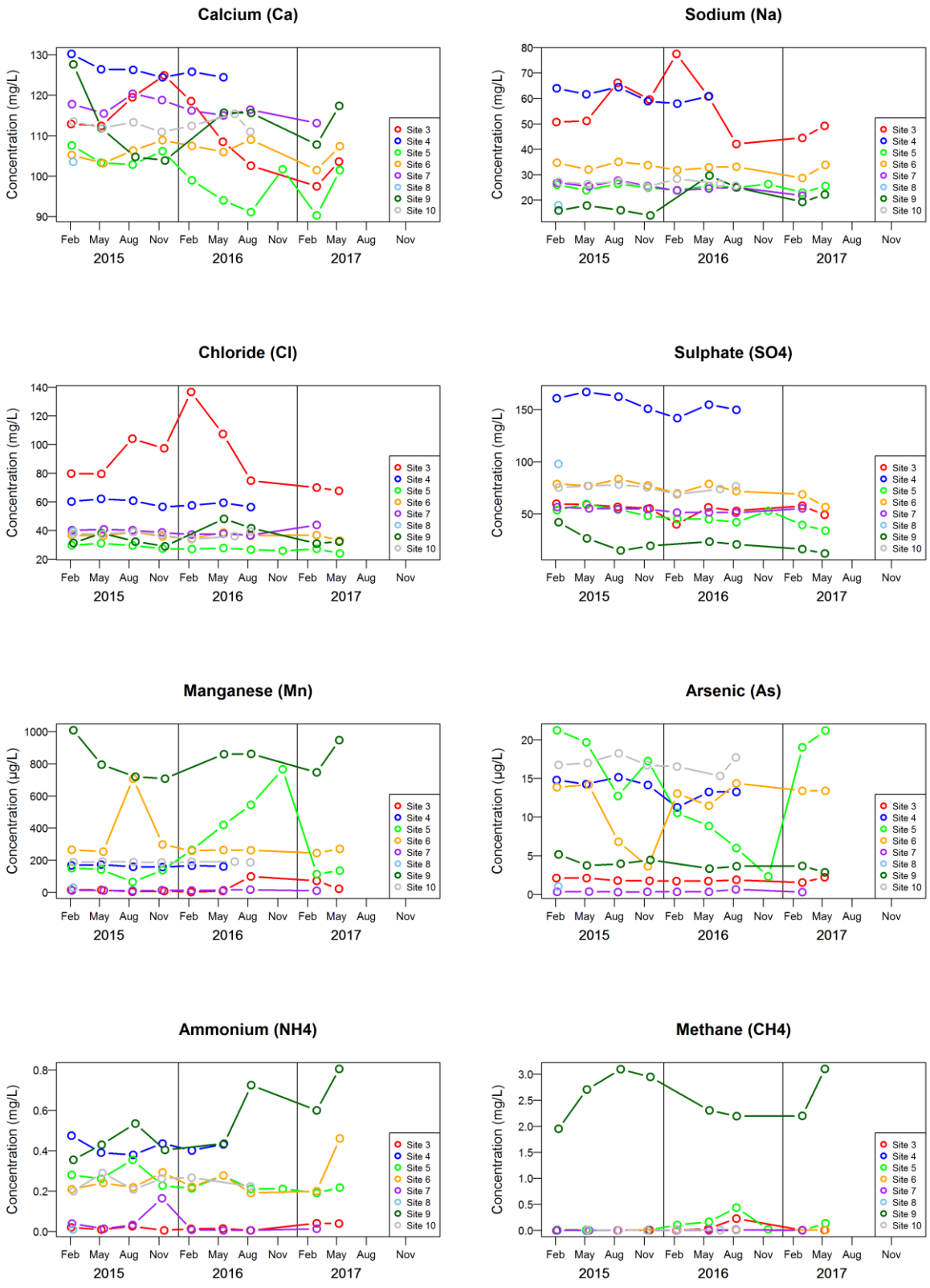

Figure 13. Temporal variation in concentrations of selected solutes from groundwater in the Superficial aquifer.

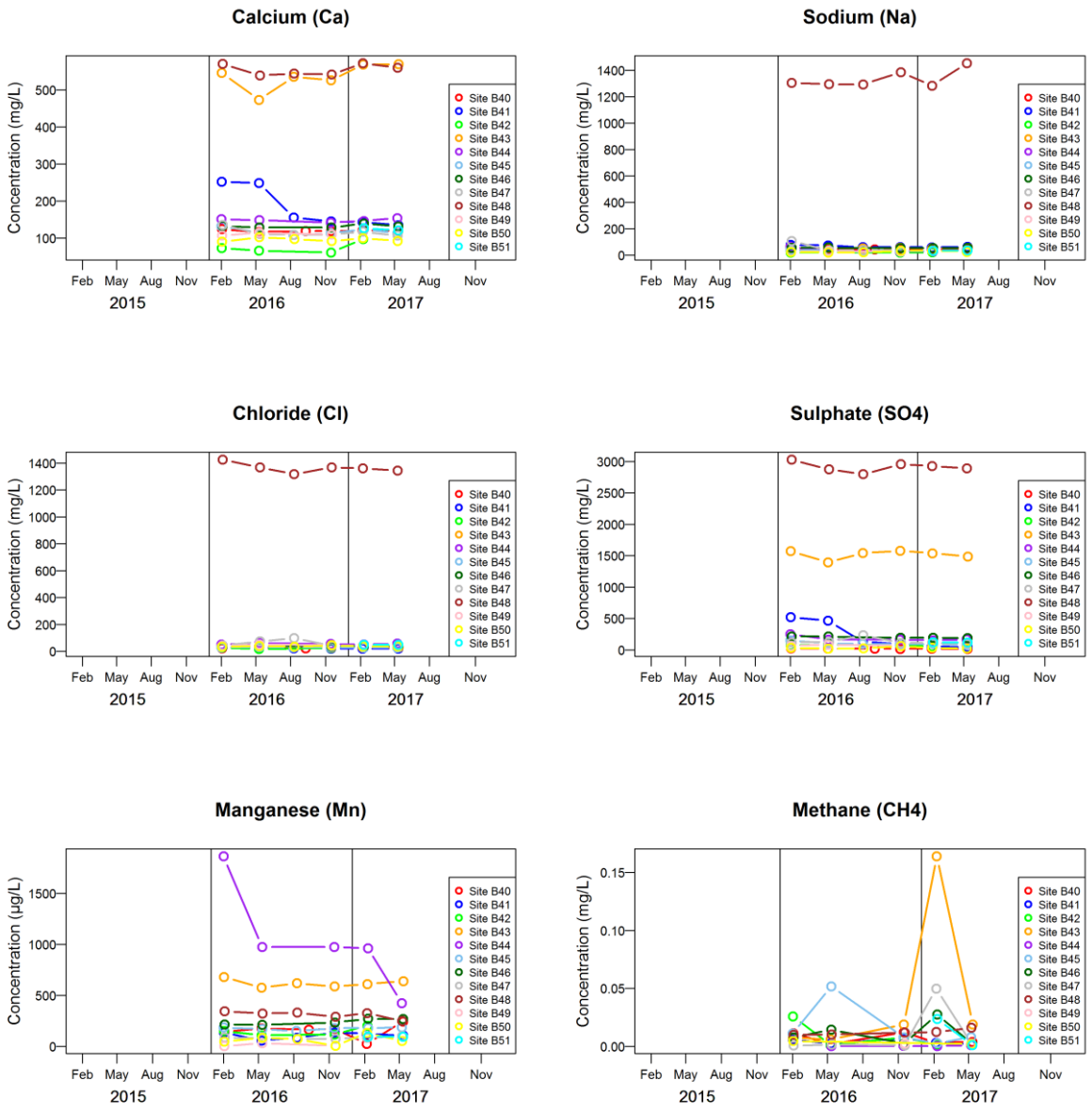

Figure 14. Temporal variation in concentrations of selected solutes from groundwater in the BGS boreholes (Superficial aquifer)

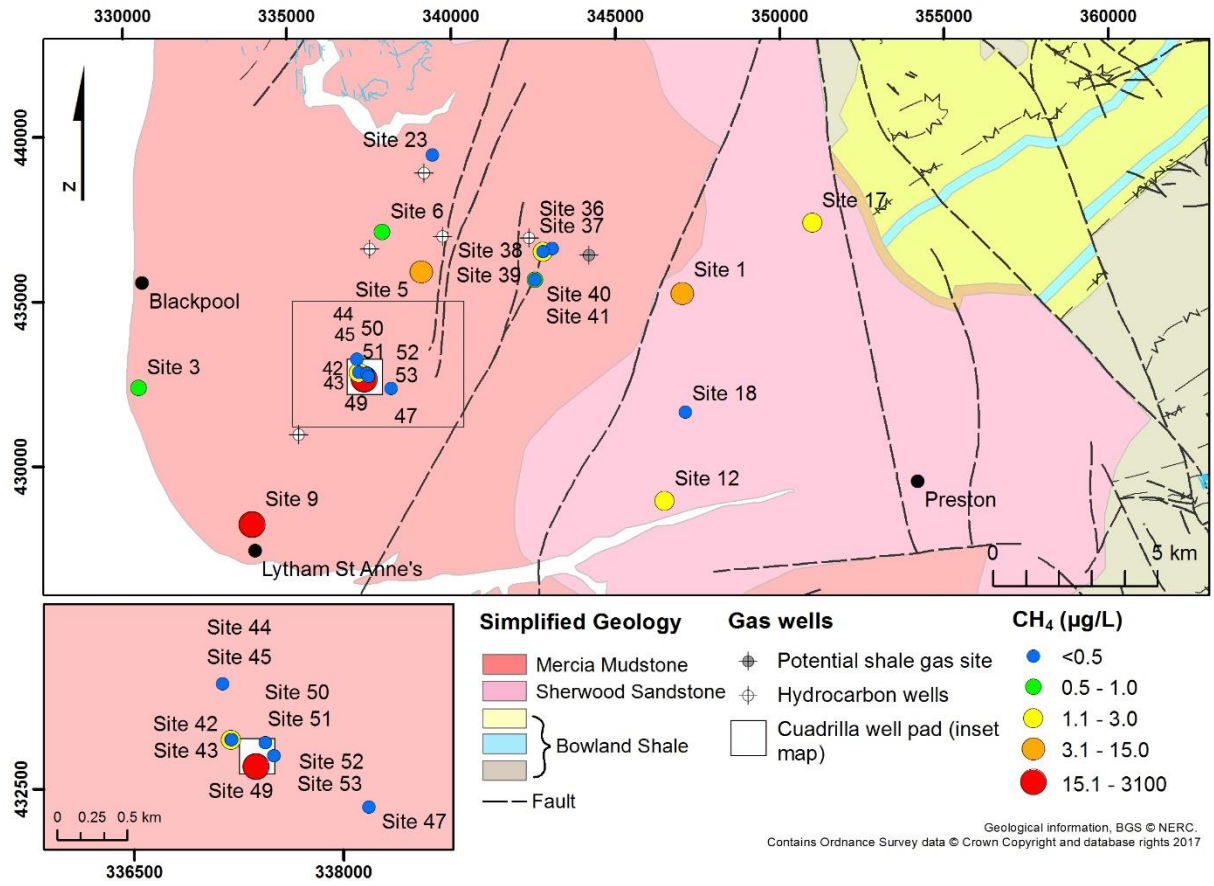

Figure 15. Spatial distribution of dissolved methane in groundwater measured at groundwater monitoring points where measurement possible.

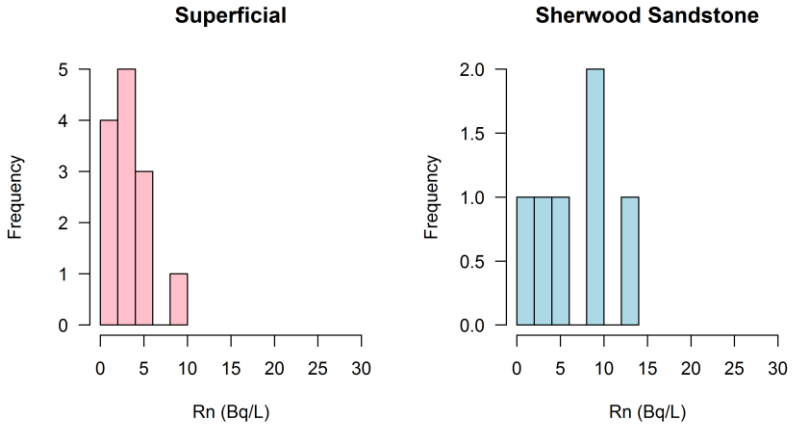

Figure 16. Histogram of representative radon distributions in groundwater samples from the Superficial (Quaternary) and Sherwood Sandstone aquifers from the monitoring network during a single sampling round

3.4.2 Sherwood Sandstone aquifer

Groundwater from the samples in the Sherwood Sandstone aquifer in the eastern part of the study area has a much less variable chemical composition. Here, Ca and HCO_3 are the dominant ions, pH is neutral to slightly alkaline, and all samples have low SEC values (<1000 µS/cm; Figure 11). The groundwater in the Sherwood Sandstone is also anoxic because of the confining condition imposed on the aquifer by the presence of overlying Quaternary Superficial deposits. Groundwater in the Sherwood Sandstone has correspondingly low concentrations of NO_3 and

high concentrations of Fe and Mn (Figure 12); NH_4 concentrations are relatively high in some samples. Methane is almost invariably detectable, though concentrations are low and in the µg/L range (Figure 12). Temporal variability has been more limited over the period of monitoring than for the Superficial aquifer (Figure 14). Spatial variations are sporadic, although few data exist to make a detailed assessment (Figure 15).

Activities of dissolved radon in the Sherwood Sandstone groundwater typically have a larger range than those in groundwater from the Superficial aquifer, although values are still not high. Activities up to 15 Bq/L were recorded in one representative sampling round (Figure 16). These values are consistently below the national parametric value for Rn in drinking water of 100 Bq/L.

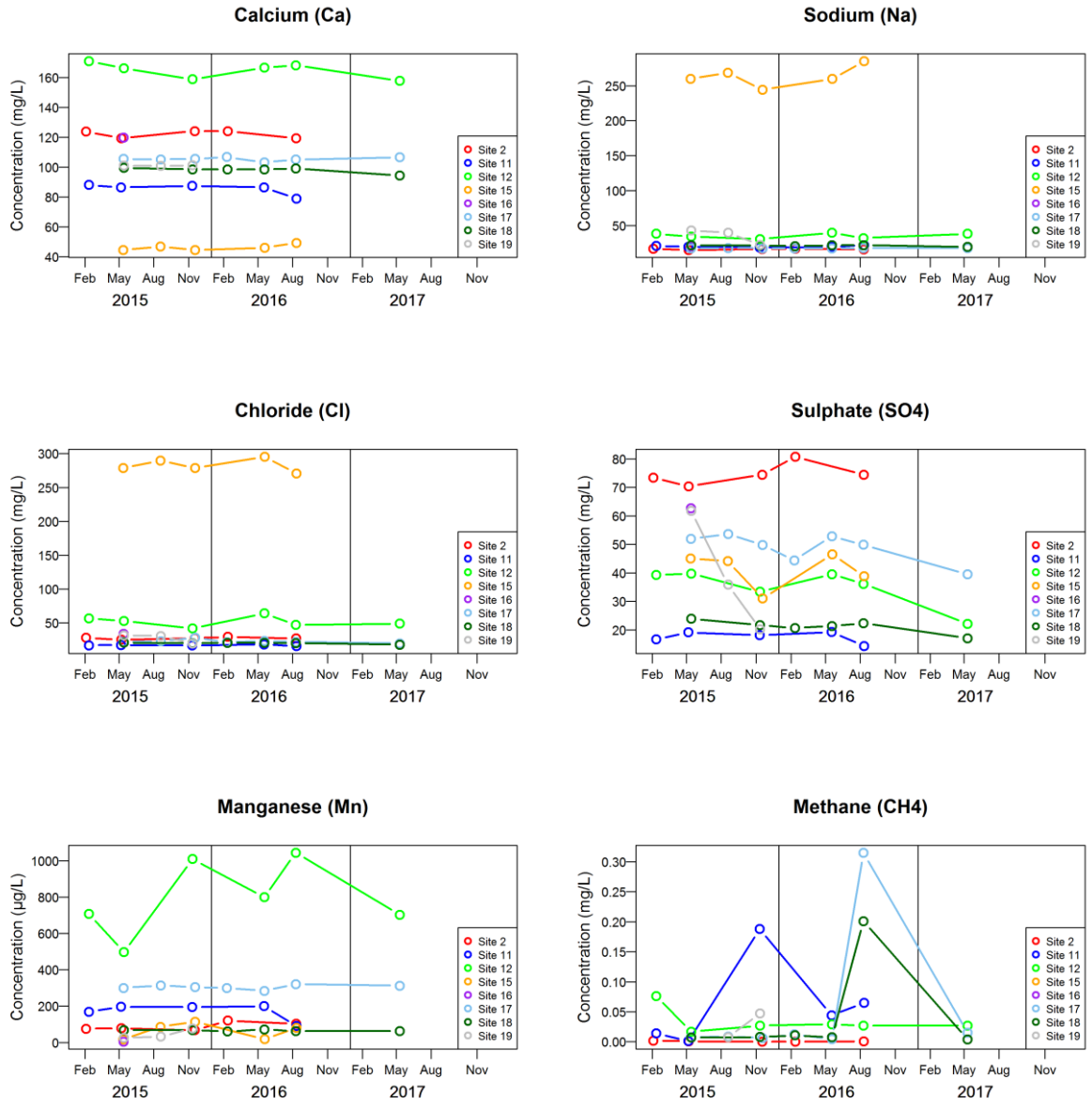

Figure 17. Temporal variation in concentrations of selected solutes from groundwater in the Sherwood Sandstone aquifer

3.4.3 Stream water

Stream compositions are also dominated by Ca and HCO_3 and low SEC values (<1000 µS/cm) are indicated (Figure 11), although relatively high concentrations of Cl and SO_4 are observed infrequently (Figure 18). The greater variability in observed compositions over time could be due to varied rainfall and contributions from runoff. Methane has not been measured in the

stream water because rapid degassing is likely and concentrations are expected to be low. Figure 18 indicates some high (and variable) concentrations of NO_3, especially in the earliest phases of monitoring. This is likely due to inputs from surface pollutants (agricultural and/or domestic discharges).

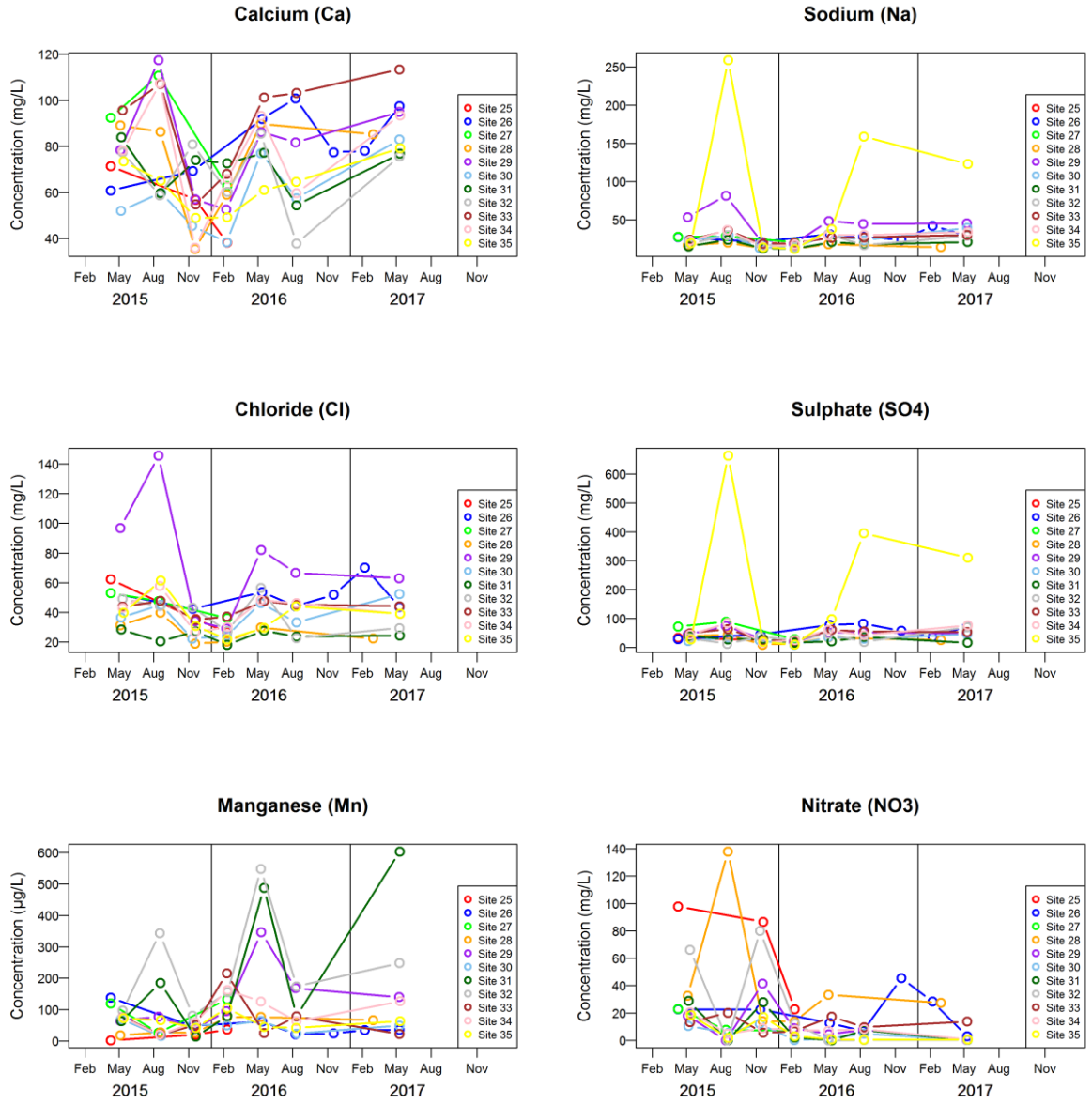

Figure 18. Temporal variation in concentrations of selected solutes from stream water

3.4.4 Organic compounds

In samples from the monitoring network monitored over the period February 2015 to May 2017, concentrations of organic compounds measured by quantitative methods are low, almost invariably being non-detectable.

Semi-quantitative determinations of compounds from a representative sampling round are shown in Figure 19. The presence of some pesticides is indicated, along with components of plastics (including Bisphenol A, BPA) and a number of perfluorinated compounds. Concentrations of these are also low however, almost all <1 µg/L. The only exceptions are benzenesulphonamide, DEHP and BPA. The low concentrations of PAH (<0.1 µg/L, Figure 19) support the non-detects determined for PAH by quantitative methods (e.g. fluorene and pyrene).

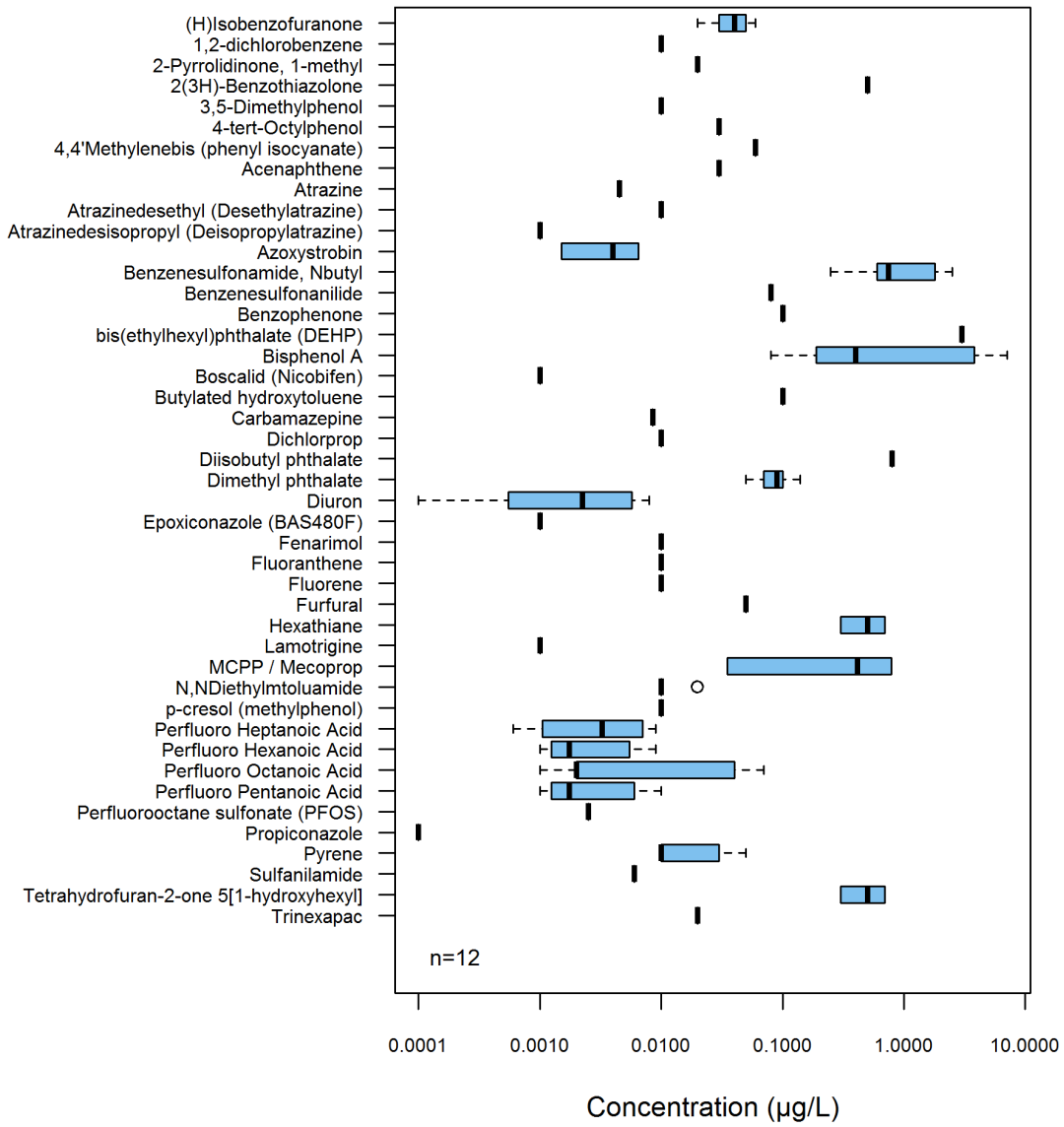

Figure 19. Representative plot of observed organic compounds in samples from the water monitoring network.

3.4.5 Deep Sherwood Sandstone groundwater

Sampling of groundwater from the deep (500 m) borehole in the Sherwood Sandstone close to Roseacre Wood has shown that the groundwater in the borehole is saline and salinity is stratified with depth (Table 2). The dominant ions in seawater are Na and Cl (ca. 10,500 and 19,000 mg/L respectively). The concentrations in the borehole water show that salinity values are more concentrated than solutes in seawater, in the case of the first analysis from a sample at 500 m depth, around fivefold more. Concentrations in the second round of sampling at 360 m depth increased slightly relative to the first analysis.

The salinity values observed indicate that the groundwater quality is notably different from that in the Sherwood Sandstone to the east of the Woodsfold Fault and suggest a lack of any significant hydraulic connection between the two. The high salinity also suggests a lack of significant groundwater flow below the Mercia Mudstone Group. The high salinity, albeit from only one borehole source, suggests that the deep Sherwood Sandstone in the Fylde (west of the Woodsfold Fault) is unlikely to be suitable for drinking water.

Table 2. Chemistry of depth samples taken from groundwater in the 500 m borehole into the Sherwood Sandstone near to Roseacre Wood; concentrations in mg/L

Sample depth (m)	Sample date	Ca	Na	Cl	SO_4
360	12-05-16	448	15,200	24,000	1,530
500	12-05-16	1,120	56,100	92,000	3,100
360	08-05-17	795	41,100	62,700	2,150
430	08-05-17	835	43,000	67,100	2,240

3.4.6 Real-time monitoring

Sondes have been inserted into a sub-set of the new BGS boreholes in the Fylde, monitoring pH, SEC, water temperature and water level hourly, with data transfer to BGS by telemetry. Five sondes (EBM 1–5) have been monitoring since early 2016, a further one (EBM 12) since May 2017. Results of the monitoring are shown in Figure 20. The vertical spikes in data represent the short intervals when sondes were removed from the boreholes for maintenance or calibration. The plots demonstrate the instrument drift in pH values over time and the need for frequent recalibration. SEC shows broad consistency over time in each borehole. Water temperature varies most in EBM 2, consistent with it being the shallowest deployed sonde and hence reflecting response to surface air temperature.

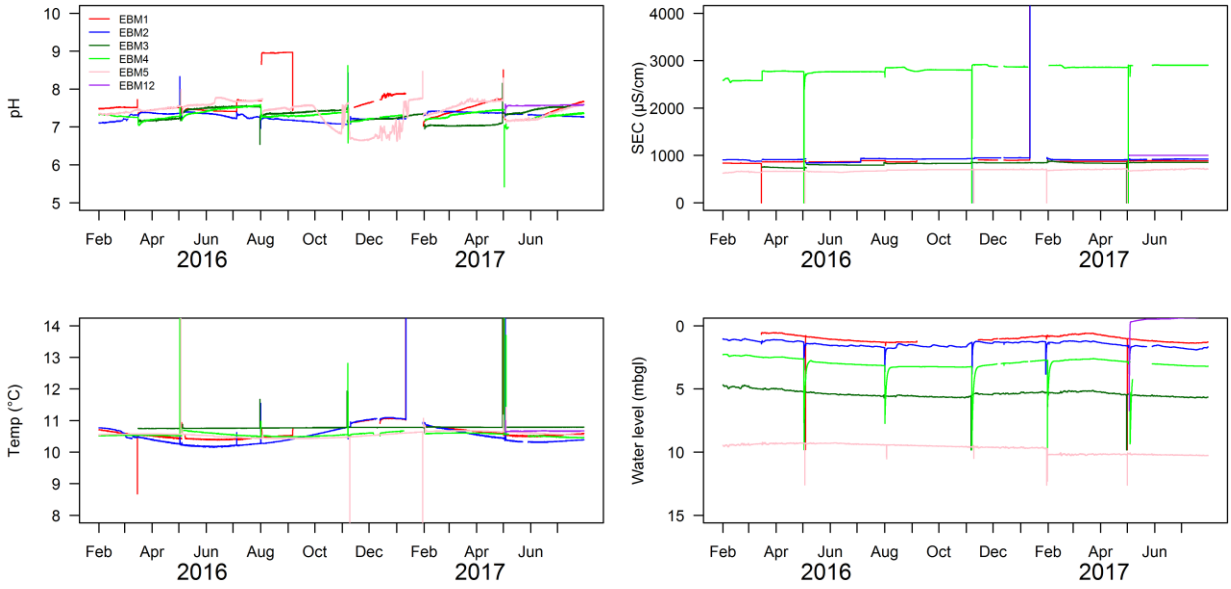

Figure 20. Real-time monitoring data for pH, SEC, water temperature and water level in groundwater from the Superficial aquifer

3.5 SUMMARY

Collated water-quality data for water from the monitoring network, BGS boreholes and sondes, indicate some distinct compositional differences between groundwater from the Superficial aquifer, from the Sherwood Sandstone and from streams. Groundwater from the Superficial aquifer is typically of Ca-Na-HCO_3 type, pH-neutral, and almost universally anoxic. Compositions are consistent with interaction with clay minerals in the aquifer. Concentrations of dissolved methane are typically low (µg/L) but up to some 2–3 mg/L at a small number of locations. Occurrence of methane is consistent with derivation by natural reactions with organic material, e.g. peat, in the Superficial deposits. Activities of dissolved Rn are low. Monitoring shows much consistency over time.

Groundwater from the Sherwood Sandstone aquifer to the east of the Woodsfold Fault is more typically a Ca-HCO_3 water, also pH-neutral and also anoxic because of the continuous layer of Superficial deposits overlying the Sandstone aquifer. Concentrations of dissolved methane are universally low (µg/L range). Activities of dissolved Rn are higher than in the Superficial groundwater but still low (<100 Bq/L). Monitoring also shows some consistency in compositions over time.

Data for one deep borehole (500 m) into the Sherwood Sandstone aquifer below the Fylde (Roseacre Wood area), indicate that the groundwater below the thick Mercia Mudstone (ca. 350 m) is highly saline, increasing with depth, and is unsuitable for water supply.

Streamwaters show greater variation in compositions over time than the groundwaters, as expected as a response to varying rainfall and surface runoff.

Concentrations of analysed organic compounds (VOCs, SVOCs, TPH, PAHs) are usually low in the groundwater and stream samples investigated, almost all being repeatedly non-detectable. Semi-quantitative analysis by GC-MS and LC-MS has detected some occurrences of organic contaminants, including pesticides, plasticisers, and perfluorinated compounds. These are at low concentrations, usually much less than 1 µg/L, but nonetheless, indicate effects of human activity on shallow groundwater and streamwater.

The water monitoring data collated over the 2015–2017 sampling period are facilitating the detailed characterisation of the baseline condition of the waters in the Fylde area. This work will be completed once a full set of baseline data has been compiled.

4 Atmospheric Composition

4.1 INTRODUCTION

An atmospheric baseline is a set of measured data at a specified fixed location that is statistically representative of the local atmospheric composition, and which reflects the role of existing local, regional and global pollution sources. The dataset should include inputs to air sampled over a period of time that is sufficient to capture typical ranges in meteorological conditions. An atmospheric baseline provides a set of statistical values against which the incremental impacts of new emissions, new pollution sources, or policy interventions, can be assessed at a later date using analogous comparative data. The baseline in air pollution conditions may be expected to vary by wind direction, time of day, and season, and meaningful statistics are established through long-term continuous observations.

The analysis in this report uses greenhouse gas concentration, principal air quality trace gas and particulate matter concentrations, and meteorological data, collected at the monitoring site at Preston New Road, Little Plumpton close to the shale-gas development site. These data represent the first full year of data. Monitoring is continuing and these further data will be reported in due course as part of a full baseline assessment.

The method of baseline interpretation used here allows us to explore the statistical climatology of the atmospheric environment at each site and to explore the mix of pollutant source-types that influences the local area by comparing meteorology (especially wind direction and wind speed) and trace gas concentrations (and correlations) as a function of time, such as time of day, day of week, seasonal and annual. We do this by discussing the mean state and variability of the measured data within relevant subsets of time over which we may expect the dataset to behave consistently and comparatively, e.g. days of the week versus weekends, winter versus summer, day versus night and differing wind directions, wind speeds, and surface pressure conditions. By comparing the differences between such regimes, we can attempt to unpick the causes of observed systematic differences and variability, and use data such as back-trajectory analysis to facilitate potential sources of gas emission upwind or nearby.

The analysis here often refers to what we describe as the *airmass history*. In atmospheric science, this term refers to the character of a volume of air in terms of any impacts on the air's composition as air moves over and through its upwind environment. Airmass composition (e.g. trace gas concentrations) is continually perturbed as air moves through Earth's atmosphere, experiencing chemical and dynamical changes associated with inputs (e.g. pollution sources), chemical modulation (due to atmospheric chemistry), physical modulation (due to dry and wet deposition) and diffusion/dispersion processes as airmasses mix as a function of the prevailing meteorology. The sum of all of these processes results in the measurements that we might see at a fixed location. Put simply, these impacts - in the context of air pollution - can be additive, representing a mix of pollution added to the airmass as it advects over various sources upwind, subtractive due to chemical and physical removal, and dispersive as airmasses mix with each other.

Detailed airmass characterisation in atmospheric science research requires the use of cutting edge chemical transport models and highly detailed and comprehensive (global) measurement datasets and remains the subject of much academic research well beyond the scope of this report and this project. Therefore, in this project, which is concerned with impacts on the local environment, we limit ourselves to the interpretation of local and regional pollutant sources and a relatively recent airmass history to interpret how these factors impact the measurement sites in a statistical framework to obtain a representative and meaningful baseline climatology.

A further objective was to advise on the spatial transferability of the climatology, (i.e. the wider area that the baseline can be extended to represent), and the temporal lifetime of the baseline (i.e. how far into the future the statistics can be reasonably assumed to be valid). This is because

different locations will typically have very different existing local pollution sources and future development plans, such that baselines have finite extrapolation potential. As the greenhouse gas baseline is intended to provide a contextual source of information from which to compare any future measured increment in local pollution attributable to shale-gas activity, it will be important to establish the utility of the baseline for this future purpose.

In an earlier report (Smedley et al., 2015), we discussed the technical specifications of the instrumentation at the atmospheric composition monitoring site built for the purpose of environmental baselining. We also described the rationale for site location, sampling frequency (1-minute resolution) and sampling duration (12 months) in the context of providing meaningful statistical comparative datasets and interpretation of local (defined here as <10 km from site) and far-field (>10 km from site) generalised sources of gas emissions that may predate any future exploration for shale gas in each location. For further information on the instrumentation, siting, and atmospheric composition baseline rationale, consult the project website: www.bgs.ac.uk/lancashire.

4.2 SITE SELECTION

The position of the atmospheric composition measurement site (see Figure 21) was selected so as to be downwind of exploratory shale gas extraction infrastructure (to optimise potential future operational monitoring) in order to obtain a representative local baseline ahead of any exploratory activity. The site consists of a mains-powered outdoor weatherproof enclosure containing all scientific instrumentation and a meteorological station to record local thermodynamics (winds and meteorological variables) to aid qualitative source apportionment based on airmass history.

4.2.1 Monitoring site details

On beginning the project in September 2015, new instrumentation was procured and site locations were selected for installation. By late January 2016, the monitoring site was fully operational and collecting the full suite of data detailed in Table 3 below.

The LP site is situated on privately-owned farmland near to the village of Little Plumpton, Lancashire, where planning permission has been granted to Cuadrilla to carry out drilling and hydraulic fracturing for shale gas exploration. The site has been established with the land-owner's permission and a full risk assessment carried out prior to installation of the monitoring station.

Figure 21. Left: photograph of the Little Plumpton (LP) measurement site; right: map showing location of the measurement site and proposed Cuadrilla site to the north of the A583 at Little Plumpton. © University of Manchester, 2017

4.3 INSTRUMENTATION

Air-quality instruments at LP were purchased using grant funding from the Department of Business, Energy and Industrial Strategy (BEIS) and administered through the British Geological Survey, including the Whole Air Sampling (WAS) system used here to derive concentrations of hydrocarbons in free air. Greenhouse gas measurement instrumentation has been provided by the University of Manchester.

Air inlets positioned on 2–3 m high pylons draw air into the instruments to record instantaneous concentrations of trace gases and particulate matter in the air moving over the measurement sites with the prevailing wind. Data were recorded locally and also transmitted wirelessly to a data storage facility, from where the science team can monitor performance and nominal operation.

Table 3. Measurements at both sites, dates when measurements became active, and measurement frequency (as streamed via the cloud). Note that NMHC refers to non-methane hydrocarbons and PM refers to particulate matter

Species	Little Plumpton	Frequency
Meteorological Data (T, q, p, 3D wind vector)	Nov 2014	1 minute
NO, NO_2, NO_x	Dec 2015	1 minute
O_3	Dec 2015	1 minute
PM_1, $PM_{2.5}$, PM_4, PM_{10}	Nov 2015	1 minute
NMHCs	Jan 2016	weekly
CH_4	Nov 2014	1 minute
CO_2	Nov 2014	1 minute

4.4 MOBILE BASELINE METHANE MONITORING

In addition to fixed-receptor-site monitoring, two 2-day measurement campaigns were undertaken using the Royal Holloway University of London (RHUL) mobile greenhouse gas laboratory following the procedures and protocols outlined in Zazzeri et al. (2015). These surveys were designed to characterise the types of existing greenhouse gas sources in the wider local area around each monitoring site. The results from these mobile surveys will be presented in Section 4.7.2. The dates and locations of the mobile surveys were 9–10 March 2016 and 27–28 July 2016.

Where repeatable plumes of methane were identified, with significant elevation of methane concentrations recorded for at least 20 seconds on forward and reverse driving profiles, the plumes were sampled for isotopic analysis by pumping air into Flexfoil bags. On average, 25 bags were filled during each 2-day campaign for subsequent analysis in the laboratory at RHUL.

Some source emissions might be expected to be continuous and measured on consecutive days and repeat campaigns, while others such as gas leaks may be repaired or pressure dependent, and emissions associated with animals may vary as they move around from barn to field. Plume receptor points sampled by the mobile laboratory were along accessible roads and tracks, so transecting a plume can be conceived to be entirely wind-dependent.

Each methane source has a typical carbon isotopic signature. These are conventionally assigned to a per mil (‰) scale for global carbon sources, which for methane gives $\delta^{13}C$ ranging from -75 ‰ for biological sources to -15 ‰ for combustion sources. Well-mixed background air contains methane with an isotopic signature between -48 and -47 ‰. Background CH_4 is typically between 1.9 and 2.0 parts per million (ppm), depending on meteorological conditions. These classifications will be used as the basis for interpretation of results.

4.5 CALIBRATION AND QUALITY ASSURANCE

Quality assurance (QA) and quality control (QC) procedures have been employed for air quality and greenhouse gas concentration data covering all aspects of network operation, including equipment evaluation, site operation, site maintenance and calibration, data review and ratification. All instrumental calibrations are traceable through an unbroken chain to international standards to ensure high accuracy and known uncertainty in the gathered dataset. Metadata concerning the precision and guidance on use of the data is prepared for each measurement reported and will be available to view publicly on the Centre for Environmental Data Analysis (CEDA) after final QC approval. Data were checked online initially before being uploaded to the CEDA repository will be quality checked. Site visits occur at 3-weekly intervals to check the instruments physically, and to perform checks on analyser accuracy, precision and response times as well as calibration.

The calibration and maintenance procedures for each instrument are detailed in Table 4 below. Measurements of CO_2 and CH_4 were made using an Ultra-portable Greenhouse Gas Analyser (UGGA; Los Gatos Research Inc., USA). This instrument was calibrated on site using two standards traceable to the WMO greenhouse gas scales: X2007 and X2004A for CO_2 and CH_4 respectively. One standard was chosen to contain roughly ambient concentrations (403.69 ppm CO_2 and 1901.00 ppb CH_4), while the other was enhanced in both gases (603.02 ppm CO_2 and 5051.07 ppb CH_4). The concentration of both gases within the standards has been determined by EMPA, Switzerland, relative to the corresponding WMO scales. The instrument uncertainty can be quantified by the 1σ values given for the calibration parameters above. These values include uncertainties associated with instrument drift and the uncertainties associated with the calibration cylinder certification. Assuming these uncertainties are uncorrelated and normally distributed, CH_4 measurements of 1900 ppb and 5000 ppb would have 95 percent confidence intervals equal to 10.49 ppb and 22.40 ppb respectively. Similarly, CO_2 measurements of 400 ppm and 600 ppm would have 95 percent confidence intervals equal to 2.92 ppm and 3.83 ppm respectively.

Table 4. Detailed descriptions of the QA/QC for data collected at LP measurement site

Parameter	Calibration and maintenance procedure
NO and NO_2	Traceable calibration cylinders from the National Physical Laboratory. Monthly checks of analyser accuracy, precision convertor efficiency.
Ozone	Six monthly calibrations in the field by a calibration unit links to a primary UV photometric standard that is itself calibrated against a certified national source annually at the National Physical Laboratory.
Particulate matter	Six monthly calibration in the field by a monodust (CalDust), monthly maintenance checks
CO_2 and CH_4	Calibration of greenhouse gas concentration data is performed by routine reference to certified gas standards, traceable to the World Meteorological Organisation scale.
NMHCS	Calibration of NMHCs is performed by reference to an NPL ozone precursor mix. This calibration scale has been adopted by the GAW-VOC network and hence the measurements of NMHCs made by this instrument are directly comparable to those made by all of the WMO-GAW global observatories. Calibrations are performed each month or more frequently if field deployment allows. A long-term data set of the response of the instrument is held and regularly updated to ensure that the instrument responses do not change and to highlight any issues with stability of components within the gas standards used.

4.6 METEOROLOGICAL BASELINE

The principal meteorological variable of interest to baseline characterisation and pollution source interpretation is the local wind speed and direction, as an indicator of the local airmass history (i.e. what source of pollution the sampled airmass may have passed over upwind). The instantaneous wind speed and direction can point us to relatively nearby sources of pollution (within ~ 10 km) where repeated and consistently elevated concentrations of trace gases are observed to correlate with wind direction and wind speed. When discussing more long-range sources of pollution (such as may be added over cities many 10s or 100s of km upwind), the timescales of interest to airmass history typically extend to no more than around 5 days. Beyond this time, the uncertainty in the path of air upwind (and the chemical changes in such air) increases rapidly and interpretation becomes meaningless. Therefore, we limit our analysis to these timescales of advection only.

We now describe the climatology of wind observed at the baseline sites and discuss what this means in the context of pollutant gas concentrations and sources that have been observed at the measurement stations.

4.6.1 Little Plumpton wind climatology

The wind speed and wind direction statistics observed at the LP site over the full measurement period are shown in Figure 22 as a conventional wind rose. This type of illustration simply shows the frequency (in percent of total time) of instances when wind blows from various directions (seen as the vector and radius in Figure 22). The colour scale in Figure 22 then illustrates the corresponding proportion of winds in each direction for a range of surface wind speeds (see colour legend in Figure 21).

As expected at the LP site (as for any exposed site in the UK) the dominant wind direction is from the western quadrant (~35% of the time), consistent with Blackpool's location on the west coast of the UK mainland and exposed to the Atlantic mid-latitude storm track. This is also the direction from which the strongest winds are observed (red and dark red colours in Figure 22), typically coinciding with the passage of mid-latitude cyclones over the UK mainland. Within this westerly quadrant, the dominant wind speed is between 6-12 m/s (dark red colours), with extremely strong winds peaking up to 20 m/s in very rare storm conditions (<0.5% of the time).

This has important implications for the local baseline. The position of the LP site near to the Blackpool shoreline means that winds bringing air from the Atlantic may typically be expected to carry relatively well-mixed and background airmasses to the LP measurement site. In this context, a *background* can be conceived to be an airmass relatively unaffected by local or regional pollution sources, broadly representative of the average composition of Northern Hemispheric air at the time. These airmasses often represent the Northern Hemispheric seasonal average concentrations of greenhouse gases especially, as these gases are relatively inert on the time and spatial scales of advection across the Atlantic in mid-latitude cyclones. As these airmasses dominate the statistical climatology at the LP site, the baseline for this wind direction provides a very useful background from which to assess future local changes in pollution sources in the immediate upwind vicinity. The position of the LP site just 300 m directly to the east of the Cuadrilla site makes the dominant westerly wind direction highly favourable for any future operational comparative assessment.

Winds from the south-east were also frequent, accounting for 22% of the period, while northerly and easterly wind directions were less frequent, representing <20% in each quadrant over the course of the 12-month baseline. Wind speeds for these quadrants (all other than westerlies) were also typically much lighter (dominated by light breeze winds in the range 2-4 m/s). This is due to a number of factors: 1) that winds from these directions are moderated by passage over the mainland UK land surface, and 2) that winds from these directions usually represent flow in less frequent high-pressure regimes to the north and east or from low-pressure systems to the south and west. Light winds from these directions will typically carry airmasses that have spent a

significant time in dynamic contact with the surface of the UK mainland and may also represent air that has passed over Western Europe. These airmasses may be expected to typically contain pollution added to the surface air as they pass over a range of anthropogenic (manmade) and biogenic (natural) sources of greenhouse gases and other pollution upwind of the measurement site; such as cities, landfill, industry, transport, agriculture etc. This air may be a mix of both local (<10 km distant), regional (UK mainland) and more distant (Western Europe) pollution sources, making it difficult to deconvolve the relative inputs of each. However, the frequency and duration of transient enhancements seen in trace gas concentration data offers important clues on the proximity (and type) of pollution source, as regionally impacted airmasses will typically display broad (longer timescale) and more invariant enhancements relative to background westerly airmasses, while local inputs are often seen as sharper and shorter-lived enhancements. This will be discussed further in the following sections, making use of additional airmass history tools such as back-trajectory analysis.

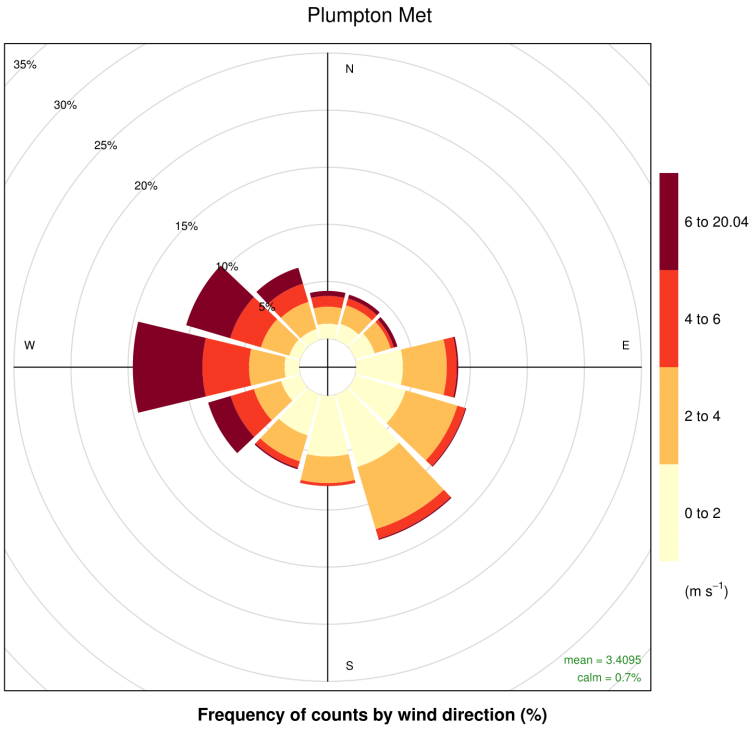

Figure 22. Wind rose for the LP site, showing wind speed and direction statistics for the period 1 Feb 2016 – 30 Jan 2017. The radius defines the percentage of total time in each of 12 wind direction cones (30 degree span), while the colour scale defines the wind speed (redder colours indicating strong wind speeds > 6 ms^{-1} and yellower and pale colours indicate light or stagnant winds, respectively). © University of Manchester, 2017

4.7 GREENHOUSE GAS BASELINE

In this section, we present the statistical analysis of the greenhouse gas baseline dataset for LP and mobile vehicle surveys of nearby greenhouse gas sources in turn. We interpret this in the context of sources of emission and background using meteorological (and other) data to aid analysis. We conclude each sub-section by discussing the authors' recommendations on the appropriate use of the baseline dataset for each site and how this concerns future monitoring for future comparative assessments.

4.7.1 Fixed measurement site climatology

Figure 23 illustrates the measured ambient CO_2 and CH_4 ambient concentrations at LP as a function of time across the full baseline period sampled at the fixed measurement site. Figure 24 and Figure 25 go on to illustrate how the measured concentrations relate to their coincidently-

measured wind direction for each greenhouse gas, while Figure 26 and Figure 27 show the same information but also display the relationship between measured concentration and wind direction as a function of time. When interpreted together, these figures distil several important and internally-consistent summary features, which can be seen in the baseline dataset when comparing salient concentration features with wind direction:

- There are clear periods of what can be defined as a "background" (accounting for 50% of the period) - where CO_2 and CH_4 concentrations appear relatively flat at around 400 parts per million (ppm) and 2 ppm, respectively (as seen in Figure 23). These periods coincide with times of westerly winds seen in Figure 24 and Figure 25, and as the orange and red colours in the times series of Figure 26 and Figure 27; and represent a typical seasonally-variant Northern Hemispheric average concentration.
- There are prolonged periods (several consecutive days) of marginally enhanced CO_2 and CH_4 (between 400-450 ppm and 2-4 ppm, respectively). These periods coincide most often with moderate south-easterly winds as seen in Figure 24 and Figure 25, when comparing with Figure 26 and Figure 27 (where green and yellow colours indicated easterly and south-easterly wind directions). These features are consistent with an interpretation that these episodes represent regional pollution inputs from cities to the south and east such as Manchester, and the cities of Central and Southern England.
- There are short-lived (less than a few hours) but large enhancements (often referred to as "spikes") in the time-series data (greater than 4 ppm CH_4 and 500 ppm CO_2). These coincide most often with light easterly and south-easterly and northerly wind directions seen in Figure 24 and Figure 25, compared with Figure 26 and Figure 27 (where easterly winds are seen in green colours). These features in the data, often superimposed on the regional increment describe above, are expected to represent local (<10 km upwind) sources such as nearby agricultural activities, roads, and landfill.
- That, for most of the time (>90% of the period), CO_2 and CH_4 display common patterns, in that both gases are often seen at their respective background concentrations, or are mutually enhanced with a scalable linear relationship (as shown in Figure 28 and discussed further below).

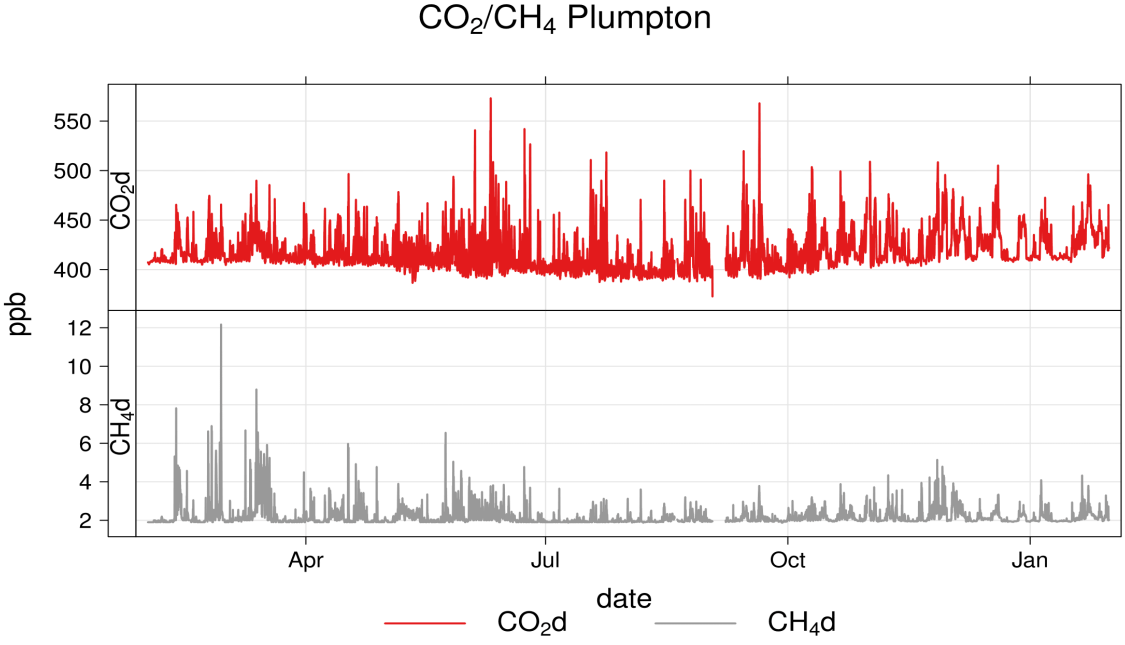

Figure 23. Time series of carbon dioxide (red) and methane (grey) in units of ppm measured at LP between 1 Feb 2016 and 31 Jan 2017. Note: "d" refers to the water-vapour-corrected (or dry) measurement by the UGGA instrument. © University of Manchester, 2017

Interpreting this further, it can be seen that westerly wind directions invariably bring relatively unpolluted air to the LP site. Other wind directions deliver more complex airmasses likely comprising a wide mix of pollutant sources upwind, both local and regional, requiring additional interpretation (see below).

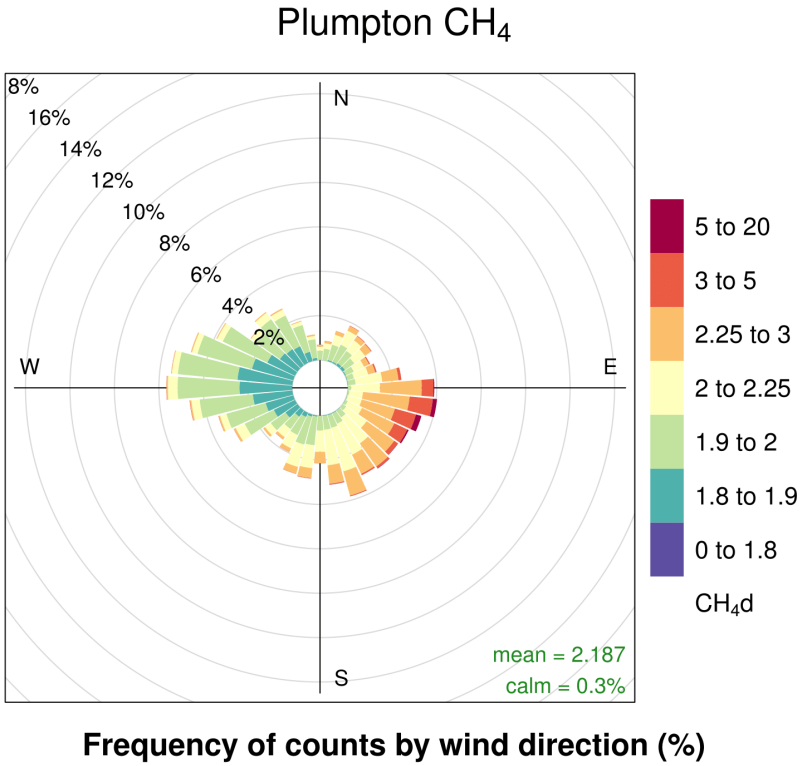

Figure 24. Concentrations (as per colour scale) in air as a function of wind direction for methane (units of ppm), as measured at LP in the baseline period. © University of Manchester, 2017

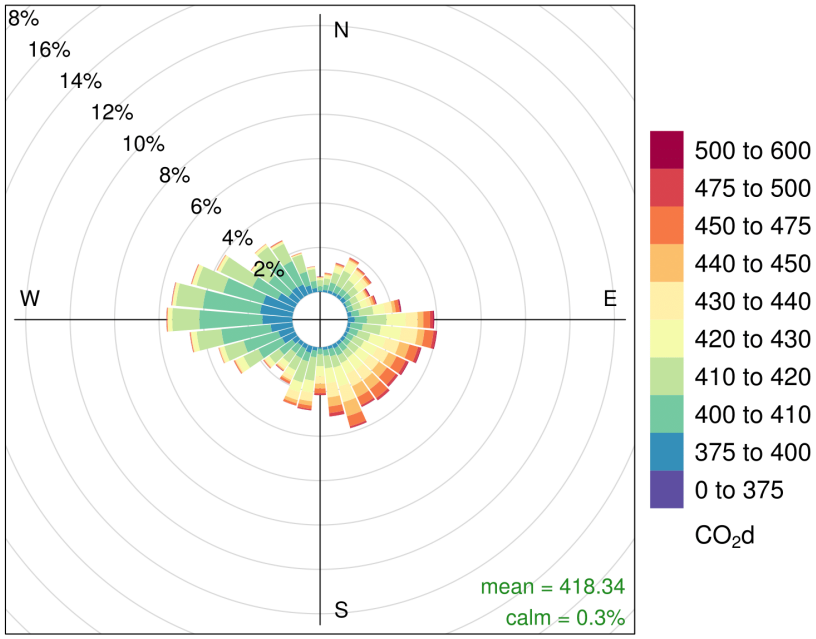

Figure 25. Concentrations (as per colour scale) in air as a function of wind direction for carbon dioxide (units of ppm), as measured at LP in the baseline period. © University of Manchester, 2017

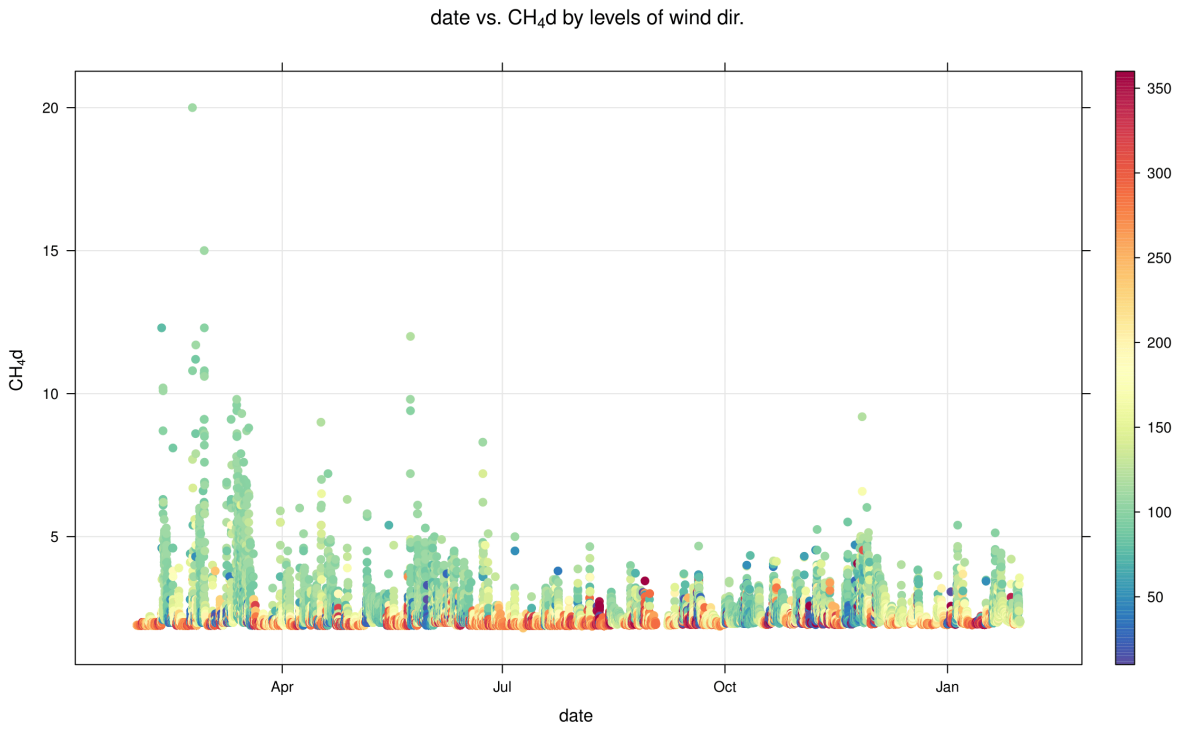

Figure 26. Methane concentration time series, colour-coded for wind direction as per legend as measured at LP in the baseline period. © University of Manchester, 2017

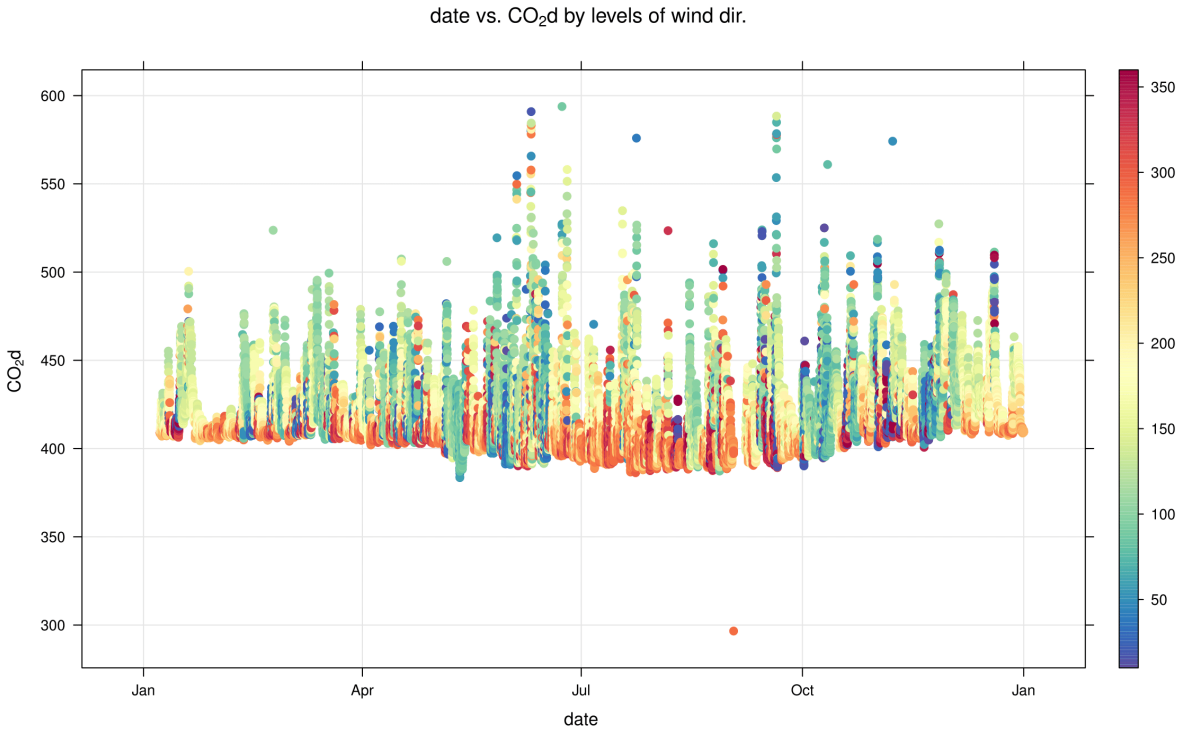

Figure 27. Carbon dioxide concentration time series, colour-coded for wind direction as per legend (in degrees) as measured at LP in the baseline period. © University of Manchester, 2017

Figure 28 illustrates the correlation between simultaneously-measured CO_2 and CH_4 concentration in air, colour-scaled for sampling density (each count representing a one-minute data interval). Warmer colours indicate more frequent sampling. Clear correlations between the concentrations of the two greenhouse gases seen in plots of this type delineate so-called mixing

lines. Such correlations (or mixing lines) often correspond to specific airmass types where co-emission from specific sources, or common airmass chemistry, may be active.

In Figure 28, we see that there are two broad correlations and one dominant feature, seen, as follows:

1. A dominant mixing line (traced by red and yellow colours) with a relationship of $[CO_2]=132.1[CH_4]+386.5$ ppm – representing co-emission (or bulk mixing) of nearby CO_2 and CH_4 sources upwind to the east and north east (based on understanding of how such concentrations relate to wind direction in Figure 25 to Figure 28).
2. A weaker but clear mixing line with a relationship of $[CO_2]=7.5[CH_4]+386.5$ ppm - representing co-emission (or bulk mixing) of CO_2 and CH_4 regional UK and longer-range sources upwind to the east and south east.
3. A dominant red cluster centred at ~400 ppm CO_2 and 2 ppm CH_4 – this represents the dominant and frequent background signal seen in westerly Atlantic airmasses (Figure 24 and Figure 25). Note that the darkest red colours in this cluster correspond to >40 total days of measurement each within the baseline period.

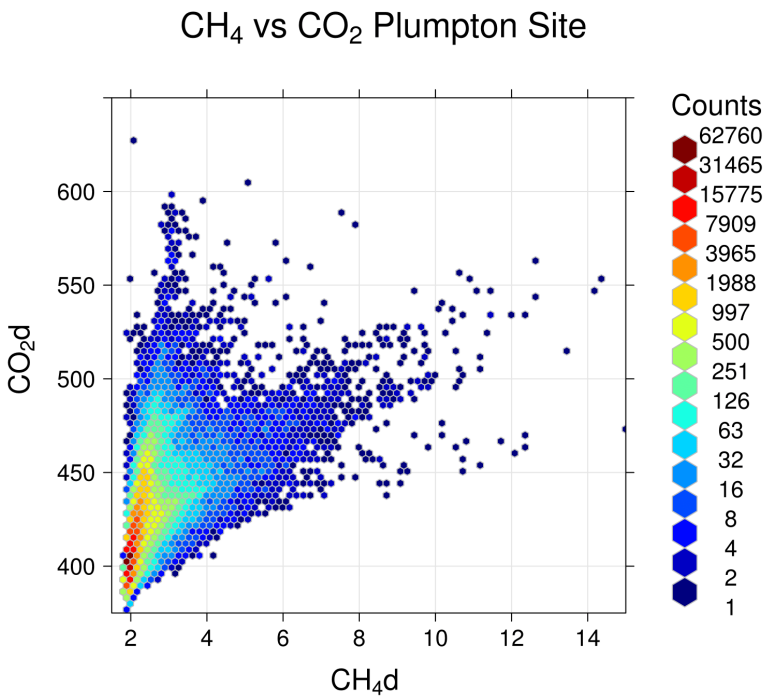

Figure 28. Coincident CO_2 and CH_4 concentrations measured at LP. Colours indicate the frequency density of sampling (number of coincident measurements). One count refers to a one-minute period of data. © University of Manchester, 2017

Mixing lines such as these are a powerful differentiator of source types, especially at the regional and national scale. When temporally averaged (as in Figure 28), they characterise airmasses that have passed over a large fetch of similar pollution source types and where the airmass has had time to mix internally. The two dominant mixing modes seen in Figure 28 are seen to correspond to the less frequent easterly, southerly, and south-easterly wind directions. Considering the location of LP, these wind directions represent air that has passed over the Pennines and the cities of Manchester, Leeds and Sheffield in the case of easterlies, and the cities of Birmingham and London in the case of south easterlies. While cities and infrastructure are a principal source of UK pollution (including greenhouse gases), biogenic sources of greenhouse gases, such as the biosphere, landfill and agriculture would also be expected to feature in the fetch of such airmasses when upwind of the LP site. The summative mix of these longer-range pollution types upwind for easterly and south-easterly wind directions gives rise to the dominant mixing line observed as the red and yellow trace in Figure 28 and described in summary point 2 above.

To interpret more local sources of pollution (within ~10 km), we must focus in detail on the more transient features in the high temporal resolution dataset. To do this on an event-by-event basis for a year of data would be meaningless (and impractical) in the context of the baseline analysis here, though event-led (case study) analysis may well be advisable during any operational monitoring. However, it is possible to interpret the relative role of proximal pollutant sources to the overall baseline by considering short-lived but significant excursions from the average baseline and comparing these with wind speed and direction.

Figure 29 and Figure 30 illustrate a polar bivariate representation of the relationship between both wind speed and direction and greenhouse gas concentration. The colour scale in Figure 29 highlights the wind speed and wind direction conditions that dominate the overall concentration average seen at the measurement site (as a weighted mean of concentration x frequency of occurrence). The red areas seen in both panels (CO_2 and CH_4) in Figure 29 correspond to light winds (0–2 m/s) from the south-east indicating a well-constrained local source for both gases. Figure 30 shows how the absolute measured concentration relates to wind direction and wind speed, which again shows the dominant south-easterly origin of elevated CH_4 concentrations, but also demonstrates a subtly different origin of the greatest enhancements in CO_2, which appear from both the south and south-east. Given the site's location, these local CH_4 sources to the south-east are likely to be the nearby dairy farm (on which the site is located) and the nearby A583 main road, while the southerly dominance in CO_2 is likely mostly associated with passing traffic on the A583 main road. The fact that the red area does not extend to higher wind speeds in the south-east is consistent with an interpretation that longer-range sources of pollution may not contribute significantly to periods where the greatest enhancements in concentrations are sampled at the site, i.e. that local sources dominate the strongest enhancements. The role of longer-range (regional, national and continental) sources is therefore to add a smaller increment to the much larger local emission sources that dominate periods of enhancement in south-easterly wind conditions. The lighter blue areas seen in Figure 29 to the west indicate a long-range and diffuse source of the greenhouse gases, which is consistent with longer-range transport of moderately enhanced airmasses, from Ireland and in intercontinental transport from the United States, although this source's relative contribution to the baseline is very much weaker than those upwind sources when airmasses are received from the south-east.

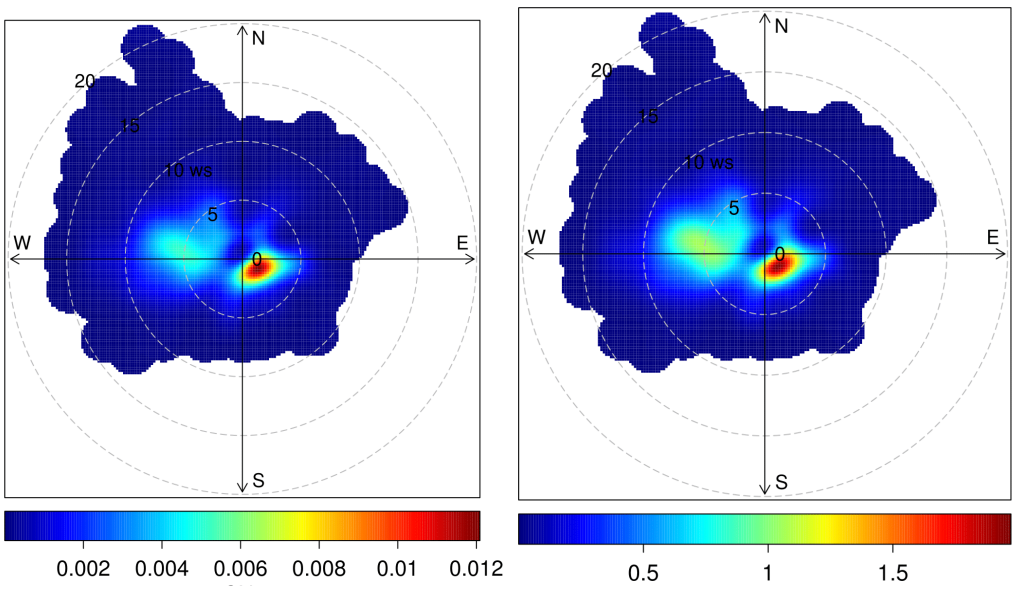

Figure 29. Polar bivariate representation of methane (left) and carbon dioxide (right) as a function of wind direction. The colour scale represents the fraction of total measurement time weighted for concentration enhancement relative to the global mean (as scaled for colour in units of ppm) and wind speed (defined by the radial component - each contour representing 5 m/s). See text for further details. © Univ Manchester, 2017

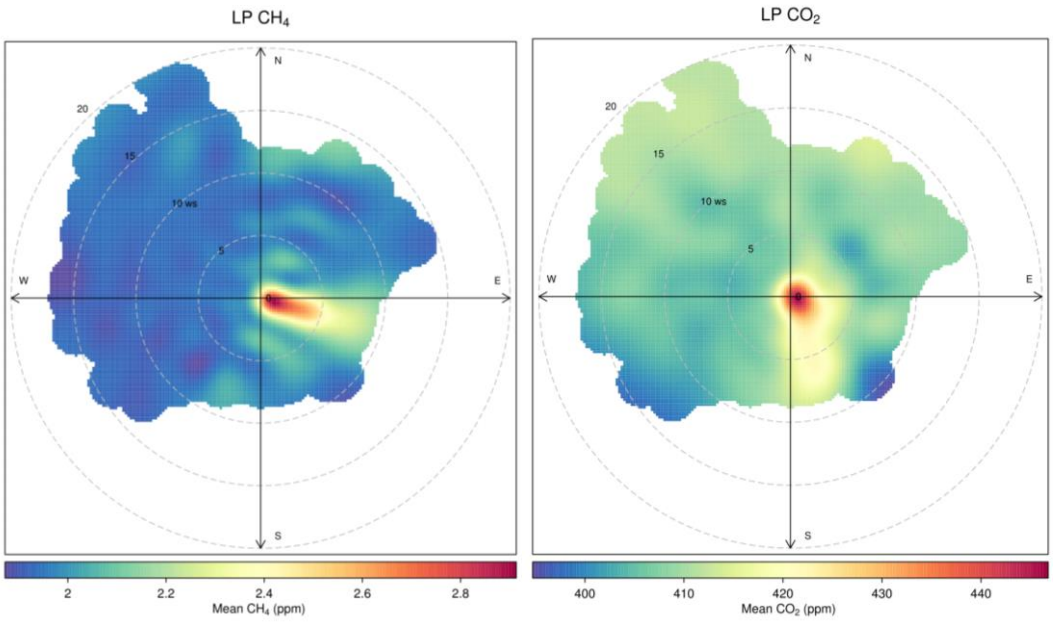

Figure 30. Polar bivariate representation of methane (left) and carbon dioxide (right) as a function of wind direction and wind speed. The colour scale represents the absolute measured concentration (as scaled for colour in units of ppm) and wind speed (defined by the radial length component - each contour representing 5 m/s). See text for further details. © University of Manchester, 2017

To differentiate the role of local, regional and more distant (long-range inter-continental) pollution sources further, we now examine the airmass history, which can be interpreted using Lagrangian back trajectories. Back trajectories are a useful indicator of the path that air has taken in the atmosphere up to and over the previous 5 days. Beyond this time, the accuracy of hindcasted trajectories degrades rapidly due to numerical and meteorological uncertainty associated with Lagrangian transport models and the accuracy of reanalysed meteorological data. Put simply, back trajectories attempt to trace back the path of neutrally buoyant single particles in the atmosphere as they are carried on the wind (this is known as Lagrangian advection). Back-trajectory models use wind fields from meteorological reanalyses (hindcasted winds calculated by forecast models that use assimilated measured data).

In this analysis, we have used the Hybrid Single Particle Lagrangian Integrated Trajectory Model (HYSPLIT) and hourly United States National Centre for Environmental Prediction Global Forecast System reanalysis meteorological data at a spatial resolution of 0.5°x0.5°. We have then calculated 5-day back trajectories with endpoints at the location of the LP site at 6-hourly intervals across the measurement period (~1200 trajectories in total between 1 Feb 2016 and 31 Jan 2017).

Figure 31 shows the airmass history of air sampled at LP throughout the baseline period. This statistical representation of the history of air can be interpreted as a surface "footprint", illustrating a surface area over which air measured at LP has been influenced by potential surface sources. Figure 31 shows the frequency (as a fraction of total time, in this case as a percentage of the 12-month baseline period) that air has passed near to the surface in a latitude-longitude grid with a 1-degree spacing. The red colours indicate that air received at LP is most characterised by air that has previously passed over Ireland and the Atlantic Ocean. It also shows less frequent contact with the near-surface to the north.

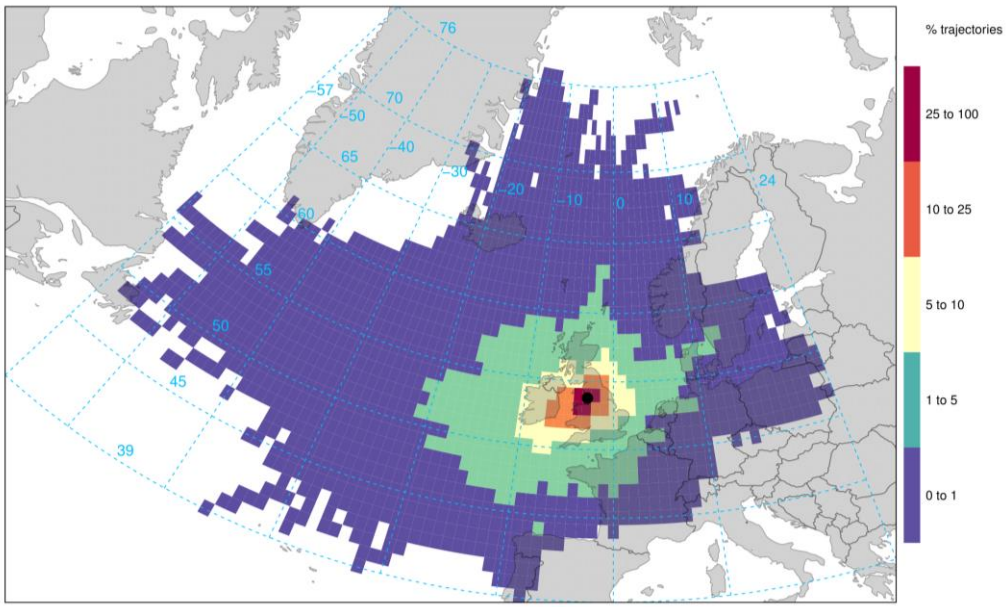

Figure 31. 5-day airmass history surface footprint statistics for the period 1 Feb 2016 to 31 Jan 2017, as seen from the LP site at a spatial resolution of 1 x 1 degree. Frequency refers to the fraction of the total trajectories passing over each lat/long grid cell. © University of Manchester, 2017

Figure 32 shows the same trajectories but sub-sampled by meteorological season. This figure illustrates that for all but the winter season, airmasses arriving at LP in the baseline period display a variety of upwind histories from all directions (dominated by the Atlantic region to the west). In the winter season, we see that airmasses originate (within the past 5 days) almost exclusively from latitudes to the south of the LP site. This is not to say that airmasses in winter have no longer-range history in more northern latitudes, simply that contact with the near-surface over the preceding 5 days before sampling at LP is dominated by latitudes south of the LP site, i.e. that longer-range (>5 day) airmass histories may well be seen further to the north before being advected over the UK mainland in westerly (or other) flow regimes. This pattern is consistent with the analysis and conclusions drawn about the local meteorology discussed earlier and suggests that land-based long-range sources of pollution from the east (over the UK and mainland Europe) are experienced relatively infrequently compared to maritime air received from the west and the Atlantic at LP.

To investigate further the nature of the 4 broad airmass types arriving at LP identified earlier, we now examine the temporal patterns and airmass history for each airmass classification. To achieve this, the polar bivariate data seen in Figure 11 have been used to categorize the baseline dataset into four principal clusters by the method of K-means clustering. The resulting clusters can be seen in Figure 33, which illustrate (as defined zones) the dominant relationships between concentration, wind direction, and wind speed, which we have discussed earlier. Each zone can be thought of as representing an internally consistent subsample of the data based on the correlation between gas concentration, wind speed and wind direction.

For methane (Figure 33 left), we see the dominant westerly airmass (Cluster 1 - green), a less frequent background airmass from the north-west (Cluster 4, yellow), a regionally (enhanced GHG concentration) airmass (Cluster 2 - blue) and a highly enhanced airmass (Cluster 3 - orange). For carbon dioxide, we see similar features for clusters 1, 2, and 3, but with the more dominant southerly zone cluster (Cluster 2 in Figure 33 right - shown in purple).

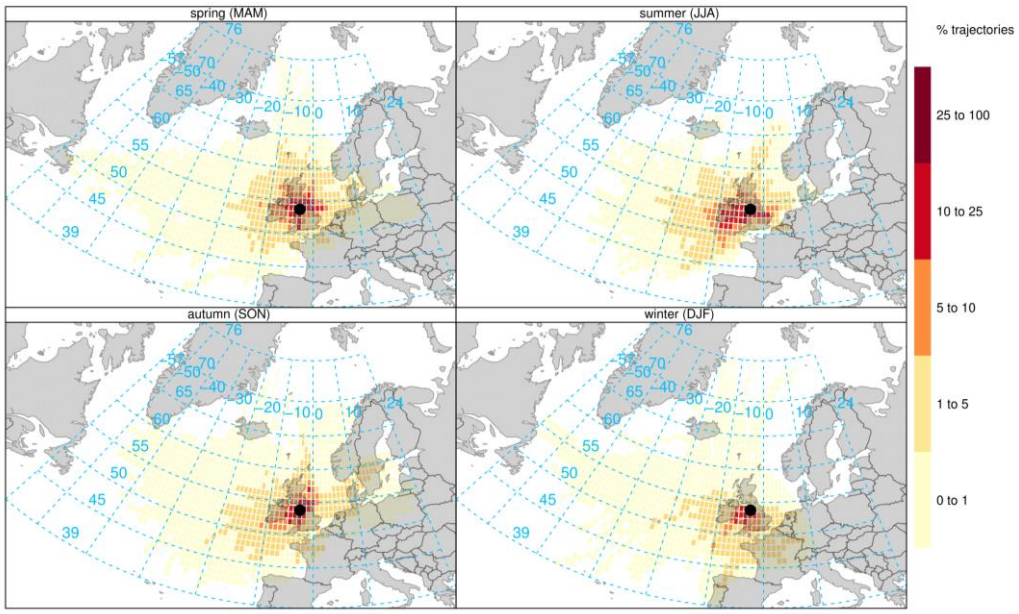

Figure 32. 5-day airmass history surface footprint statistics for the period 1 Feb 2016 to 31 Jan 2017 by meteorological season (e.g. DJF refers to Dec, Jan and Feb), with trajectory endpoints at the LP site at a spatial resolution of 1 x 1 degree. Frequency refers to the fraction of the total trajectories passing over each lat/long grid cell. © University of Manchester, 2017

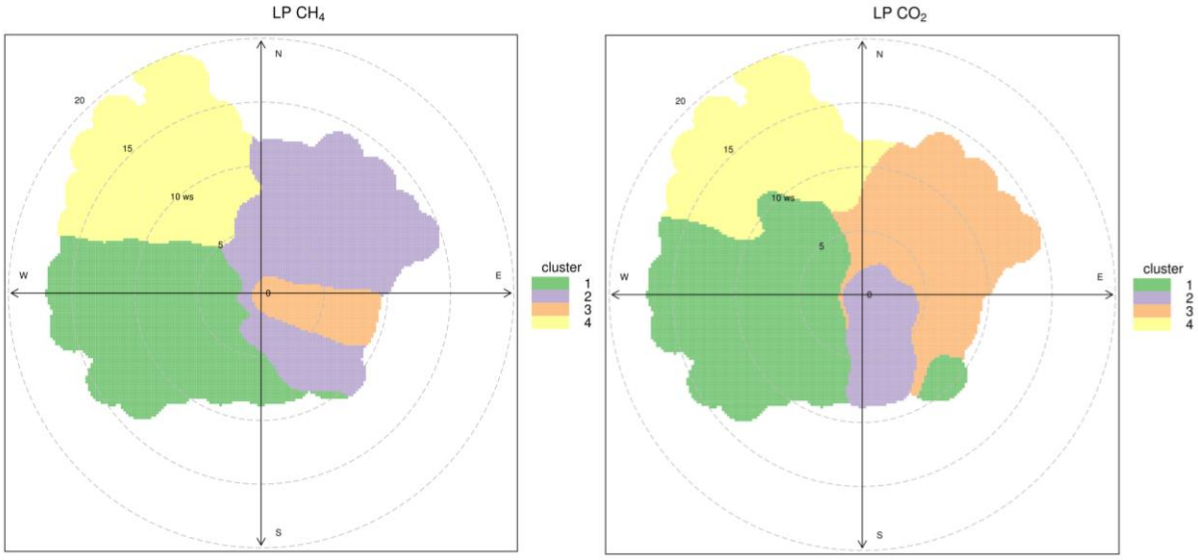

Figure 33. Derived 4-mode K-means clusters of dominating wind-concentration relationships for: left (methane); and right: carbon dioxide as sampled at LP. Radial direction indicates wind direction, while radial length defines wind speed. © University of Manchester, 2017

We have used this clustering approach to sub-sample the dataset to investigate airmass histories corresponding to each zone (or cluster) by calculating back trajectories for meteorological conditions at the time of measurement of each data point inherent to each cluster. This is illustrated in Figure 34, which shows the trajectory climatology for each cluster corresponding to methane. When illustrated in this way, the difference between the 4 airmass classification origins can be observed readily as distinct surface footprints over different upwind areas. The westerly and northerly zones (clusters 1 and 4 in Figure 33 left) define Atlantic maritime origins (seen as the blue and purple trajectories in Figure 34, consistent with our earlier conclusion that air received at LP from these locations broadly represents a Northern Hemispheric average

composition. The regionally enhanced (elevated concentration) cluster is seen in the green trajectories, which pass over the UK mainland to the west and continental Europe. The highly elevated trajectories (seen as orange in Figure 34) show an Atlantic and English Channel footprint, which further reinforces our conclusion that the observed elevations associated with this wind direction are associated with more localised (<10 km upwind) emission sources (added to a smaller UK mainland increment), as the longer-range airmass history would otherwise deliver cleaner airmasses than from Clusters 1 and 4. The mean trajectory path for each cluster is shown in Figure 35, which illustrates the divergent nature of each cluster in terms of their long-range airmass histories. Figure 35 also shows the percentage of time over the baseline period associated to each cluster, further reflecting the conclusions discussed using the simpler wind rose analysis described for Figure 24 to Figure 27 earlier.

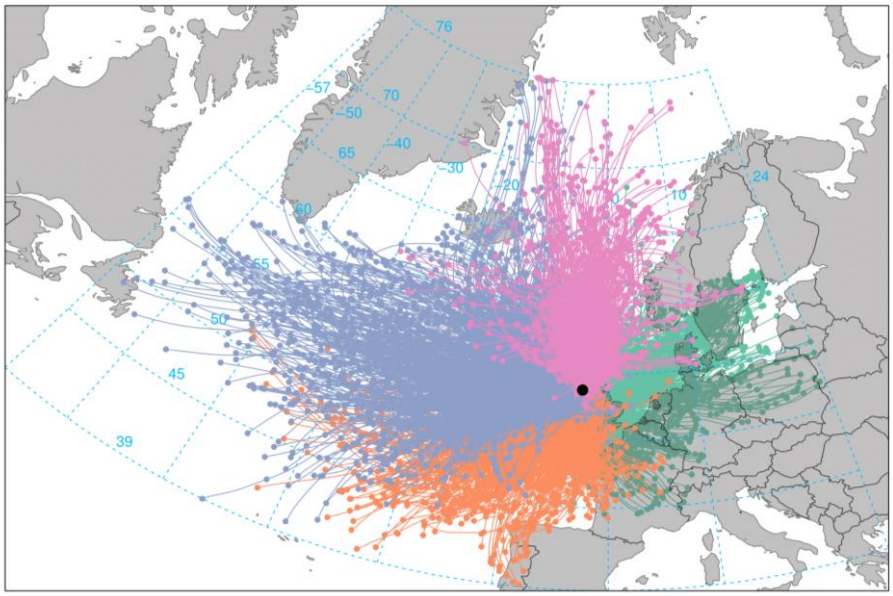

Figure 34. 5-day back trajectories ending at LP corresponding to the time of each data point associated with the 4 principal clusters identified in Figure 14 left for methane. © University of Manchester, 2017

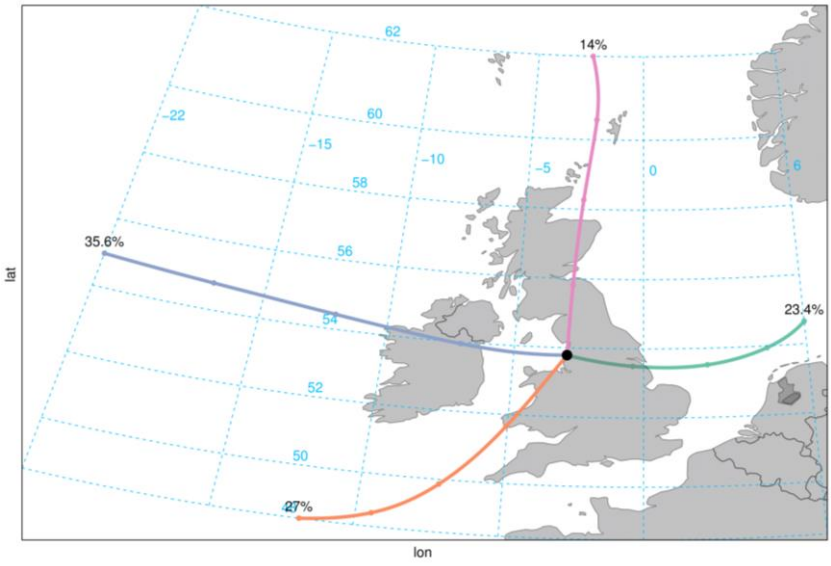

Figure 35. Mean path of 5-day back trajectories seen in Figure 15, ending at LP for each of the 4 principal airmass clusters. The percentage associated with each mean trajectory path defines the fraction of time (as fraction on 12 months in the baseline period) that airmasses arriving at LP are classified within each principal cluster defined in Figure 14

We can now examine the temporal patterns associated with measured concentrations within each of these principal clusters. The diurnal, weekly, and seasonal variability observed for each cluster can give additional clues as to the nature of sources and their proximity to the receptor site. Figure 36 shows this for methane. The top panel shows the mean diurnal pattern and statistical variability (at the 95% confidence level of sampled variability around the calculated mean) in methane concentration as a function of time of day (and day of week) for each cluster (represented as an average over the entire baseline period). When illustrated in this way, we can clearly observe very different diurnal behaviour for cluster 3 (the most elevated airmass) especially, relative to clusters 1, 2, and 4. In particular, we see a consistent and repeatable diurnal minimum at around midday on every day of the week across the whole year. This diurnal minimum on Cluster 3 is best observed in Figure 36 (bottom left), which shows the average over all days of the year. We also see a marked increase in late winter months for Cluster 3. This pattern is consistent with the ventilation of the local boundary layer, as the height of the planetary boundary layer is lifted by convection in daylight hours (enhanced in summer months relative to winter), further indicating a dominant role for local sources, which might be expected to accumulate overnight before being diluted and detrained in daytime. Clusters 1, 2 and 4 do not display such a minimum, suggestive of longer-range origins where the timescales of diurnal boundary-layer ventilation (24 hours) are shorter than the timescales of advection (many days) between regional and distant sources and the baseline receptor site.

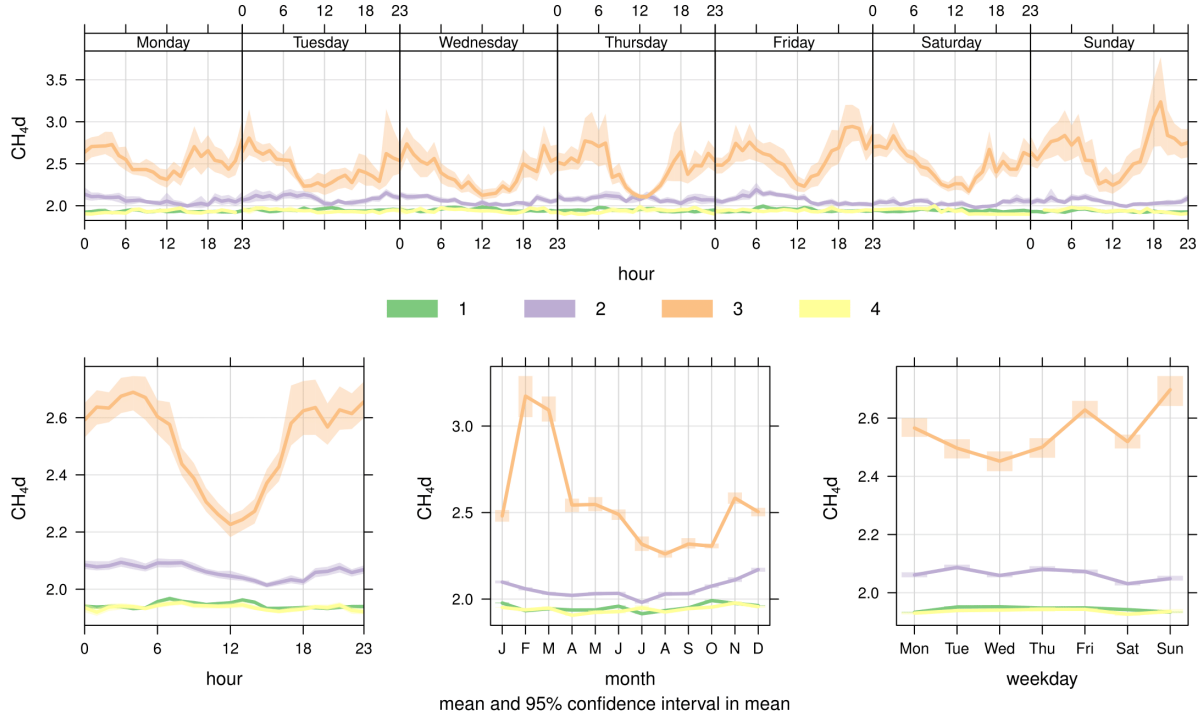

Figure 36. Temporal statistics of methane climatology at LP by time and day of week (top panel), time of day over all days (bottom left), month of year (bottom middle), and day of week (bottom right). © University of Manchester, 2017

We now examine Clusters 1 and 4 for methane in more detail. These clusters represent the background airmasses from the west and north and therefore might be expected to display a more seasonal pattern associated with biospheric respirational activity across the Northern Hemisphere. This is illustrated in

Figure 37. Same as Figure 36, but rescaled to illustrate temporal variability for less-enhanced clusters 1 and 4 for methane concentration patterns. © Univ Manchester, 2017

, which is essentially the same as Figure 36 but rescaled to illustrate the variability of methane concentration better for these (less enhanced) airmass clusters. Several salient features emerge: 1) that both clusters display a diurnal maximum at midday (the opposite of that seen in cluster 3); 2) that there is evidence for a mid-week maximum; and 3) that there is a summer minimum. Together, these features suggest that these clusters represent the northern hemispheric methane summertime minimum (as methane is oxidised by photochemistry), and that there may be a role for mid-week enhancements associated with long-range anthropogenic emissions (perhaps associated with intercontinental transport in westerlies from the United States). It should be noted that these much longer-range enhancements are very small (just 20 ppb peak-to-peak) relative to those in Cluster 3, which are up to 2 orders of magnitude (100 times) higher for more local sources.

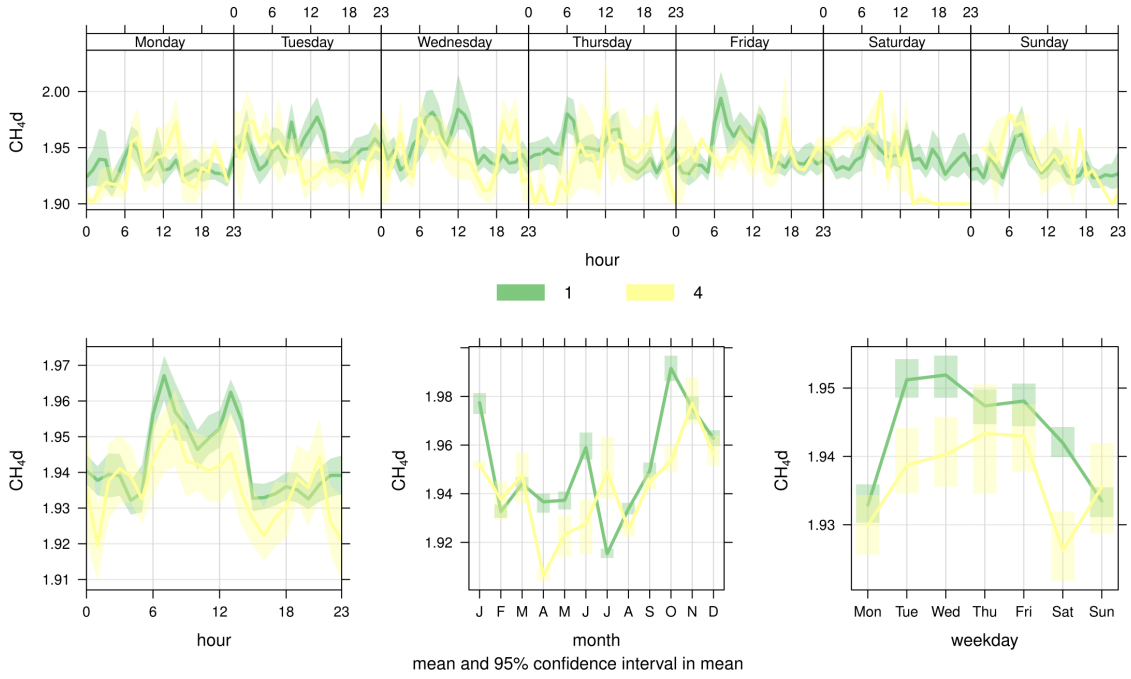

Figure 37. Same as Figure 36, but rescaled to illustrate temporal variability for less-enhanced clusters 1 and 4 for methane concentration patterns. © Univ Manchester, 2017

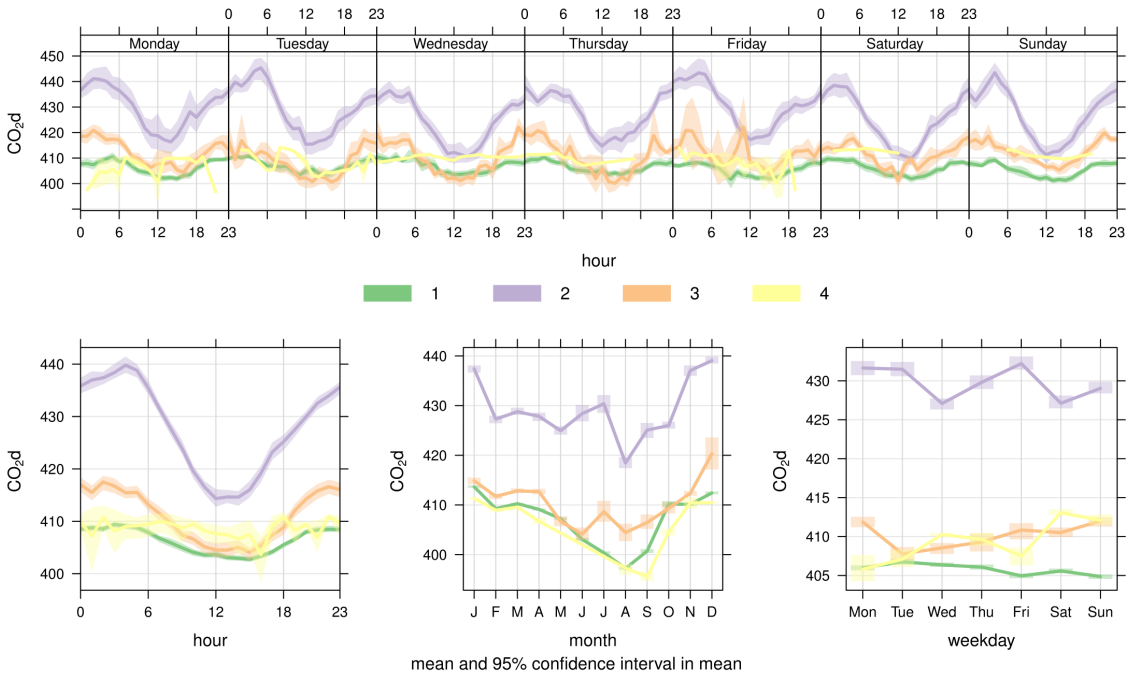

Figure 38. Temporal statistics of carbon dioxide climatology by time and day of week (top panel), time of day over all days (bottom left), month of year (bottom middle), and day of week (bottom right), averaged for the whole baseline period. © Univ Manchester 2017

we see similar diurnal patterns due to boundary layer ventilation (Fig 19 top panel) for all clusters except cluster 4, which represents the relatively clean northerly airmass type seen in Figure 33. The largest diurnal variability is seen for cluster 4, which represents the southerly airmass, linked earlier to local CO_2 emission sources and the nearby main road. However, unlike methane, a clear seasonal minimum is observed in August in all clusters. This feature is typical and expected to be due to the summer minimum in northern hemispheric CO_2 concentration due to biospheric respiration (uptake), which peaks in the summer months. This is seen for all clusters simply because the relative change in the seasonal background CO_2 concentration is significant when compared with the signal due to even very nearby CO_2 emission sources, unlike CH_4 (by virtue of the very small absolute mean global concentration of CH_4 around 2 ppm, which means that small mass fluxes of CH_4 can contribute a much greater relative signal on this much lower background). In the case of CO_2, clusters 1 and 4 represent more background (less elevated conditions) from westerly and northerly origins, respectively. These are shown in more detail in Figure 39. While clusters 1 and 4 are seen to have very similar seasonal trends, there are some marked differences, especially in the diurnal variability (Figure 39 bottom left) and when comparing weekday with weekend (Figure 39 bottom right). Cluster 4 (northerly and north-westerly origin) does not display a clear diurnal signal and also appears to peak on Saturdays and Sundays relative to weekdays. The lack of a diurnal signal is consistent with an absence of local sources for this cluster. However, the weekend peak is suggestive of something quite different. Often, weekend signals may indicate a change in human social behaviour (e.g. increased traffic flow to recreational destinations). This could indicate weekend traffic movements to the town of Blackpool, which is to the north west of the baseline site. However, we might expect this to manifest in a daytime (or rush hour) maximum, which is not observed. We may speculate that the night-time weekend economy of the Blackpool area may explain the lack of such a diurnal trend on weekend days. However, this may be at the risk of over-interpreting the data available. Moreover, clusters 1 and 4 for CO_2, like clusters 1 and 2 for methane, represent only small enhancements compared with their more elevated clusters and therefore such a signal is small compared with the role of more local emission sources.

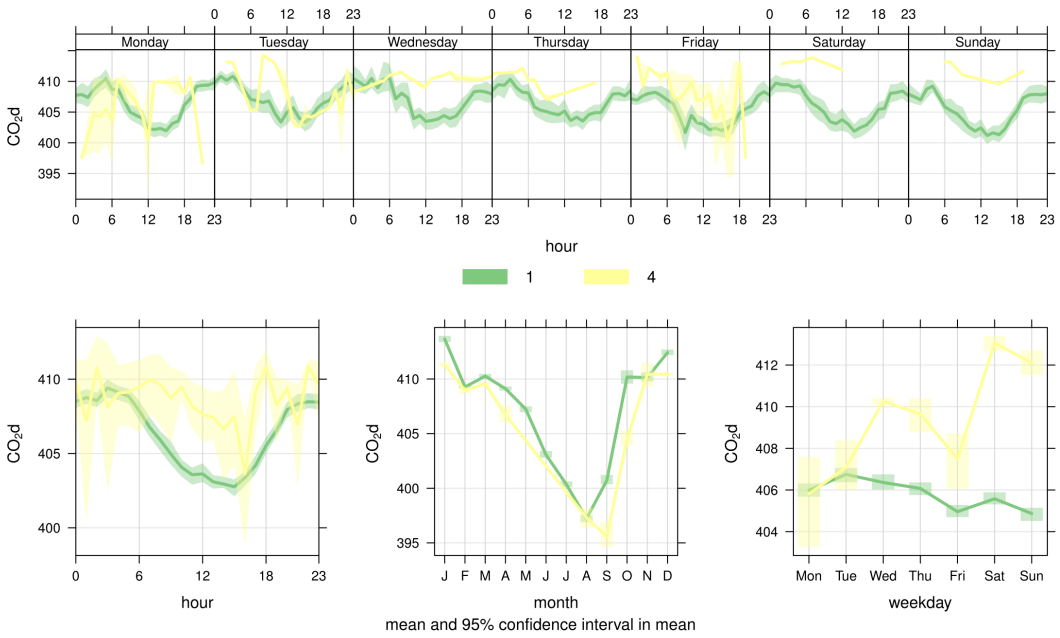

Figure 39. Same as Figure 38, but rescaled to illustrate temporal variability for less-enhanced clusters 1 and 4 for carbon dioxide concentration patterns. © University of Manchester, 2017

To investigate the nature of local methane emission sources (biogenic and anthropogenic) in cluster 3 in Figure 34**,** the results from the mobile vehicle surveys are discussed in the following Section.

4.7.2 Little Plumpton mobile vehicle surveys of methane emission sources

Maps of the area sampled by the mobile vehicle campaign in March 2016 can be seen in Figure 42 and Figure 43, colour-coded for sampled CH_4 concentration. The same, but for the July 2016 survey, can be seen in Figure 44 and Figure 45. The March campaign is summarised in the Figure 40 Keeling plot with individual source plumes identified by both surveys in Figure 41 a-f. A summary of the findings is given in Table 5.

The main persistent methane plume in the Fylde region is the landfill at Fleetwood, which was detected on all measurement days despite different wind directions and detected up to 3 km from source across the River Wyre estuary. Concentrations up to 2.5 times the atmospheric background level were recorded peripheral to site. This has a distinctive isotopic signature of -57 ‰ (Table 5), which is typical of all active landfills measured to date by the RHUL group. The Clifton restored landfill gave a signature of -55 ‰, within the range of -56 to -53 ‰ measured for other pre-gas extraction landfill cells. Composting at -52 ‰ and natural gas leaks at -41 ‰ were detected during the March Fylde campaign but not during the July campaign (Figure 44 and Figure 45).

Ruminant emissions (dairy cows) were measured during both campaigns. During March, these were mostly emissions from barns, which formed sharp but narrow (<50 m wide) plumes with excess more than 50% above background. During July the cows were dispersed across fields, resulting in broad (>100 m wide) plumes with excess less than 20% above background. When the cows are in barns, the isotopic signature represents a mixture of emissions from breath and slurry (-60 ‰), whereas the breath source is much more predominant when the cows are in the fields and the waste liquids are partly absorbed by the ground (-64 ‰). Two cow barns emitting methane are close to the proposed well pad, at Plumpton Hall and Moss House. In July, outside of milking time, these cows were dispersed throughout neighbouring fields. The strong inversion on the morning of July 28 resulted in background methane at 2.2 ppm (Figure 45), which dispersed only after 11:00 am. Background samples were collected throughout this period, and a

resulting Keeling plot for these suggests that the mixed source emissions entering Fylde from the south have a signal of -61 ‰ indicating dominance of ruminant and landfill emissions.

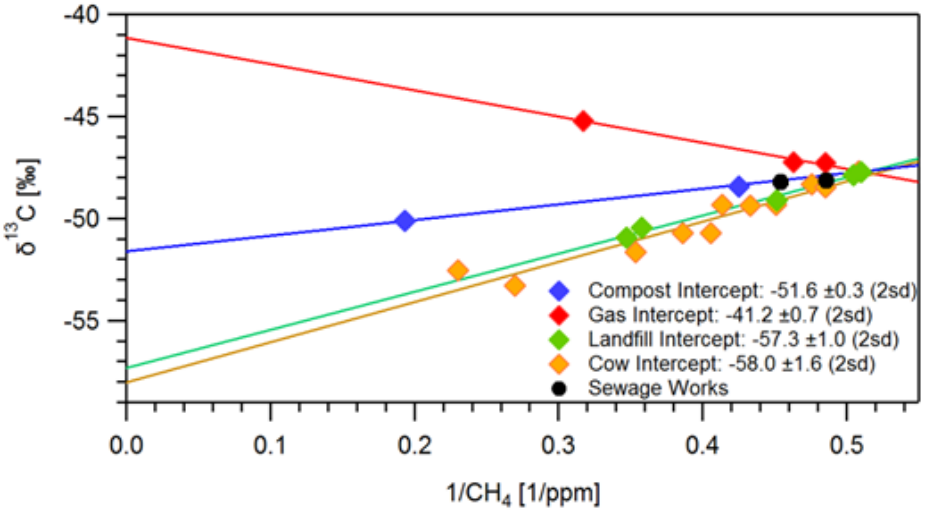

Figure 40. Summary Keeling plots of 1/CH_4 ppm vs measured $\delta^{13}C$ for all major methane sources located during the March 2016 campaign, highlighting the difference in line slope. © Royal Holloway Univ London, 2017

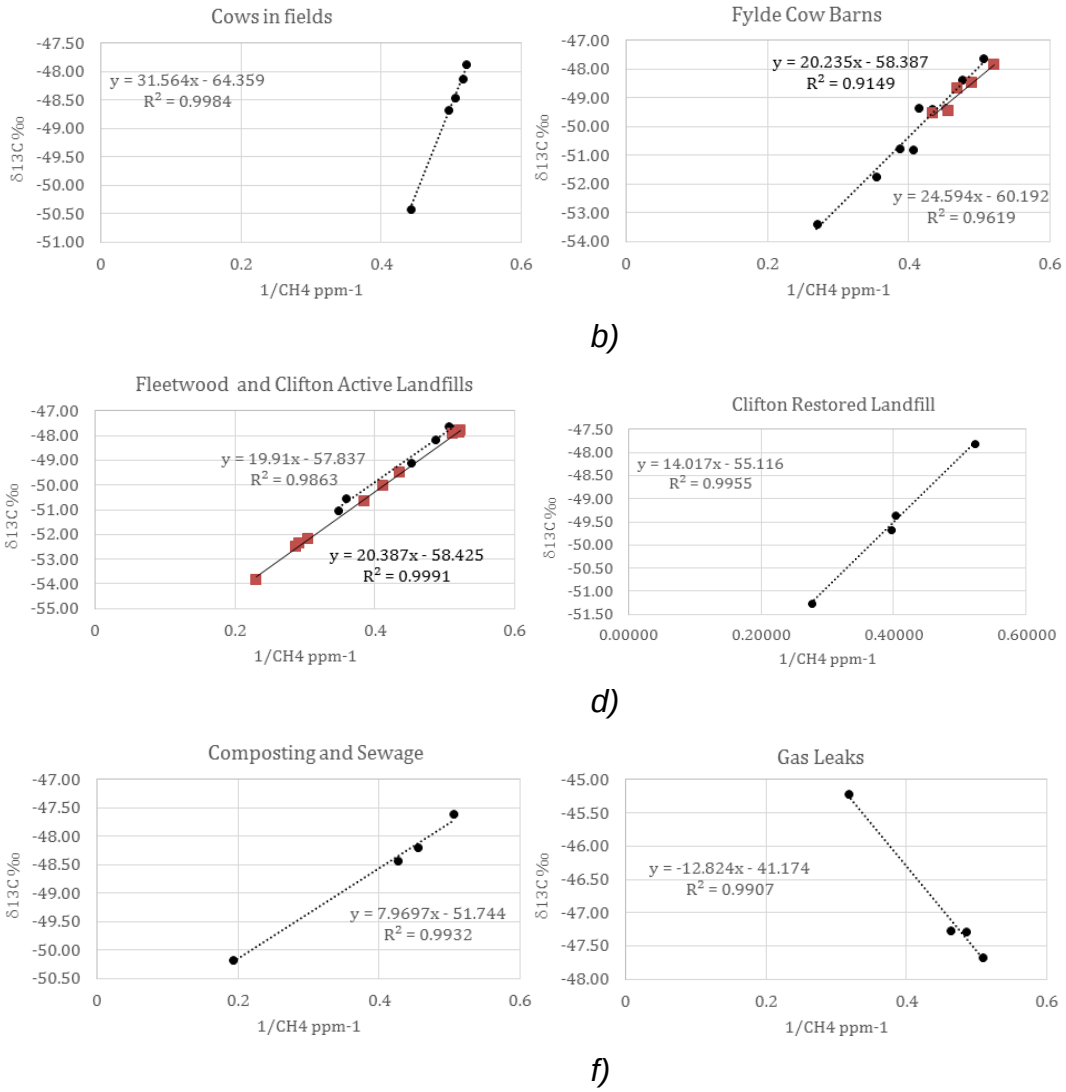

Figure 41. Keeling plots of 1/CH_4 ppm vs measured carbon-13 for each major methane source identified in the Fylde region in March and July 2016: a) Cows in fields, b) Cows in

barns, c) Active landfills, d) Restored landfill, e) Composting and sewage, f) Gas leaks. Sources observed in both campaigns show March in Black and July in Red (where observed). © Royal Holloway Univ London, 2017

Table 5. Summary of bag sampling in the Fylde region. Source methane excess and carbon isotopic signatures identified from Keeling plot analysis

Source (bag samples)	Max. excess over background (ppm)	$\delta^{13}C$ signature (‰)
Gas Leaks	1.3	-41
Composting and sewage	3.3	-52
Restored landfill	1.7	-55
Active landfill	2.4	-58
Cow barns	2.4	-59
Cows in fields	0.4 (2.9 within 2m of a cow)	-64 (-70)

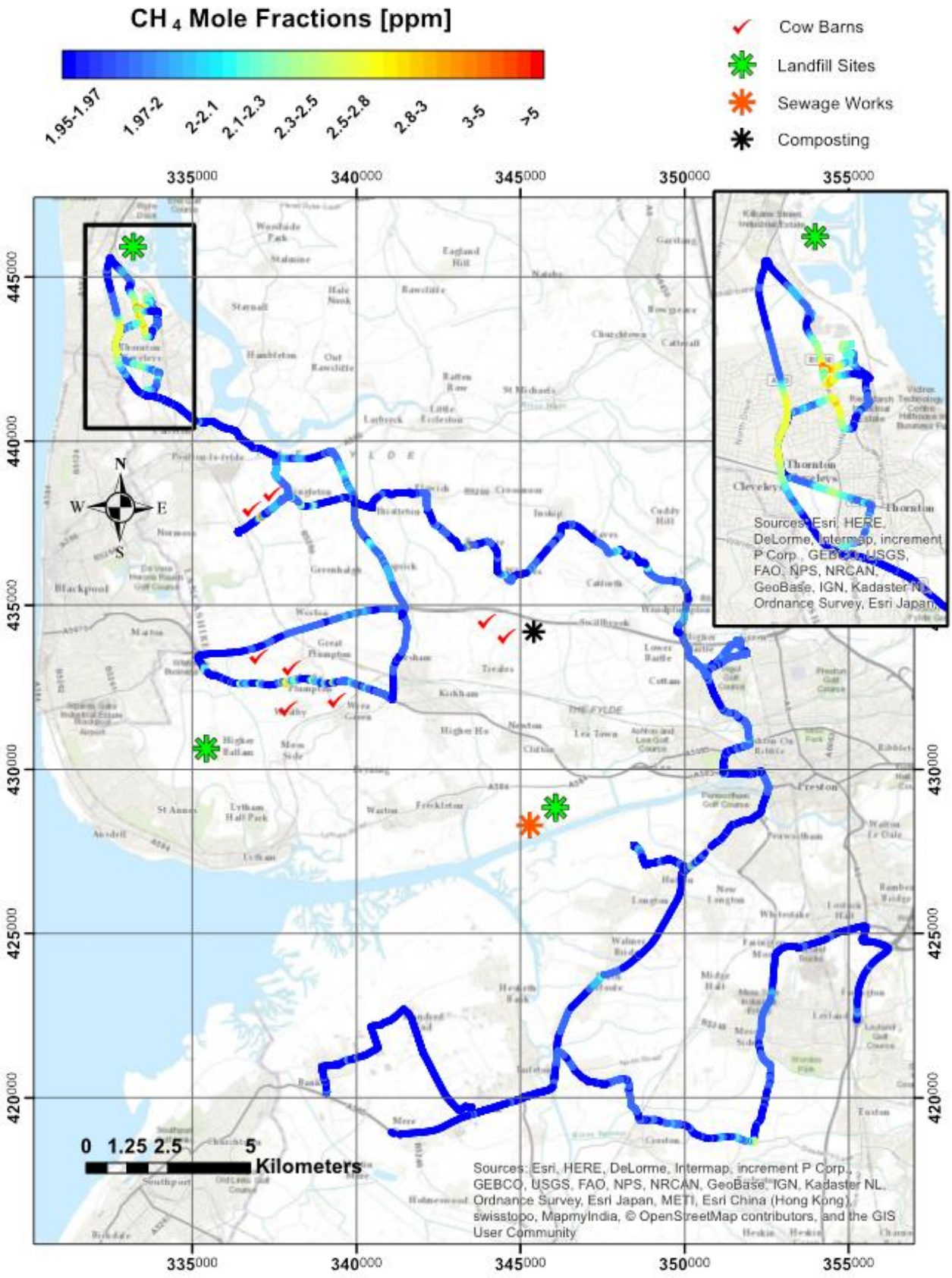

Figure 42. Survey route for March 9 2016, starting at Charnock Richard services. The largest methane plume observed was emanating from the Jamieson landfill at Fleetwood. © Crown Copyright and/or database right 2018. Licence number 100021290 EUL. © Royal Holloway Univ London, 2017

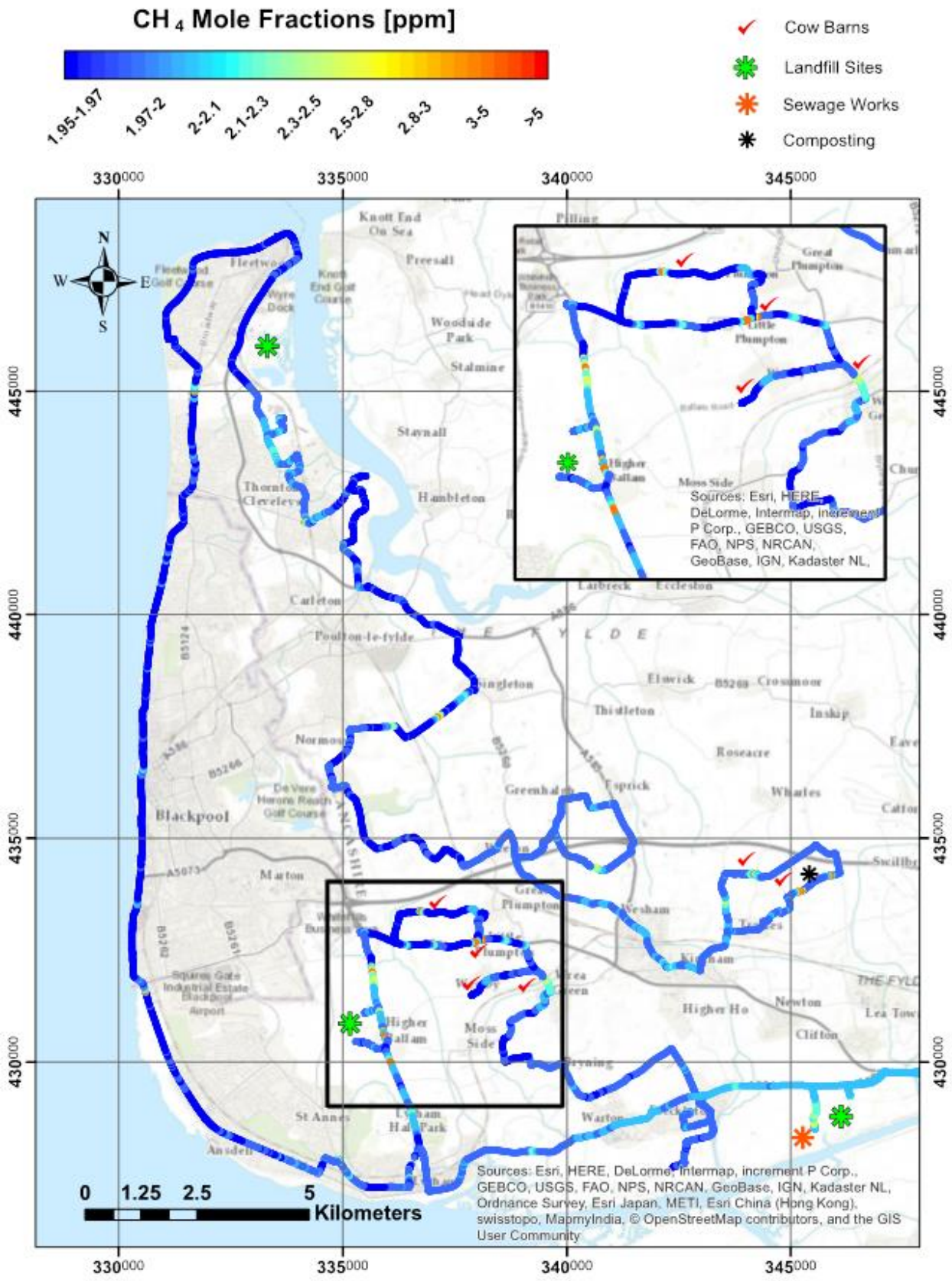

Figure 43. Survey route for 10 March 2016, ending in Preston. The largest methane plumes observed were from gas leaks and cow barns (see inset). © Crown Copyright and/or database right 2018. Licence number 100021290 EUL. © Royal Holloway Univ London, 2017

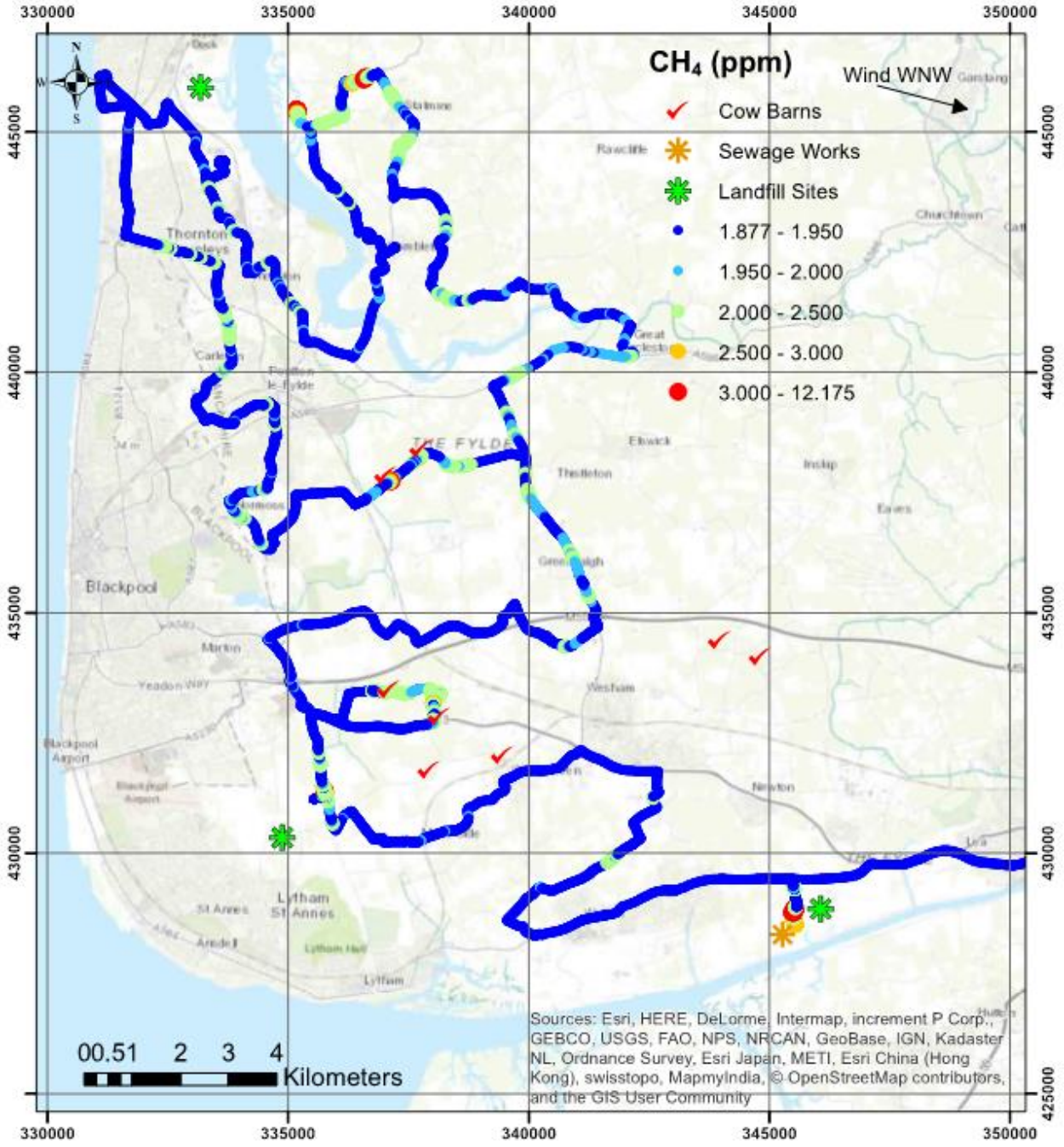

Figure 44. Survey route for 27 July 2016, starting in Preston. The largest methane plumes observed were from landfill and cows. © Crown Copyright and/or database right 2018. Licence number 100021290 EUL. © Royal Holloway Univ London, 2017

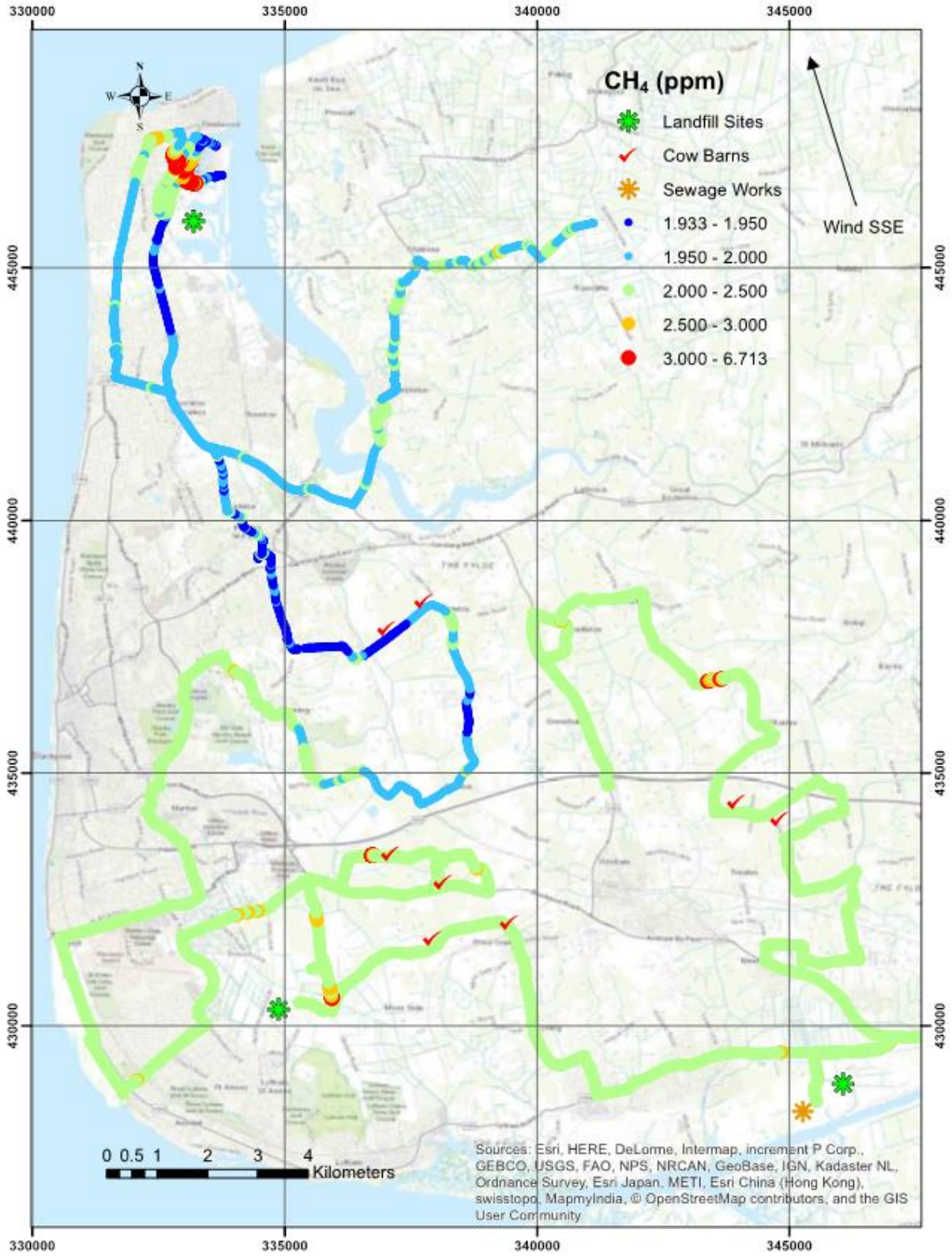

Figure 45. Survey route for 28 July 2016, starting in Kirkham. The largest methane plumes observed were from landfill and cows. A well-developed inversion resulted in a high methane background until late morning as shown by the green colours along the route track. © Crown Copyright and/or database right 2018. Licence number 100021290 EUL. © Royal Holloway Univ London, 2017

4.7.3 Summary

The summary features of the greenhouse gas baseline at LP can be defined broadly as follows.

- There are clear periods of what can be defined as a "background" (accounting for 50% of the period) - where CO_2 and CH_4 concentrations appear relatively flat at around 400 parts per million (ppm) and 2 ppm, respectively (Figure 23). These periods coincide with times of westerly winds seen in Figure 24 and Figure 25, and as the orange and red colours in the times series of Figure 26 and Figure 27. They represent a typical seasonally-variant Northern Hemispheric average concentration.
- There are prolonged periods (several consecutive days) of marginally enhanced CO_2 and CH_4 (between 400-450 ppm and 2-4 ppm, respectively. These periods coincide most often with moderate south-easterly winds as seen in Figure 24 and Figure 25, when comparing with Figure 26 and Figure 27 (where green and yellow colours indicated easterly and south-easterly wind directions). These features are consistent with an interpretation that these episodes represent regional pollution inputs from cities to the south and east such as Manchester, and the cities of Central and Southern England.
- There are short-lived (less than a few hours) but large enhancements (often referred to as "spikes") in the time-series data (greater than 4 ppm CH_4 and 500 ppm CO_2). These coincide most often with light easterly and south-easterly and northerly wind directions seen in Figure 24 and Figure 25, compared with Figure 26 and Figure 27 (where easterly winds are seen in green colours). These features in the data, often superimposed on the regional increment described above, are expected to represent local (<10 km upwind) sources such as nearby agricultural activities, roads, and landfill.
- For most of the time (>90% of the period), CO_2 and CH_4 display common patterns, in that both gases are often seen at their respective background concentrations, or are mutually enhanced with a scalable linear relationship (as shown in Figure 28).

The climatological annualised GHG statistics for the LP site are shown in Table 6. The mean concentrations of CO_2 and CH_4 are slightly elevated (4.5% in the case of CO_2, and 18.4% for CH_4) compared with the Northern Hemispheric tropospheric average for 2016 (~400 ppm and ~1850 ppb, respectively). This is expected due to the position of LP on land and exposed to sources of emission both locally and regionally. The one-standard-deviation variability around the mean is large (4.8% for CO_2 and 29.5% for CH_4), reflecting the variable airmasses that impact the site. The higher CH_4 variability is suggested to be linked to the nature of local sources (such as agriculture and landfill identified in the mobile surveys discussed in Section 4.7.2). The interquartile and interdecile ranges for both gases are constrained to 6.5% for CO_2 and 17% for CH_4 relative to the mean, while the extremes (99th percentiles), extend to 16% and 215% of the mean for CO_2 and CH_4, respectively. This demonstrates that for the vast majority of the period (80%), concentrations do not vary by more than ~20% at most). However, shorter-period, extreme events (accounting for 1% of the baseline period), can see concentrations of CH_4 double that of the mean climatological concentration. Such periods are identified with episodic local emissions, lasting for a few hours at most.

In all cases, it must be stressed that the levels of greenhouse gas concentrations seen at this site do not represent any known hazard to human health and are well within the typical range seen for any land-based measurement site. Even the largest transient enhancements seen in the collected dataset are in what would be considered to be a normal modern range and the conclusions drawn in this report on the existing sources of local pollution in our opinion do not represent any cause for local concern.

The statistics defined in the baseline period can be used in the following ways when comparing to analogous datasets collected in the future or during periods of new localised activity:

- The background (hemispheric average concentrations) seen in airmasses associated with westerly and south-westerly origins lend themselves optimally to assessment of any

incremental signal due to hydraulic fracturing in Little Plumpton. This is because the location of the baseline site directly to the east of the field where Cuadrilla holds an exploratory licence, which means that any significant fugitive emission should be readily observable against the otherwise very flat and clean signal seen for this wind direction in the baseline dataset. This will allow future work to positively identify (but not quantify mass flux for) the source of emissions on site as a function of time, linking such emissions (should they exist) to site activity and phases of production.

- The observed statistics concerning pre-existing sources of nearby and regional pollution allow any shale-gas-linked emission (in future, should analogous data be collected for comparison) to be compared numerically with concentration statistics in the baseline for other (more elevated pre-existing) wind directions and emission source origins. This allows for a contextual comparison - where any localised elevations due to shale gas can be quantified statistically, as a fraction of the contribution to atmospheric composition due to non-local emission sources.

To summarise, the purpose of this analysis was to establish the baseline climatology for the area to allow future comparative interpretation. In the context of greenhouse gases, this concerns the future quantification of greenhouse gas mass flux to atmosphere (fugitive emissions) from shale-gas operations.

Table 6. Summary climatological statistics evaluated over the baseline period for GHG concentrations measured at the baseline site at LP

	CO_2 (ppm)	CH_4 (ppb)
Mean	417.91	2191.04
Std Dev	20.17	646.10
Q0.1	387.21	1864.75
Q1	390.56	1893.93
Q10	397.75	1923.52
Q25	405.67	1942.68
Q50	412.04	2004.45
Q75	426.63	2202.35
Q90	444.25	2566.38
Q99	485.64	4730.81
Q99.9	542.37	9546.12

4.8 AIR QUALITY BASELINE

This section reports the Air Quality (AQ) baseline for the LP site. The statistical analysis of the AQ baseline dataset will be presented and interpreted in context of sources of emissions using meteorological data to aid analysis. The analysis provides information on the annual climatology of air pollution along with representative insight into shorter-term variability in air pollution. The baseline analysis is framed specifically with reference to the attainment of EC Directive air quality standards and this uses a range of metrics including annual, 1 hour and 8 hour means.

4.8.1 The baseline dataset

The dataset used in this report was from data collected for the first full year of monitoring (to 31 January 2017). The dataset includes local meteorology (2 m above ground), nitrogen oxides (NO and NO_2, collectively NO_x), particulate matter in a number of aerodynamic size ranges (PM), ozone (O_3) and speciated non methane hydrocarbons (NMHCs). The data are archived and publicly-accessible at the NERC Centre for Environmental Data Analysis (CEDA) at 1-minute intervals, except NMHCs, which are reported as weekly values. Data are available via the following link: http://browse.ceda.ac.uk/browse/badc/env-baseline.

The environmental baseline is examined and then compared with other similar regional UK monitoring sites operated by Defra and other agencies.

4.8.2 Results and discussion

Managing and improving air quality in the UK is driven by European (EU) legislation on ambient air-quality standards and also commitments to limit transboundary emissions, through the National Emissions Ceiling Directive and the Gothenburg Protocol. The 2008 Ambient Air Quality Directive (2008/50/EC) sets legally binding limits for outdoor air pollutants that impact on human health, and includes NO_2, O_3, benzene, 1,3 butadiene, PM_{10} and $PM_{2.5}$. All these species have been measured as part of the baseline project.

Within the UK, ambient air quality is controlled with the aspiration that all locations meet either the prescribed Limit Values or Target Values depending on the species. EU Limit Values are legally binding concentrations that must not be exceeded. There are prescribed averaging times associated with each pollutant and for some, a number of exceedances are allowed in each year. Target values are meant to be attained where possible by taking all necessary measures not entailing disproportionate costs, often reflecting natural impacts on those pollutants that can lie outside of regulatory controls.

All EU directives are listed on http://ec.europa.eu/environment/air/quality/standards.htm.

The national air-quality objectives for data parameters measured as part of the AQ baseline are shown in Table 7.

Table 7. Air Quality EU directives for parameters measured at the baseline sites.
[a]Conversion based on EC conversion (temperature 20 °C and pressure 1013 mb)

Pollutant	Concentration	Averaging period	Legal nature	Permitted exceedances	Approx conversion to ppb[a]
Fine particles	25 µg/m^3	1 year	Limit value	none	n/a
Nitrogen dioxide	200 µg/m^3	1 hour	Limit value	18	104.7 ppb

(NO_2)	40 μg/m^3	1 year	Limit value	none	20.9 ppb
PM_{10}	50 μg/m^3	24 hours	Limit value	35	n/a
	40 μg/m^3	1 year	Limit value	none	n/a
Benzene	5 μg/m^3	1 year	Limit value	none	1.88 ppb
Ozone	120 μg/m^3	Maximum daily 8 hour mean	Target value	25 days averaged over 3 years	60.1 ppb

4.8.2.1 SUMMARY STATISTICS OF ANNUAL MEANS OF AIR POLLUTANTS AT LP

Table 8 shows a summary of the annual means of various air pollutants at LP and a restatement of the annual directive limit value. An important immediate conclusion that can be drawn by the baseline study over the first year is that in terms of annual mean values, none of the monitored air pollutants exceeds annual mean Limit Values. For planning guidance, air-quality issues must be taken into account when ambient air pollution concentrations approach 75% of the Limit Values. No air pollutants at either site reach this threshold.

Table 8. Summary of annual statistics for LP for various air pollutants and comparison against annual mean limit values.

Pollutant	Annual mean at LP	Annual mean Limit value
Ozone	19.6 ± 10.1 ppb	60.1 ppb
$PM_{2.5}$	9.3 ± 7.8 μg/m^3	25 μg/m^3
PM_{10}	7.9 ± 8.9 μg/m^3	40 μg/$m^{3\pm}$
NO	2.5 ± 6.4 ppb	No limit value
NO_2	6.1 ± 6.6 ppb	20.9 ppb
NOx	8.9 ± 12.1 ppb	No limit value
Benzene	0.2 ± 0.01 ppb	1.88 ppb

Thresholds with short-term mean values exist for some pollutants. These are listed in Table 9, along with the amount of times these values were exceeded. A threshold value of 75 % was used when calculating all exceedances.

Table 9. Summary of statistics for LP short-term mean values for various air pollutants and comparison against short-term mean limit values, where these apply

Pollutant	Number of 8-hours exceedances LP	8-hour limit
Ozone	1 (25 allowed per year, averaged over 3 years)	60.1 ppb
	Number of 24-hours exceedances LP	24 hour limit
PM_{10}	0	50 $\mu g/m^3$
	Number of 1-hours exceedances LP	
NO_2	0	200 $\mu g/m^3$

The O_3 exceedance in July 2106 was when temperatures in the UK were high, resulting in photochemical production of O_3.

4.8.2.2 LITTLE PLUMPTON DETAILED ANALYSIS

Metrics

Table 10 reports metrics by individual wind sector. As is common in the UK, easterly and south-easterly air masses are often the most polluted since these bring air from south-east England and continental Europe. The lowest concentrations of air pollutants are typically observed during periods of westerly airflow. The LP site also has the influence of the major road to the south and its influence can be clearly seen in the NO_x and PM measurements from those wind sectors.

Table 10. LP metrics by wind sector

	N	NE	E	SE	S	SW	W	NW
O_3 (ppb)	22.4	20.2	18.3	13.2	13.8	19.8	23.8	24.7
NO (ppb)	1.2	1.6	2.6	5.3	4.6	2.2	0.7	0.8
NO_2 (ppb)	3.6	4.9	4.0	12.1	10.4	5.4	2.3	2.4
NO_x (ppb)	4.9	6.5	5.1	18.1	15.7	8.0	3.1	3.1
$PM_{2.5}$ ($\mu m/m^3$)	4.8	5.5	10.5	13.8	10.6	5.8	5.4	4.8
PM_{10} ($\mu m/m^3$)	7.9	10.0	17.9	18.0	13.8	9.6	9.7	8.6

Diurnal variation of air pollution (Figure 46)

The O_3 diurnal concentration is lowest at night and peaks just after midday, as expected in the general context of UK oxidative air chemistry; this is a combination of boundary-layer height and photochemical production during the day and surface loss at night.

Both NO_x and PM display similar diurnal cycles. The fact that these are similar in shape is an indication that they have similar sources. The diurnal variation is heavily influenced by road traffic. The NO_x diurnal shows NO and NO_2 increasing in the morning, which is probably due to the boundary-layer height and local traffic sources. The mid-afternoon peak relates to the effect of the late afternoon/evening rush hour.

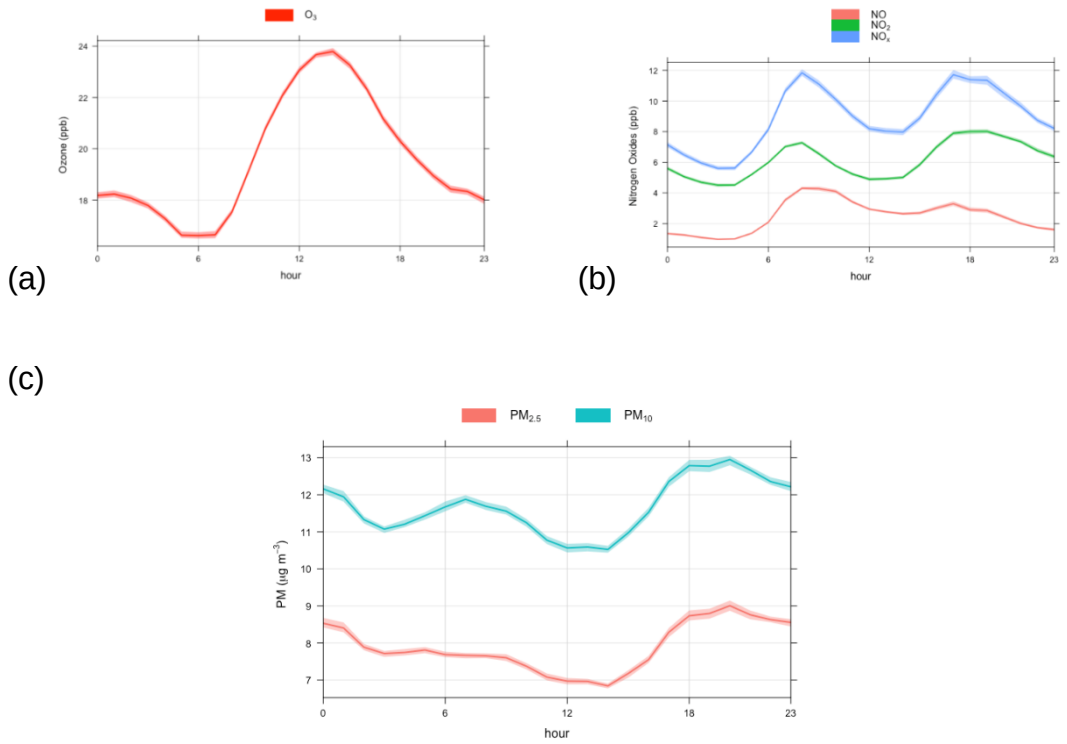

Figure 46. Diurnal variations at LP for (a) O_3 (b) NO_x and (c) PM. © Univ York, NCAS, 2017

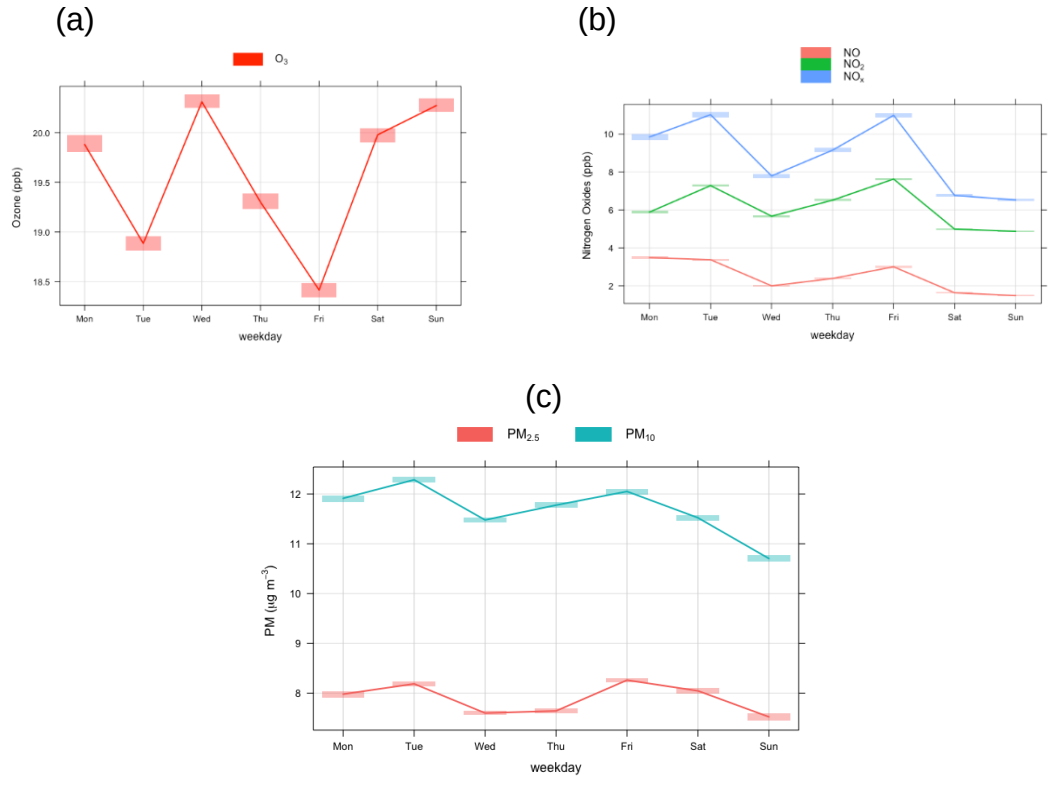

Figure 47. Hebdomadal cycles for at LP for (a) O_3, (b) NO_x and (c) PM. © Univ York, NCAS, 2017

Hebdominal variation of air pollution (Figure 47)

The working week (Mon–Fri) is clear in the O_3 and NO_x measurements, with NOx being highest during the week and decreasing at the weekend. By contrast, O_3 is highest at the weekend due to

reduced titration from NO. There is a slight anomaly mid-week when the NO_x appears to reduce. The reason for this difference is currently unclear.

Annual variation of air pollution (Figure 48)

These show typical cycles in the context of UK air quality. Annual cycles for the in-situ air quality parameters are shown in Figure 48. As in previous plots, the NO_x and PM show similar cycles; the influence of Preston New Road is seen in the results.

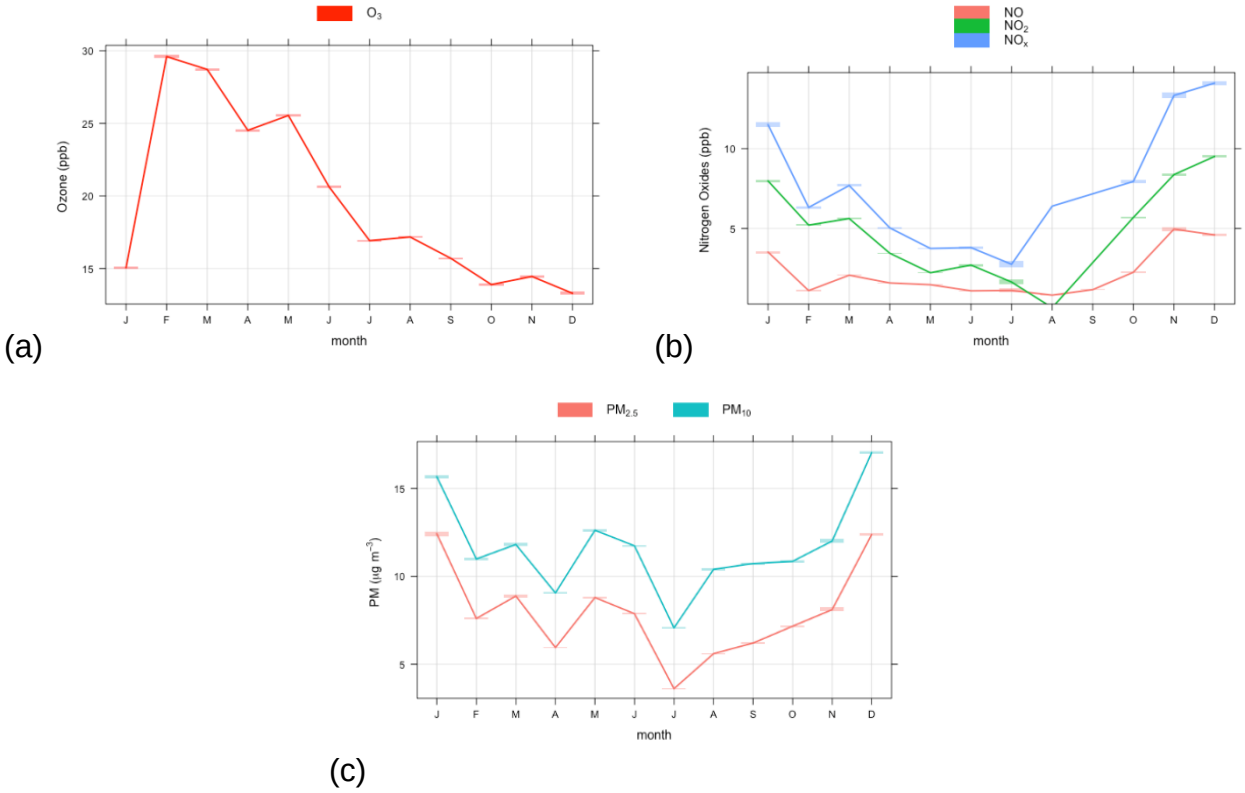

Figure 48. Annual cycles at LP for (a) O_3, (b) NO_x and (c) PM. © Univ York, NCAS, 2017

Source apportionment

Figure 49 shows percentile roses for the in-situ air quality parameters split by season. A percentile rose places the data into 5 bands (the colour-scale) and then plots each by wind direction (radial axis) and concentration. The grey line is the mean for the data set. The plots are separated into season: Spring (March, April, May), Summer (June, July, August), Autumn (September, October, November) and winter (December, January, February).

Figure 50 shows polar plots for the same pollutants, with concentrations (colour scale), wind direction (radial scale) and wind speed.

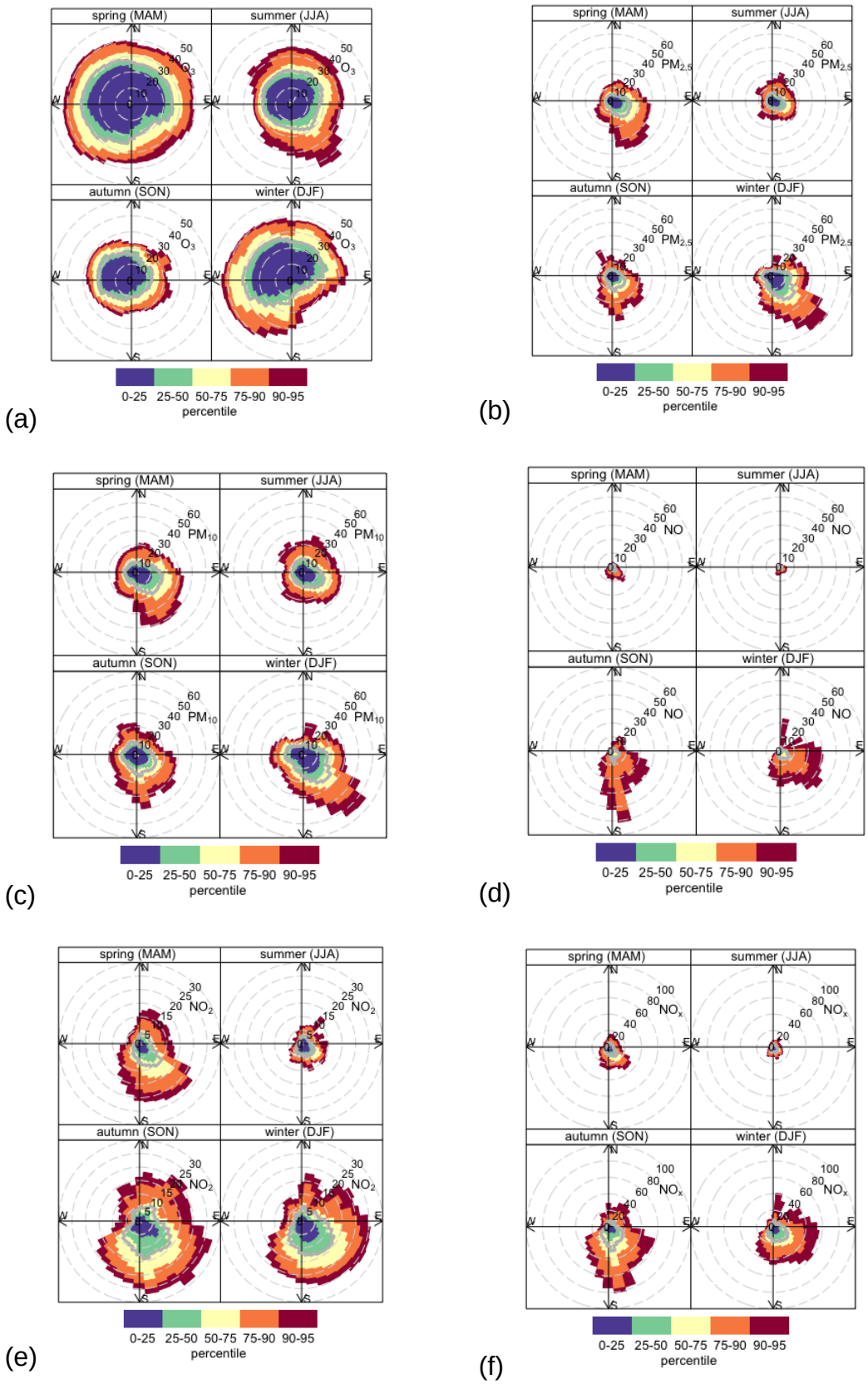

Figure 49. Percentile rose to show the 5th, and 95th percentiles for (a) O_3, (b) $PM_{2.5}$,(c) PM_{10}, (d) NO, (e) NO_2, (f) NO_X at LP, limited data is available for Summer 2016 due to instrument failure. © Univ York, NCAS, 2017

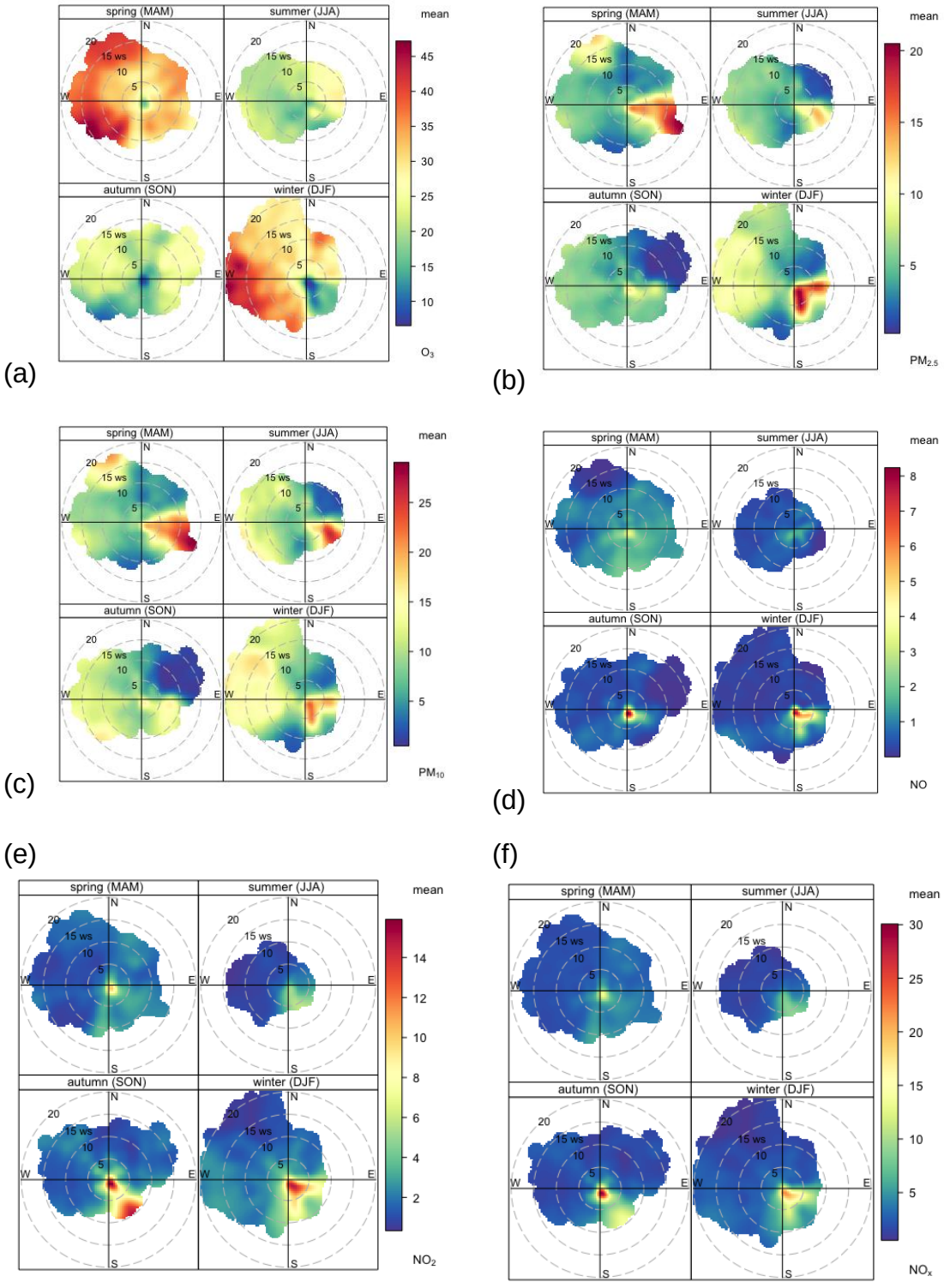

Figure 50. Polar plots for LP (a) O_3, (b) $PM_{2.5}$,(c) PM_{10}, (d) NO, (e) NO_2, (f) NO_X, limited data is available for Summer 2016 due to instrument failure. © Univ York, NCAS, 2017

We experienced instrument problems during Summer 2016 and so the NO, NO_2 and NO_x measurements are not continuous.

Ozone (O_3) concentrations are highest concentrations in the spring, arising when the wind speed is at its highest and from the west. This is likely due to peak of the Northern Hemispheric and North Atlantic O_3 and the impact of efficient long-range transport of this air to each site. Elevated O_3 is indicative of an aged air mass as it is not a primary emission but produced

through chemical reactions in the air mass. It is observed easily at the LP site due to its position on the west and clean background air observed from the west. The influence of the Atlantic Air is also shown in the PM measurements, which are all enhanced in the higher-wind-speed westerly air masses, particularly in the coarser fraction arising from maritime aerosols.

Local influence is also seen with the less frequent winds from the south and the east bringing a mix of locally and regionally polluted air masses to site. The major trunk road running alongside the site has been mentioned previously and is the source of local NO_x and PM.

4.8.2.3 NON METHANE HYDROCARBONS

Non methane hydrocarbon (NMHC) samples have been taken weekly at the site. A summary of NMHC for LP is shown in Table 11. NMHCs are able to give an indication of air-mass origin, in areas of oil and gas production, higher lighter alkanes such as ethane and propane may be due to fugitive emissions.

Table 11. Summary of NMHC measurements at KM, N =34. All NMHC have an uncertainty of <10 %

Hydrocarbon	Annual mean(ppb)	Minimum Value (ppb)	Maximum Value (ppb)
Ethane	2.75	0.77	12.59
Ethene	0.69	0.15	2.93
Propane	1.17	0.16	5.99
Propene	0.17	0.03	0.85
Isobutane	0.36	0.03	2.03
Nbutane	0.94	LOD	5.94
Isopentane	0.28	LOD	1.13
Npentane	0.21	LOD	0.95
Benzene	0.19	0.02	0.41
Toluene	0.32	LOD	3.65

The only NMHC currently regulated is benzene and the annual mean benzene concentration is well below the Limit Value for the UK at both sites.

4.8.3 Summary

The atmospheric composition work package has shown the importance of establishing a baseline before any future activities in a region. From an air-quality perspective, it is essential that this baseline cover at least a whole year. This is highlighted not only in the O_3 measurements which have a photochemical dependence, but also the PM measurements which show strong seasonal differences. The dataset also highlights the need for continuous measurements where possible to enable a full analysis of sources in the region.

5 Seismicity

5.1 BACKGROUND

The primary aim of the seismicity work package is to deploy a network of seismic sensors to monitor background seismic activity in the vicinity of proposed shale-gas exploration and production in the Fylde, Lancashire. The data collected will allow reliable characterisation of baseline levels of natural seismic activity in the region. This will facilitate discrimination between any natural seismicity and induced seismicity related to future shale-gas exploration and production. A further aim is to make recommendations for a suitable traffic-light system to mitigate earthquake risk. The initial design requirement for the seismic monitoring network was reliable detection and location of earthquakes with magnitudes of 0.5 and above in the area of two potential sites for shale gas exploration at Preston New Road and Roseacre Wood.

5.2 NETWORK PERFORMANCE

The seismic monitoring network consists of six near-surface sensors (red squares in Figure 51). We also receive real-time data from 4 stations installed and operated by Liverpool University. The latter were installed independent of this project and data from these is not guaranteed.

Continuous data are transmitted in near real-time to the BGS office in Edinburgh, where the data are processed and archived. The completeness of these data can be checked easily to gain an accurate picture of network performance. The completeness levels are shown in Figure 52.

All BGS stations show high levels of data completeness for the time period 1/4/2017 to 30 /6/2017, with over 96% available from all stations except AQ10, installed in May 2017.

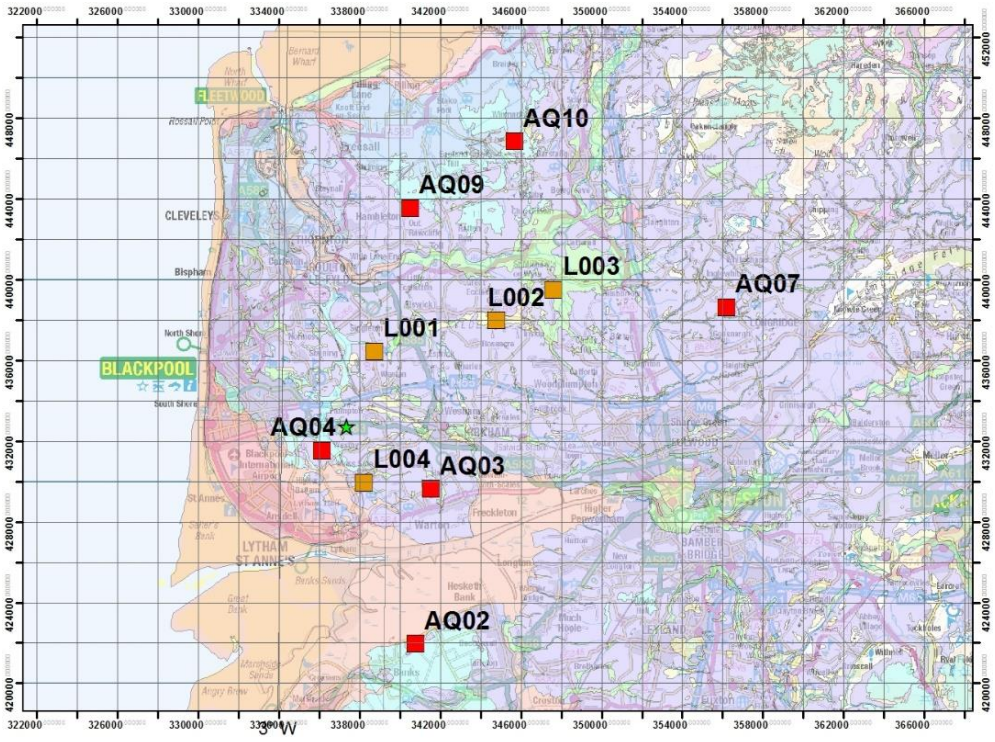

Figure 51. Ordnance Survey map of the Fylde peninsula overlain by superficial geology. Red squares show UK array sensors and the orange squares show the locations of Liverpool University sensors. The green star shows the location of the site of possible hydraulic fracturing at Preston New Road. © Crown Copyright and/or database right 2018. Licence number 100021290 EUL

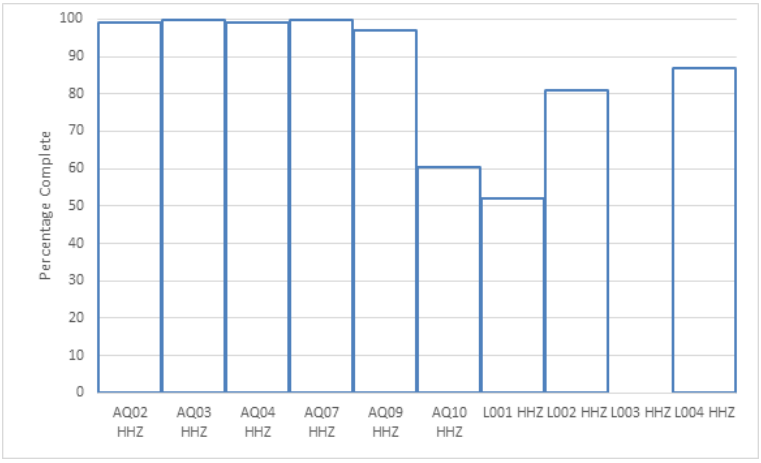

Figure 52. Data completeness for the stations on the Fylde Peninsula 1/4/2017 to 30/6/2017; AQ10 was installed on 4/5/2017.

The Liverpool stations show significantly lower levels of completeness.

The level of data completeness is an improvement on the values between 1/4/2016 and 31/3/2017. A value of over 95% is extremely good for data transmitted in near real-time using mobile phone networks and is better than many of the BGS permanent monitoring stations that use similar technology. Data losses result from failure of outstation hardware, communications problems, or failure of central data processing. The data acquisition is able to recover from short breaks in communications links to outstations by re-requesting missing packets of data from local data buffers, but failure of outstation hardware requires intervention by local operators or maintenance visits. No maintenance trips were required in the period 1/4/2017 to 30/6/2017.

5.3 STATION NOISE AND PERFORMANCE

We use power spectral density (PSD), calculated from one-hour segments of continuous data, to characterize noise levels at a range of frequencies or periods for each of the stations. A statistical analysis of the PSDs yields probability density functions (PDFs) of the noise power for each of the frequency bands at each station. Figure 53

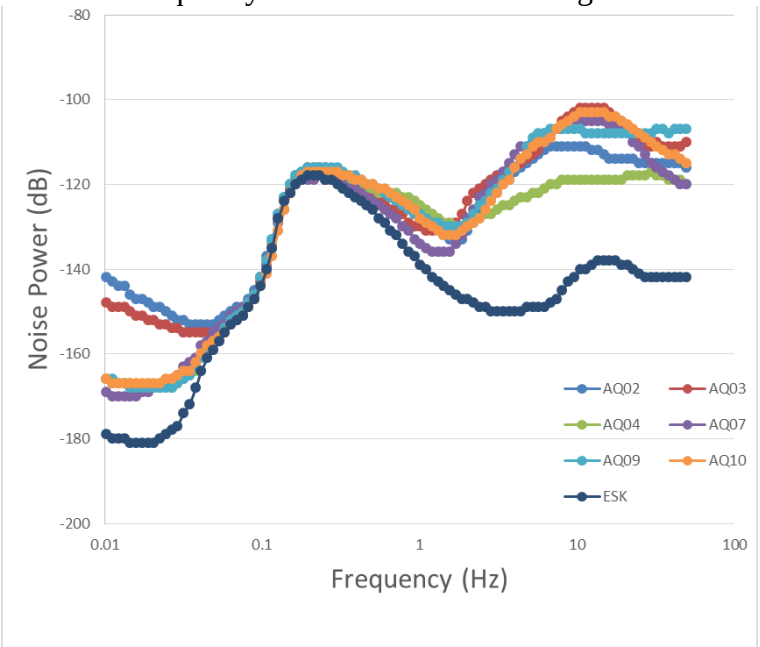

Figure 53 shows the median noise levels calculated at each BGS station. These stations are noisier than most other stations in the BGS network and noisier than those in the Vale of Pickering network. This is because the Fylde Peninsula is densely populated, with many sources

of cultural noise, while also having no bedrock near the surface. Rather, the near-surface geology comprises clays that are extremely poor transmitters of cultural noise. The permanent station ESK is given for comparison: this is one of the 'quieter' stations in the UK network. The only way to improve the signal-to-noise properties of this network would be to re-site some of the stations within boreholes.

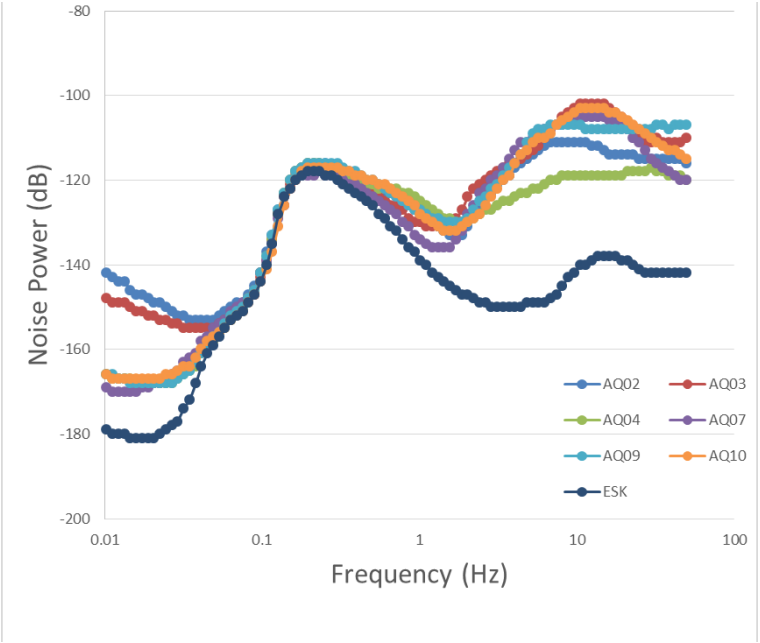

Figure 53. Median noise levels at all BGS stations on the Fylde Peninsula. ESK is a quiet national network station included for comparison.

Noise analysis has shown that:

- In general, all of the stations in Lancashire are noisier than those established in the Vale of Pickering, Yorkshire due to increased industrial noise and population density.
- There is a noticeable seasonal variation at all sites at low frequencies due to storm noise in the winter.
- The most prominent and pertinent feature for this study is the diurnal difference which is observed in both summer and winter. The day-time anthropogenic noise in the high-frequency range (5–45 Hz) can cause an increase in the mode of the station noise of over 20 dB at some sites, although it is more generally between 8 and 15 dB variation. This increase in the noise level could cause problems for the detection of small events since they will fall within this frequency range.

5.4 DATA PROCESSING AND ANALYSIS

Continuous data from all stations are transmitted in real-time to the BGS offices in Edinburgh and have been incorporated in the data acquisition and processing workflows used for the permanent UK network of real-time seismic stations. A simple detection algorithm is applied to the data from the Fylde Peninsula stations to detect possible events. All detections are then reviewed by an experienced analyst. Apart from teleseisms, only one event was detected in the period from 1/4/2017 to 30/6/2017. This was a 1.7ML earthquake at Kents Bank in Cumbria, approximately 41 km north of the Preston New Road site.

5.5 DATA AVAILABILITY

Helicorder plots showing 24 hours of data from each station are available online and can be found on the BGS Earthquake Seismology Team web site at http://www.earthquakes.bgs.ac.uk/helicorder/heli.html.

5.6 REGIONAL SEISMICITY

Figure 54 shows recorded seismicity within a 100 km square centred on the Preston New Road site. The Fylde Peninsula is an area of low seismicity even for the UK. Apart from the seismicity related to hydraulic fracturing operations at Preese Hall in 2011, most of the nearby seismicity is offshore in the Irish Sea. For example, a magnitude 2.5 ML earthquake occurred 5 km south-west of Blackpool in 1970.

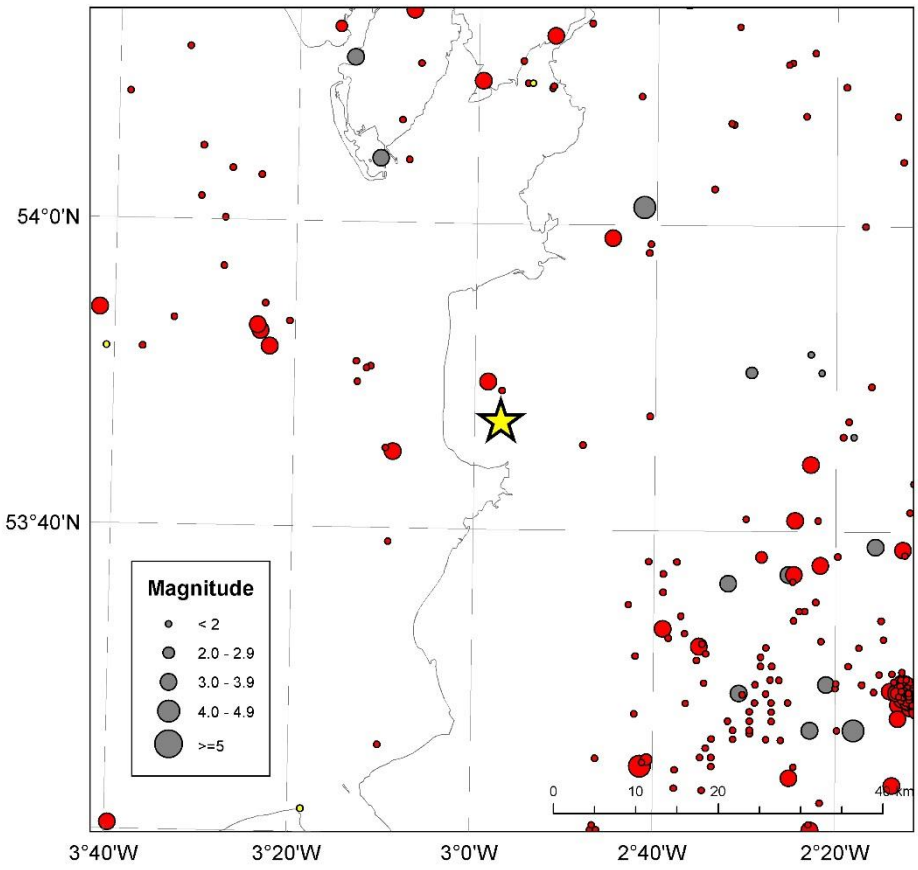

Figure 54. Recorded seismicity within a 100 km square centred on the Preston New Road site (yellow star). Grey circles show earthquakes prior to 1970. Red circles show earthquakes recorded between 1970 and 31/03/2017. Yellow circles show earthquakes from 1/4/2017.

A magnitude 3.3 ML earthquake was recorded in the Irish Sea on 25/08/2013 at 09:58, with an epicentre approximately 25 km west of Fleetwood, Lancashire. This event was preceded by a magnitude 2.5 ML foreshock in the same location at 05:37 and followed by a magnitude 2.8 ML aftershock on 31/08/2013. These were the largest earthquakes to have occurred in the Irish Sea since a series of three earthquakes, with magnitudes ranging from 3.8 to 5.0, on 16 and 17 March 1843.

BGS received over 60 reports from members of the public who felt the earthquake. Almost all of these came from inhabitants of the Lancashire coast at distances of up to 40 km from the epicentre.

The epicentres were immediately east of the Bains gas field, leading to speculation that these earthquakes could have been related to hydrocarbon production. However, the Bains field ceased

production in 2009, and although there is a long history of induced earthquakes related to gas extraction in places such as Groningen, The Netherlands, the historic earthquakes in the area show that natural seismicity predates any production.

A magnitude 0.9 ML earthquake in the Irish Sea was recorded on 5/4/2017. This was approximately 45 km west of the Preston New Road well site. It was not detected by the stations on the Fylde Peninsula.

The magnitude 3.7 Ulverston earthquake on 28 April 2009 was also felt in Lancashire. Historically, the largest earthquake in the region was a magnitude 4.4 earthquake near Lancaster in 1835 with a maximum intensity of 6 EMS.

6 Ground Motion

6.1 INTRODUCTION

There is speculation about whether the potential exists for shale-gas operations at depth to cause surface ground deformation. Conventional oil and gas operations have on rare occasions been shown to result in subsidence above compacting oil and gas reserves (Geertsma, 1973) and a recent study suggests that surface uplift in eastern Texas was due to fluid injection, which was distinguished using satellite remote sensing (Shirzaei et al., 2016). These studies do not imply that shale-gas operations at depth will cause ground motion. Nevertheless, undertaking objective and authoritative monitoring of the ground surface at operation sites and surrounding regions is advisable (a) to determine if there are any impacts on the ground surface and (b) to reassure the public that appropriate independent monitoring of all potential environmental impacts is being undertaken. Knowledge regarding the baseline ground motion conditions, compared with the current situation, would enable the provision of impartial and objective information on whether shale-gas operations have affected the status of the landscape.

Firstly, it is necessary to define 'ground motion' in the context of this baseline monitoring study. The first clarification is that the term does not refer to seismicity, which is the frequency, intensity and distribution of earthquakes (induced or otherwise) in an area. We use 'ground motion' to mean the motion of the surface of the landscape upwards (uplift), downwards (subsidence) or sideways (lateral motion). The motion is measured as the average velocity per year (in millimetres) along with profiles of motion at each point/pixel for each time period a measurement was captured. The measurements are derived by processing satellite radar data using the Interferometric Synthetic Radar (InSAR) technique, with the motion generally described in terms of Line of Sight (LOS) from the satellite or as absolute motion (vertical/ horizontal displacement). Satellite-based InSAR interrogates the differences in phase from a series of radar images to generate results of surface motion. The motion we measure does not take account of ground acceleration, i.e. peak ground acceleration (PGA).

The key monitoring question is whether shale-gas operations are altering the earth-surface processes and stress conditions that are operating at the site. We cannot assume that an area is stable prior to shale-gas operations. When considering a monitoring system, it is important to account for the dynamic nature of the earth's surface i.e. there may be some pre-existing displacement due to either natural or induced factors. Therefore, a baseline survey is vital to determine the pre-existing conditions of the site including displacement such as upwards motion (uplift), downwards motion (subsidence) or horizontal/lateral motion, and ongoing monitoring during any operations is required to characterise the current situation.

The investigation in this work package is designed to monitor surface ground motion (subsidence, uplift or stability) of the target area using LOS InSAR prior to any permitted unconventional gas production in Lancashire. InSAR is considered an appropriate technique for ground motion monitoring because:

a) archive radar data (acquired by satellites since 1992) are available and can be utilised to ascertain a baseline of motion (or lack of motion) prior to any permitted gas operations;
b) data from currently-orbiting satellites such as Sentinel-1 can be analysed to acquire information about the ongoing surface ground motion conditions in a region;
c) the analysis produces measurements over areas measuring up to thousands of square kilometres rather than at a point location, which other techniques such as GNSS provide.

InSAR can provide millimetric measurements of surface ground motion from satellite platforms such as ENVISAT, ERS1&2, RADARSAT, Sentinel-1A/B, TerraSAR-X and CosmoSKY-Med. The technology has been validated by the British Geological Survey (BGS) in projects such as

TerraFirma and was used by BGS in projects including PanGeo, SubCoast and EVOSS to develop and demonstrate viable services (e.g. Cigna et al., 2015; Jordan et al., 2017). InSAR has also been successfully used in CO_2 sequestration monitoring projects in locations such as In Salah where Mathieson et al. (2011) stated that "perhaps the most valuable, and initially surprising, monitoring method so far has been the use of satellite based Interferometric synthetic aperture radar (InSAR) to detect subtle ground deformation".

Table 12 provides a guide to the advantages and limitations of remote and in-situ systems for ground motion monitoring.

Table 12 Comparison of remote and in situ ground surface motion monitoring systems

Monitoring technique	Advantages	Limitations
InSAR	Measurements are made remotely (non-invasive) Measurements can be made using historic data to gain a baseline prior to operations. Imagery can cover a large area simultaneously. Entire deformation field can be imaged, rather than isolated points.	Conventional techniques have difficulty in vegetated areas. High magnitudes of motion (greater than the satellite detected phase difference) cannot be measured. Temporal and spatial resolution is limited by satellite set up and orbital parameters. Affected by steep topography (shown not be an issue in most of the UK).
GNSS	High precision. Does not require line of sight between benchmarks. Continuous site can operate without frequent human interaction.	Equipment can be stolen / vandalised / damaged. Sampling of deformation field is limited to individual points; several points are required. Requires at least 4 satellites in view simultaneously.
Tiltmeters	High precision. Does not require line of sight between benchmarks. Continuous site can operate without frequent human interaction.	Equipment can be stolen / vandalised / damaged. Sampling of deformation field is limited to individual points. Complex installation (e.g. in boreholes) – several tiltmeters are required.
Total Stations	High precision. Continuous sites can operate without frequent human interaction.	Requires line of sight between benchmarks. Generally they are operated manually, requiring repeat site visits to operate the system.

To date, the InSAR process has not been applied to monitoring energy operations in the UK because of the challenge of gaining coherence over non-urban areas. To resolve this challenge, we processed the data using the conventional SBAS (small baseline subset) process to gain precise results over urban areas and subsequently utilised the ISBAS (intermittent small baseline subset) process to acquire results over the non-urban areas (Cigna and Sowter, 2017).

BGS has experience of applying InSAR to several ground surface monitoring applications in the UK e.g. utilising 55 ERS-1/2 images between 1992 and 1999 to investigate ground motion linked to ceased mining operations in south Wales (Bateson et al., 2015). The deliverable in this ground motion work package is to provide "an analysis of satellite (InSAR) data". In order to achieve this, the following steps were followed:

- Obtain stacks of satellite SAR data;
- Process the data using the SBAS InSAR techniques, thereby deriving results primarily for urban areas;
- Process the data to ISBAS level, thereby extending the results to non-urban areas;
- Provide an analysis of the InSAR results.

The work package utilised the ISBAS technique of InSAR analysis as it has been found to provide results in non-urban areas where other InSAR techniques fail. The conventional SBAS technique requires that the target shows coherence in every image of the stack, while the ISBAS technique utilises coherence that is intermittent throughout the stack. Both SBAS and ISBAS processing and analysis was undertaken on each stack of radar images to provide results in urban and non-urban areas.

6.2 DATA SELECTION

This BGS-funded research project utilised archive radar images from the ERS-1/2 satellite for the period 1992–2000 (Table 13) to assess the efficacy of InSAR for ground motion monitoring as part of an integrated baseline monitoring programme. The stack of radar data consisted of 63 images that were analysed using SBAS and ISBAS InSAR techniques, i.e. two sets of analyses were undertaken and completed within this ground motion work package. Data from the ENVISAT and Sentinel satellites (covering the time period from 2007 to the present day) have not yet been utilised in this study.

Table 13. ERS-1/2 image metadata

Track	No. of scenes	Dates of image acquisition
T409	63	04/07/1992–11/07/2000

6.2.1 Ancillary data

A selection of ancillary datasets (listed below) were utilised in order to interpret the InSAR process i.e. to determine / understand the potential causes for the motion:

1. Bedrock geology (incl faults)
2. Surficial geology (incl. compressible ground)
3. Historic mining information/plans
4. Seismic records
5. Groundwater abstraction records
6. Borehole records
7. Geohazard information (e.g. landslides and shrink/swell)
8. Landcover information
9. Historic topographic maps

10. Aerial photography
11. Digital elevation models
12. Digital terrain models.

6.3 DATA PROCESSING

All of the InSAR processing was undertaken by the BGS Earth Observation Team. Our approach to acquiring, processing and interpreting the InSAR data is briefly outlined in this section. The methodology to effectively undertake the monitoring programme of ground-motion conditions using InSAR techniques is illustrated in Figure 55 with the associated actions listed below.

1. Search of catalogue satellite radar data to confirm that suitable stacks of images were available for the study area;
2. Download the stack of image datasets covering the geographic area and the time period(s) of interest;
3. Process the imagery for the region using SBAS and ISBAS InSAR technique(s);
4. Ensure that the outputs from the InSAR processing match the quality required e.g.:
    a. Suitable density of spatial coverage in the area of interest
    b. Suitable temporal coverage in the area of interest
    c. Assess output statistics to gauge if the results are fit-for-purpose;
5. Interpretation of the InSAR outputs. This is a key stage because the outputs from the InSAR image processing are dependent on the quality of the interpretation. There are two fundamental components;
    a. Ensure that interpretation is undertaken by sufficiently-experienced personnel. For shale gas applications the interpretation should be done by experienced geoscientists who compile and integrate a suite of geoscientific information
    b. The interpretation was reliant upon access to a comprehensive range of ancillary data, listed in the section above.

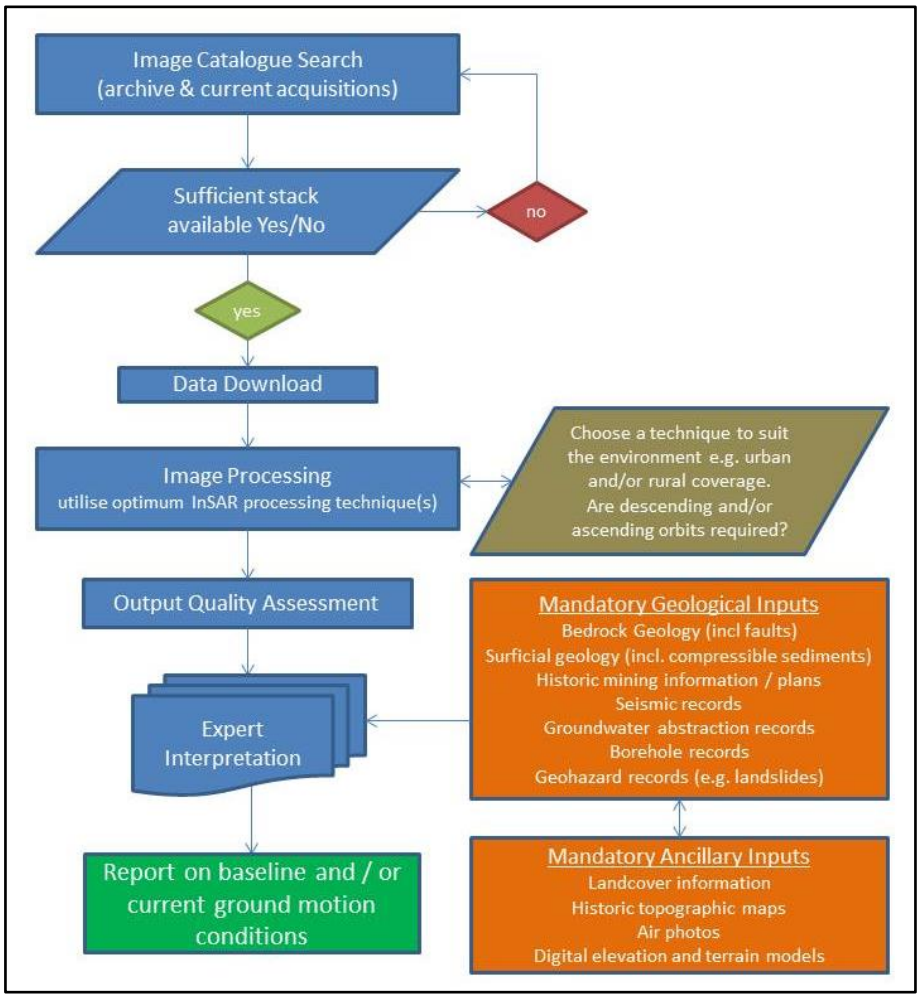

Figure 55. Flowchart of the approach and data utilised for the ground motion InSAR monitoring work package

6.4 RESULTS OF FYLDE INSAR ANALYSIS

The processing of the InSAR data has provided the first baseline assessment of land-surface deformation in the region. The analysis has not covered the full time period from 1992 to the present day as this was a preliminary study. In the Fylde, the ERS-1/2 radar data have been analysed to produce InSAR results for urban and non-urban areas. The results indicate a maximum velocity of +15.8 mm/year and a minimum velocity of -13.6 mm/year. The SBAS InSAR analysis comprises 140k points while the ISBAS analysis comprises 890k points.

The results of the ERS-1/2 InSAR analysis for SBAS and ISBAS are shown for the regional area in Figure 56 and Figure 57 respectively. Green areas are considered stable, red are subsiding on average over the time period, and blue are undergoing uplift.

A larger area than the Fylde was processed; the results highlight the potential for InSAR to detect the range of motion in the region including discrete areas of subsidence and uplift, as well as confirming the stability of large areas (Figure 58, Figure 59).

Outside the Fylde, the discrete area of uplift (blue points) north-west of Salford is likely due to the rise in groundwater levels following cessation of water pumping in abandoned coal mines. Minewater pumping data have not been evaluated to assess this hypothesis. There is an area of subsidence to the south-west of the uplift, in the Bickershaw-Goldborne-Leigh region. This is likely due to mining activity in the three collieries including water abstraction (Arrick, 1995), and formation of the Pennington Flash, illustrated in Figure 60.

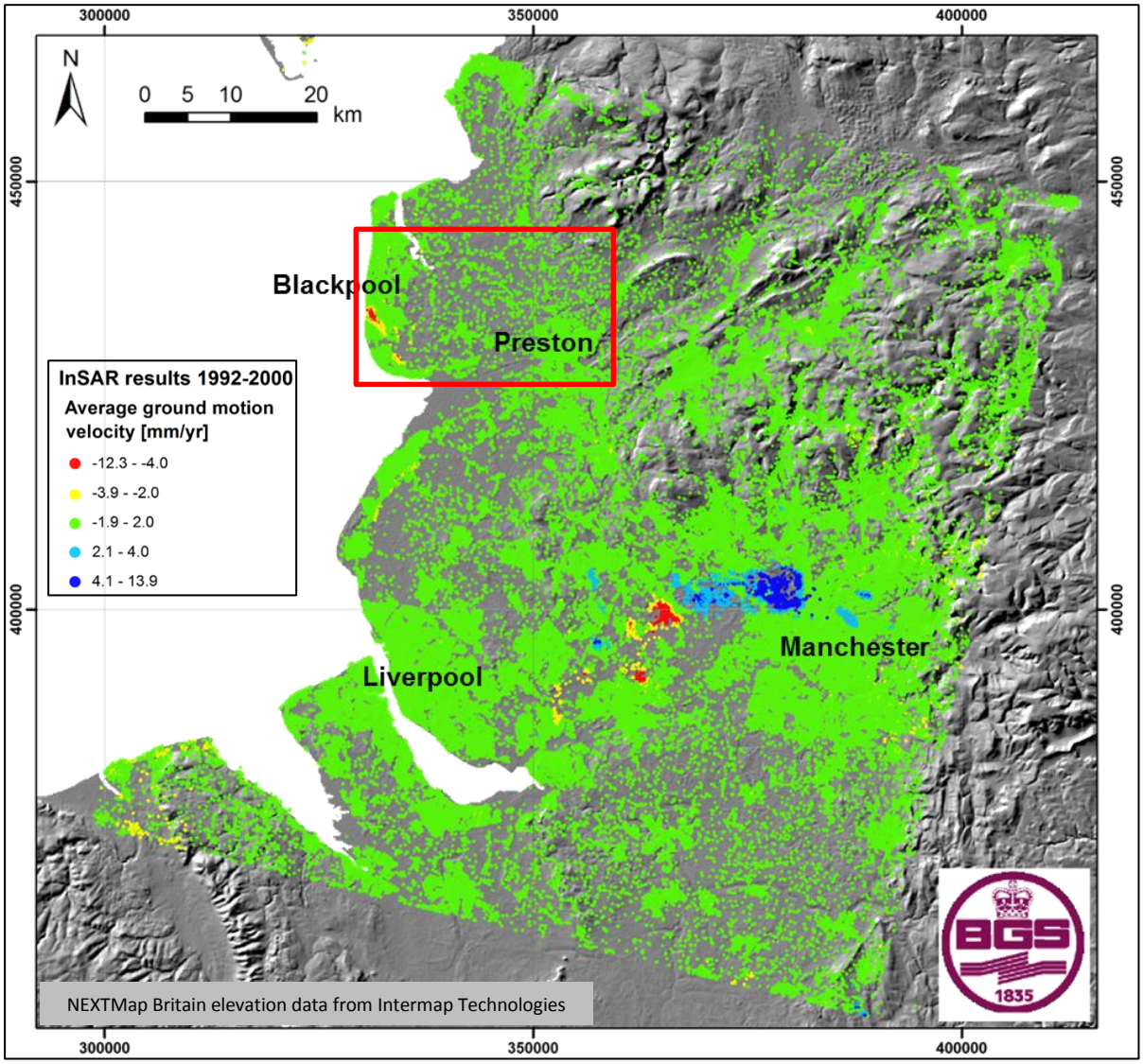

Figure 56. InSAR processing using SBAS technique of ERS-1/2 data from 1992 to 2000. The red box outlines the extents of the Fylde study area

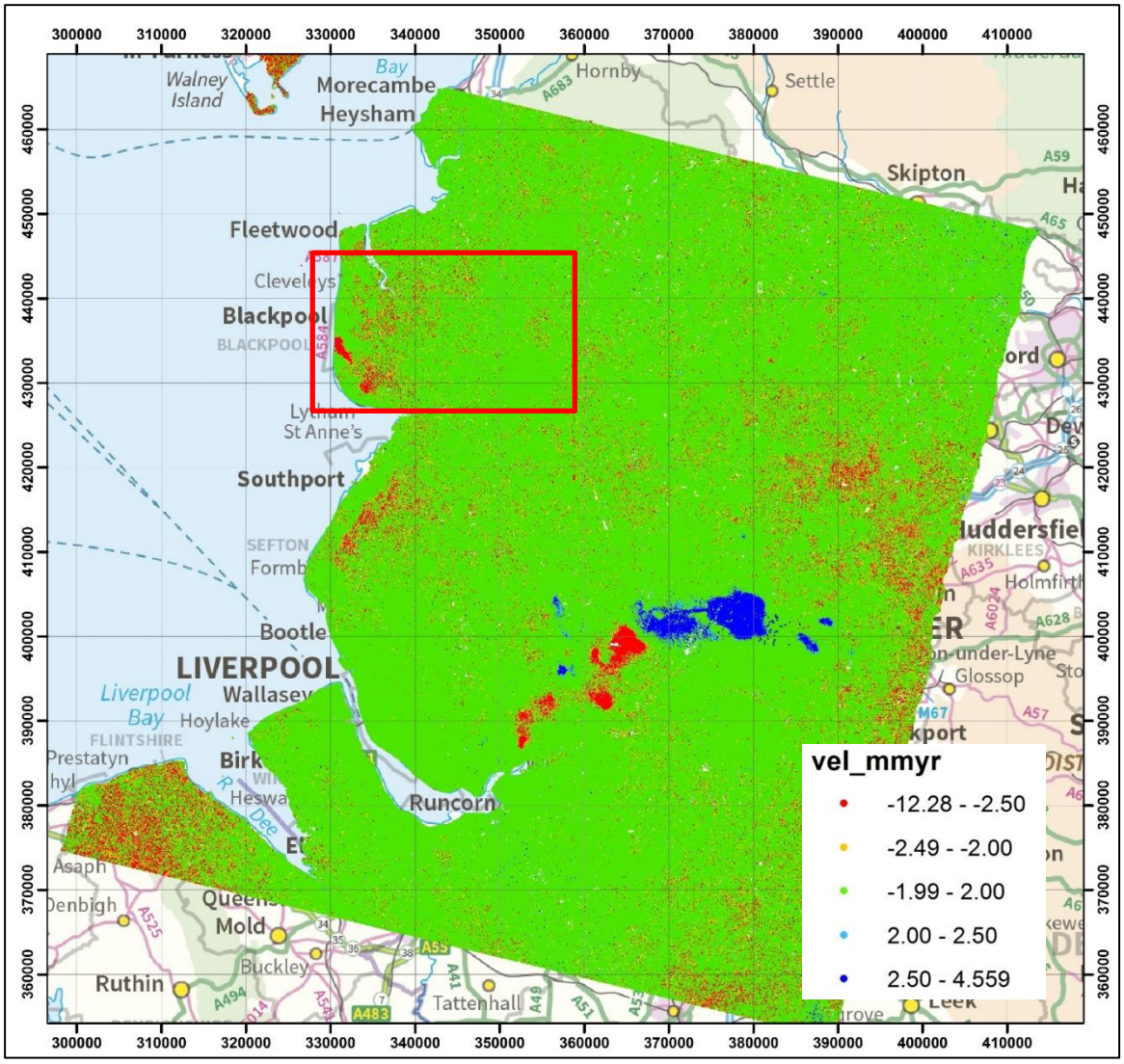

Figure 57. InSAR processing using ISBAS technique of ERS-1/2 data from 1992 to 2000. The red box outlines the extents of the Fylde study area. © Crown Copyright and/or database right 2018. Licence number 100021290 EUL

A detailed view of the InSAR results for the Fylde are seen in Figure 60. The results in this time period (1992–2000) contain discrete areas of subsidence indicating that the Fylde area is undergoing some ground motion. Sufficient resources were not available in this preliminary study to validate these with ground surveys.

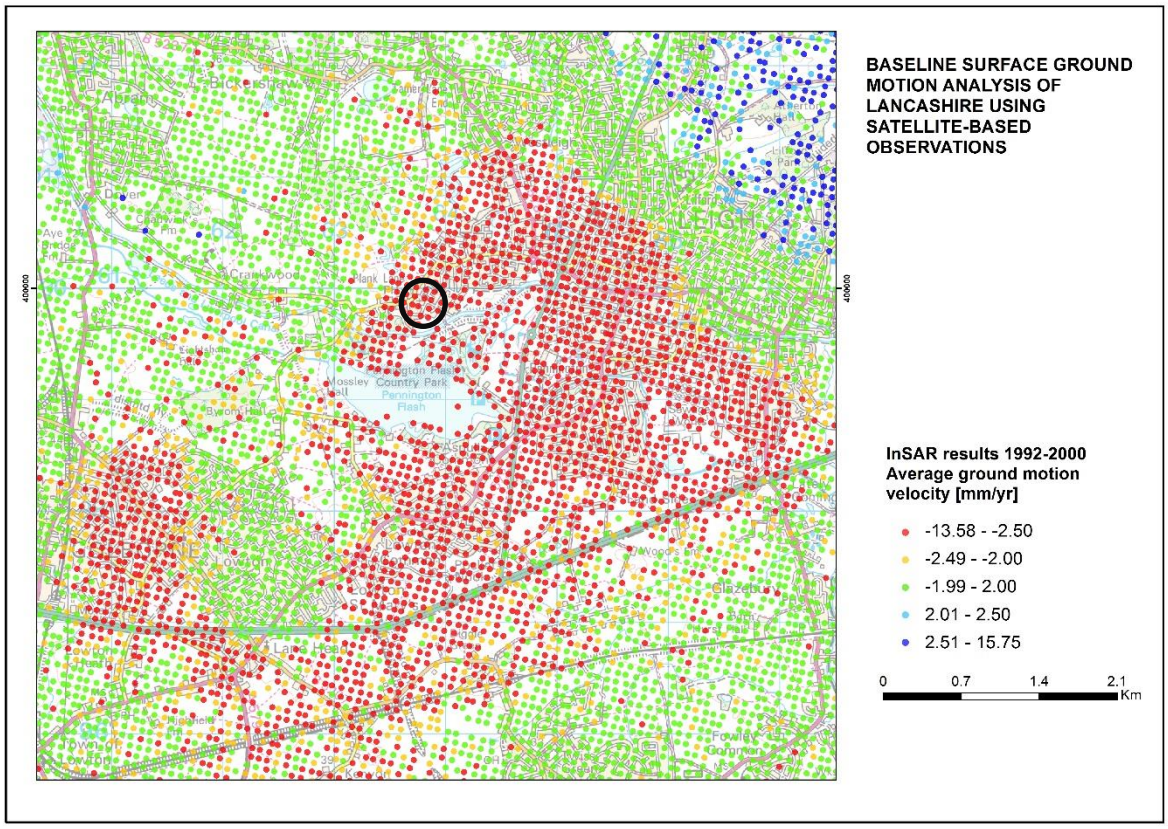

Figure 58. Areas of subsidence identified (in red) on the InSAR data in Leigh (outside of the Fylde study area) between 1992 and 2000. Black circle outlines the detailed time series results in Figure 59. © Crown Copyright and/or database right 2018. Licence number 100021290 EUL

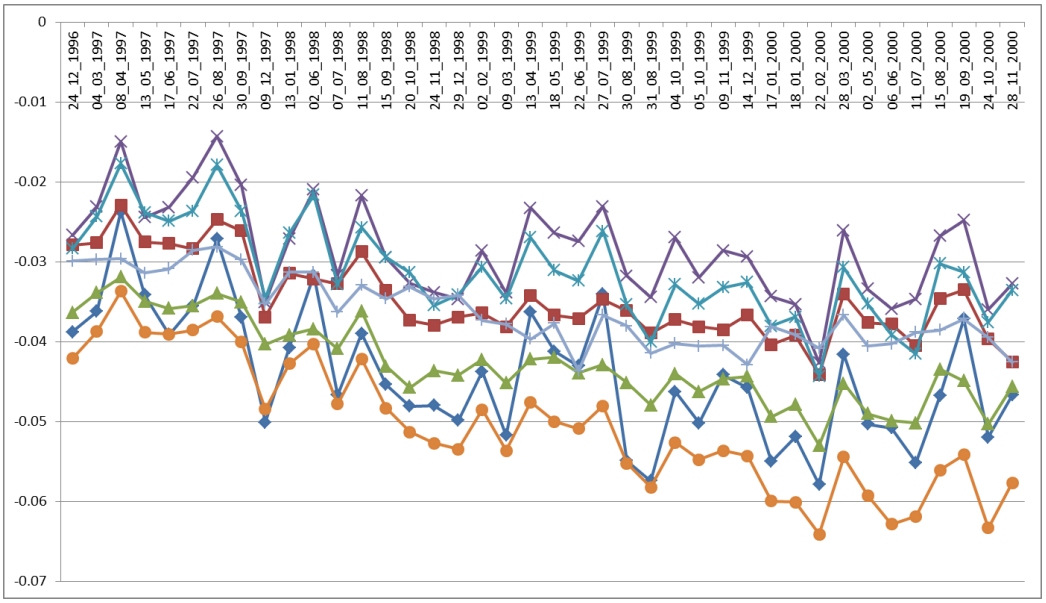

Figure 59. Time-series profiles of motion for 1996 to 2000

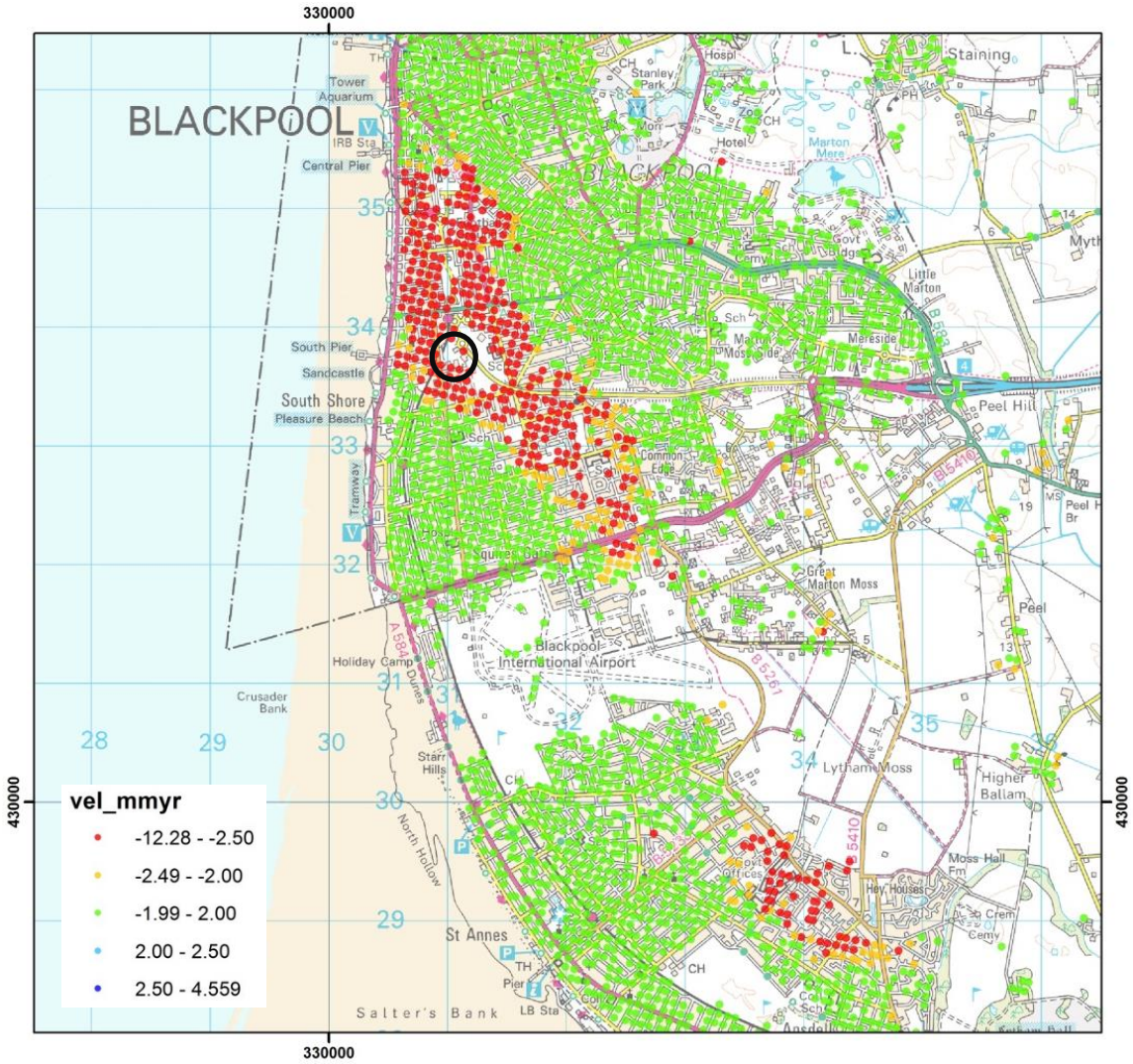

Figure 60. Areas of subsidence identified (in red) on the InSAR data in Blackpool between 1992 and 2000. Black circle indicates the location of boreholes in Error! Reference source not ound.**. © Crown Copyright and/or database right 2018. Licence number 100021290 EUL**

These areas of subsidence correspond to an area of 'peat and blown sand' on the published geological maps. Boreholes from the area indicate the presence of 'sand and peat' at the top of the stratigraphy (Figure 4), suggesting that the subsidence may be caused by the existence of compressible ground.

Additional processing of more recent satellite imagery (as conducted for the Vale of Pickering area) would provide a more complete representation of the baseline of ground motion prior to or during hydraulic fracturing operations.

6.5 DISCUSSION OF RESULTS

The preliminary Fylde ground motion InSAR analysis entailed processing one stack of ERS-1/2 (covering the period from 1992 to 2000) using SBAS and ISBAS techniques (i.e. two levels of analysis in total). The assessment indicates that zones within the wider region covered by the satellite image stack underwent both uplift and subsidence, while the majority of the region was stable. It is suggested that the uplift and subsidence in the Manchester area may be related to coal mining, while the subsidence in the west of the Fylde is thought to be related to compressible ground. These examples provide an indication of the ground motion which this monitoring technique can detect. Work has not yet been undertaken to confirm the cause of the motion.

The recently launched Sentinel-1A and 1B constellation is now orbiting the Earth and acquiring data every six days. These satellites offer the opportunity to extend ground motion monitoring for the Fylde from 2015 onwards, once a sufficient stack of data become available. Preliminary InSAR results have been obtained from these satellites for the Vale of Pickering baseline study. They indicate that higher concentrations of measurement points can be achieved using both the SBAS and ISBAS techniques when compared to ERS and ENVISAT InSAR results.

6.6 SUMMARY

It was apparent at the public engagement event in the Fylde (and the Vale of Pickering) that there is some confusion between seismic activity and ground motion. Many of the attendees link the two and presume that if there is seismic activity there must be ground motion and vice versa. It is therefore important to communicate the situation regarding baseline ground deformation and also provide evidence regarding the opportunities for monitoring in order to address public concerns. Part of this is the establishment of ground motion baselines along with monitoring of the situation throughout any shale-gas operations. This baseline allows an understanding of how the natural (and anthropogenic) processes lead to small-scale ground motions. The baseline provides evidence that small-scale motions are occurring continually and may not normally impact on day-to-day life. It also offers comfort to the public that there is a record of the existing conditions so that if operations start, there is a baseline with which to compare the up-to-date information.

The unique characteristics of satellite-based InSAR have proven it to be a valuable technique in the establishment of a baseline of ground motion for the Fylde prior to any exploitation of shale gas. There are three main benefits of using InSAR to derive ground motions:

1. In common with most remote sensing techniques, InSAR offers a regional view of the phenomena being measured. Ground deformation points are generated for the entire radar scene; this offers the opportunity to not only focus on ground motions for the immediate area surrounding the shale gas site, but also the wider area. This wider view allows an understanding of the processes, which drive the movement of the ground.
2. C-band satellites have been orbiting the Earth, and imaging the UK, since 1992–1993. These data have been archived. It is therefore possible to process the archive data and ‘look back in time’ and retrospectively establish the patterns of ground motion for an area. This is simply not possible with other techniques such as GNSS where the survey equipment must be located onsite with knowledge of the phenomena to be measured.
3. InSAR processing results in a dense network of opportunistic measurement points. For techniques such as SBAS the greatest densities are found over urban areas where the built environment acts as a good radar scatterer. However, recent advances in processing such as ISBAS increase the density of measurements, especially in rural areas, such as the Fylde. Each measurement point has an average velocity but also a time series. This offers the opportunity to understand how the ground at that point has moved through time, thereby enabling the interpretation.

7 Soil Gas

7.1 INTRODUCTION

The soil gas element of the project sought to establish baseline conditions for the concentrations of gases in the soil, flux of key gases from the soil to the atmosphere and near-ground atmospheric levels of gases. There is therefore some overlap with the atmospheric monitoring and, since radon was measured at a subset of the surveyed locations, there is also some linkage to the additional radon work (see Section 8).

Baseline soil gas measurements, like those for the other parts of the project, provide a basis against which to assess any future changes that might result from shale-gas activities. Although of low probability, there is the potential for gas to escape from depth along geological pathways (faults, fractures and other higher permeability zones) or man-made features, especially wells (either pre-existing or drilled for shale gas exploration, evaluation or development).

Whilst large faults may be known from existing geological maps and/or data acquired during hydrocarbon exploration (e.g. 3-D seismic data), or become apparent from seismicity or ground motion studies, smaller faults and fractures may be present but unknown. The completion (plugging and abandonment) of existing deep boreholes could be of variable quality depending on the age of the well; there are wells in the Fylde that are more than 50 years old. New wells also represent a potential pathway.

It is very difficult to predict where fluid migration from depth might reach the surface whether it follows natural or man-made pathways. Natural seepage of gas along faults tends to occur at limited sites, metres to tens of metres across, along only a very small proportion of the fault length (e.g. Annunziatellis et al., 2008; Johnson et al., 2017; Ziogou et al., 2013). Borehole leaks can occur at the wellhead or, if fluid escapes from the annulus of the well, can reach the surface up to several kilometres away (e.g. Allison, 2001).

7.2 MONITORING SITE SELECTION AND SUPPORTING INFORMATION

The general principles of the approach were set out in the Site Selection report (Smedley et al., 2015). The aim was to acquire a representative dataset that reflected the spatial and temporal variability of baseline soil gas conditions in the Fylde in the vicinity of the proposed shale gas activity at both Preston New Road and Roseacre Wood. This was carried out within the constraints of logistical requirements and budgetary limits. For example, landowner permissions are needed for access and continuous monitoring needs to be in secure locations, safeguarded against human or animal interventions, where mains power is an advantage.

This soil gas study included field measurement of methane, CO_2 (which could be produced from methane oxidation or present in reservoir gas), O_2 (useful in helping determine the source of CH_4 and CO_2) and Rn (a possible tracer of gas migration pathways). The trace gases H_2S and H_2, were also included.

A mix of survey mode (single point and mobile) and continuous measurements at selected sites was carried out. Surveying large areas for discrete surface gas outlets is conducted best with mobile equipment to identify locations of specific interest. However, due to dilution in air, sensitivity is reduced. Single-point measurements provide the highest sensitivity as the gas is extracted from the soil or soil surface where concentrations are highest, and a sufficient number of analyses over a site provides a good indication of the range of baseline conditions. Continuous measurements at a small number of sites provide information on temporal variations (e.g. diurnal or seasonal changes).

It was the intention to supplement field measurements with a subset of duplicated laboratory determinations of soil gas concentrations. This would have provided information on additional gases, such as other light hydrocarbons, and verified field determinations with higher precision

data. However, this would have significantly reduced the amount of field data, through diversion of effort and has therefore not yet been undertaken.

7.3 MONITORING AND DATA PROCESSING ACTIVITIES:

The study included:

- detailed coverage of near-ground atmospheric methane and CO_2 using mobile open path lasers;
- broad-scale grids of point measurements of soil gas (CO_2, CH_4, O_2, H_2, H_2S, Rn) and flux (CH_4 and CO_2) in the field with closer spaced coverage to investigate a major fault at one of the sites;
- at one specific location, continuous measurements using eddy covariance techniques to derive local CO_2 flux where other atmospheric measurements are being undertaken.

The soil gas surveys (mobile and point measurements) were carried close to the two proposed shale gas sites near Preston New Road and Roseacre Wood (Figure 61). They included areas of glacial till, peat and minor tidal flat deposits on Triassic mudstones (Kirkham and Breckells Mudstone Formations) and also the inferred surface location of a major NE–SW to NNE–SSW fault near Roseacre Wood.

An eddy covariance system was installed at Preston New Road (Site 1) to provide continuous CO_2 flux information in conjunction with the atmospheric monitoring.

7.4 RESULTS

7.4.1 Spatial surveys

Two separate surveys were carried out in the Fylde in August 2015 and September 2016. In general, the soil was dry at these times enabling soil gas data to be obtained at most sites except for a few low-lying waterlogged locations at Preston New Road.

Equipment availability and some instrument problems meant that obtaining full datasets was not possible with all techniques on each visit. Additional instruments were available in 2016, which widened the range of measurements possible significantly, especially of CH_4 concentration and flux but also to include mobile laser measurements of both CH_4 and CO_2. The data obtained from all the baseline surveys is summarised in Table 14.

Table 14. Summary of survey soil gas data acquisition.

Technique	Survey period	
	August 2015	**September 2016**
Mobile CH_4 laser		✓
Mobile CO_2 laser		✓
CH_4 in soil gas		✓
CO_2 etc. in soil gas	✓	✓
Rn in soil gas	✓	✓
CH_4 flux		✓
CO_2 flux	✓	✓

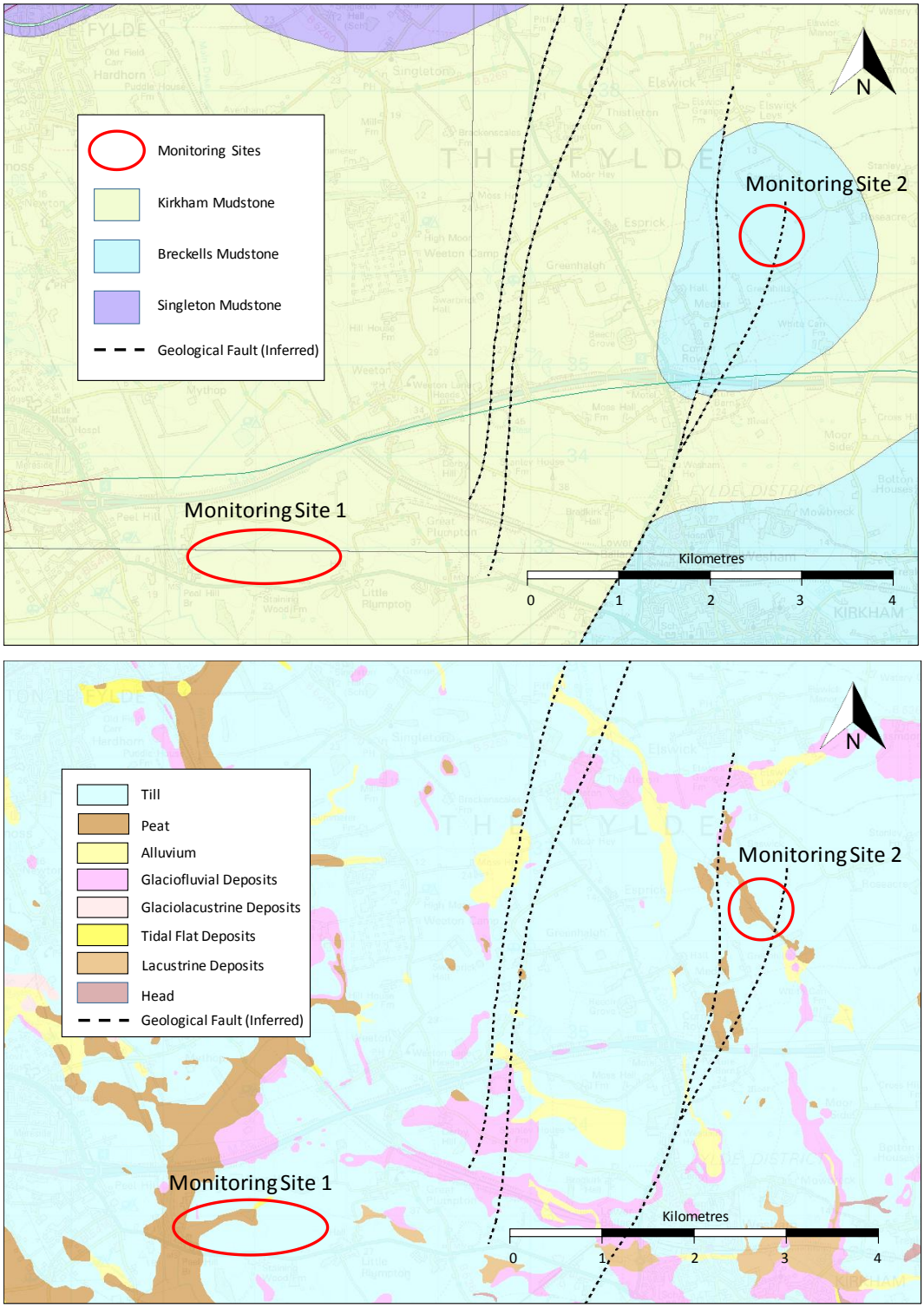

Figure 61. Soil gas study areas within the red circles with solid geology (top) and drift geology (below). Site 1 is Preston New Road and Site 2 is Roseacre Wood. Includes mapping data licensed from Ordnance Survey; © Crown Copyright and/or database right 2017. Licence number 100021290 EUL

The soil gas and flux results are summarised in Figure 62. The CO_2 flux data show general seasonal trends with higher fluxes due to enhanced biological activity in the summer compared with the autumn. There were also a greater number of outlying values in August 2015, predominantly at Site 2. Outliers aside, there was little difference in flux between the two sites on each visit.

The soil gas concentrations of CO_2 were generally higher in September 2016. This could be the result of higher soil moisture inhibiting the (relatively low) flux from the soil and creating a

build-up of gas in the soil pores. The Rn concentrations were lower in 2016 although similar between the two sites. Both moisture and temperature affect CO_2 biological production in the soil. Thus, under moist conditions more CO_2 is generated in the soil but may be retained if the soil is capped by a relatively wet surface layer. Concentrations of CO_2 above 10% are at the higher end of values for biogenic CO_2 in soil but not outside the observed range.

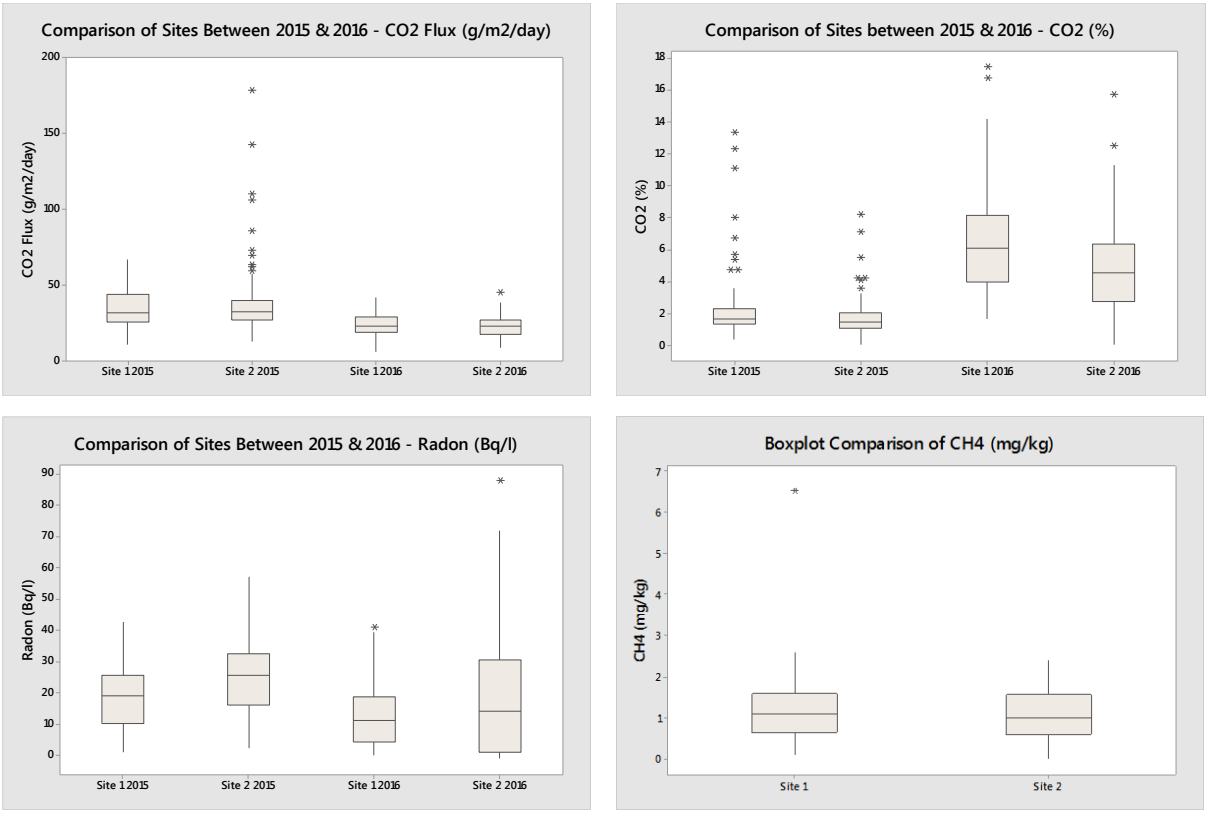

Figure 62. Boxplots summarising soil-gas data for the two sites in August 2015 and September 2016 (data for CH_4 from September 2016 only)

Methane in the soil showed a narrow range of concentrations in September 2016 with little difference between the two sites (Figure 62) and an upper limit below 3 mg/kg except for one value of 6.5 mg/kg at Site 1. Methane fluxes were very low with maxima of 0.013 and 0.008 $g/m^2/d$ at sites 1 and 2 respectively. The median methane concentration was below the atmospheric level of 1.9 mg/kg. Taken together this suggests limited methane exchange with the atmosphere and that any methane being produced is being oxidised to CO_2.

Spatial variations in soil gas and flux are compared in Figure 63 to Figure 66. Whilst there are broad patterns of relatively high and low CO_2 concentrations in the different areas of measurement (Figure 63), individual points do not tend to match well between surveys with a few exceptions. The precise re-sampling of the same site is not possible and points could differ by a few metres between surveys. Thus the differences seen probably reflect small-scale variations of the soil in terms of biological production as well as physical properties such as permeability and moisture content superimposed on seasonal effects. There is a suggestion, from the highest CO_2 concentrations for the 2015 survey, that the inferred fault at Site 2 might lie some 60–130 m to the west. However, this is not corroborated by the 2016 data.

There appears to be little consistency in the spatial patterns of CO_2 flux (Figure 64) between visits, but the 2015 survey data are affected by a small number of very high values. Direct comparison between sites for the two surveys shows very little correlation (r^2 of 0.0015 for Site 1 and 0.0052 for Site 2).

The one potentially anomalous methane concentration measurement occurs on the northern edge of Site 1 in a lower-lying area close to a stream or drainage ditch. This site also had a high CO_2 concentration (17.4%). The higher gas concentrations may be related to the relative wetness of the site. There were also higher CO_2 concentrations along the northern margin of Site 1 in 2015. This part of Site 1 generally has low Rn concentrations.

Radon values (Figure 66) also show little consistency between the two surveys (r^2 of 0.0409 for the 32 points common to both surveys) despite not being affected by seasonal biological effects. They may however be subject to small-scale variability and are known to be influenced by soil moisture and temperature, atmospheric pressure and wind speed (e.g. Klusman, 1993).

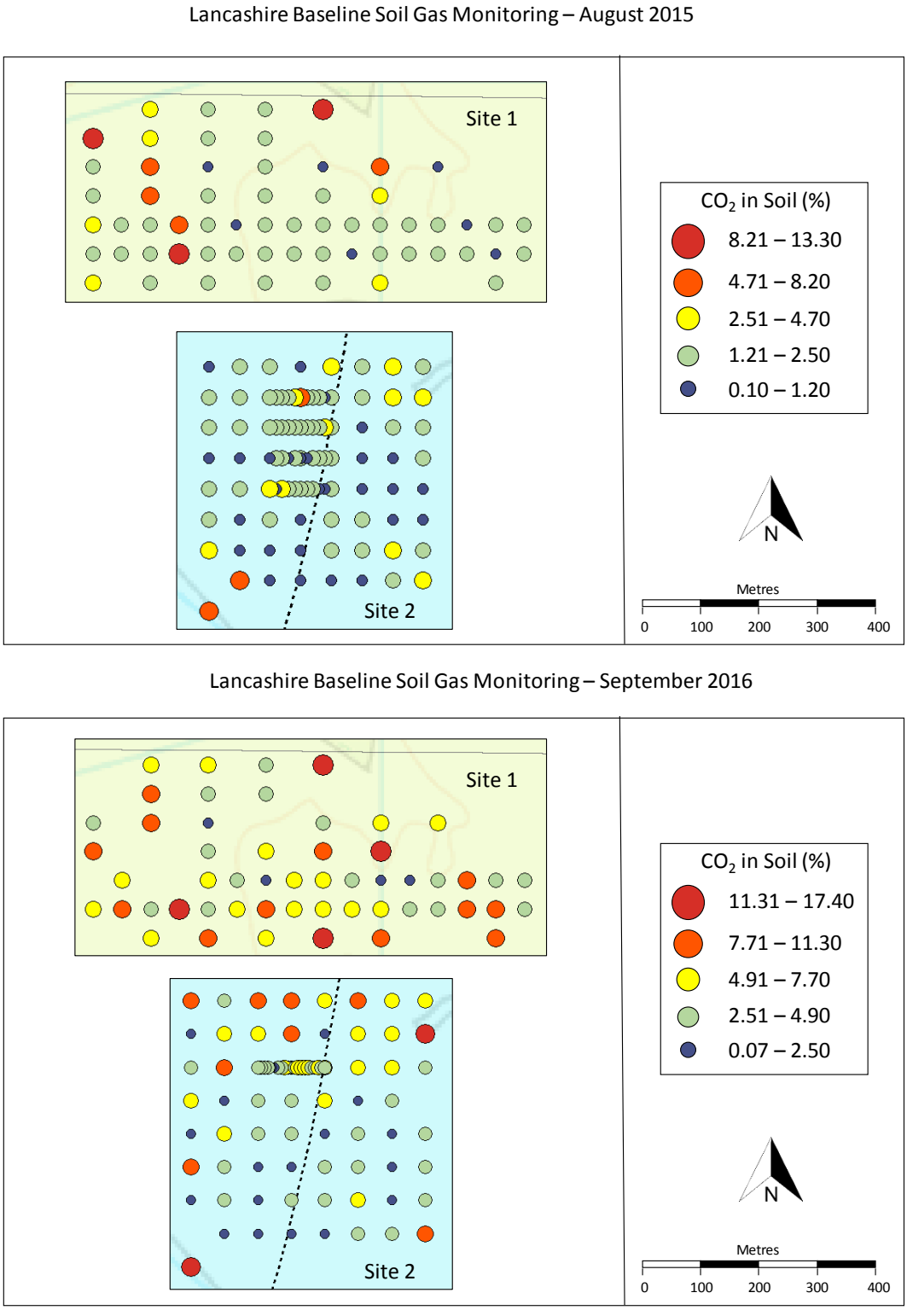

Figure 63. Spatial plots of CO_2 in soil gas for the different surveys

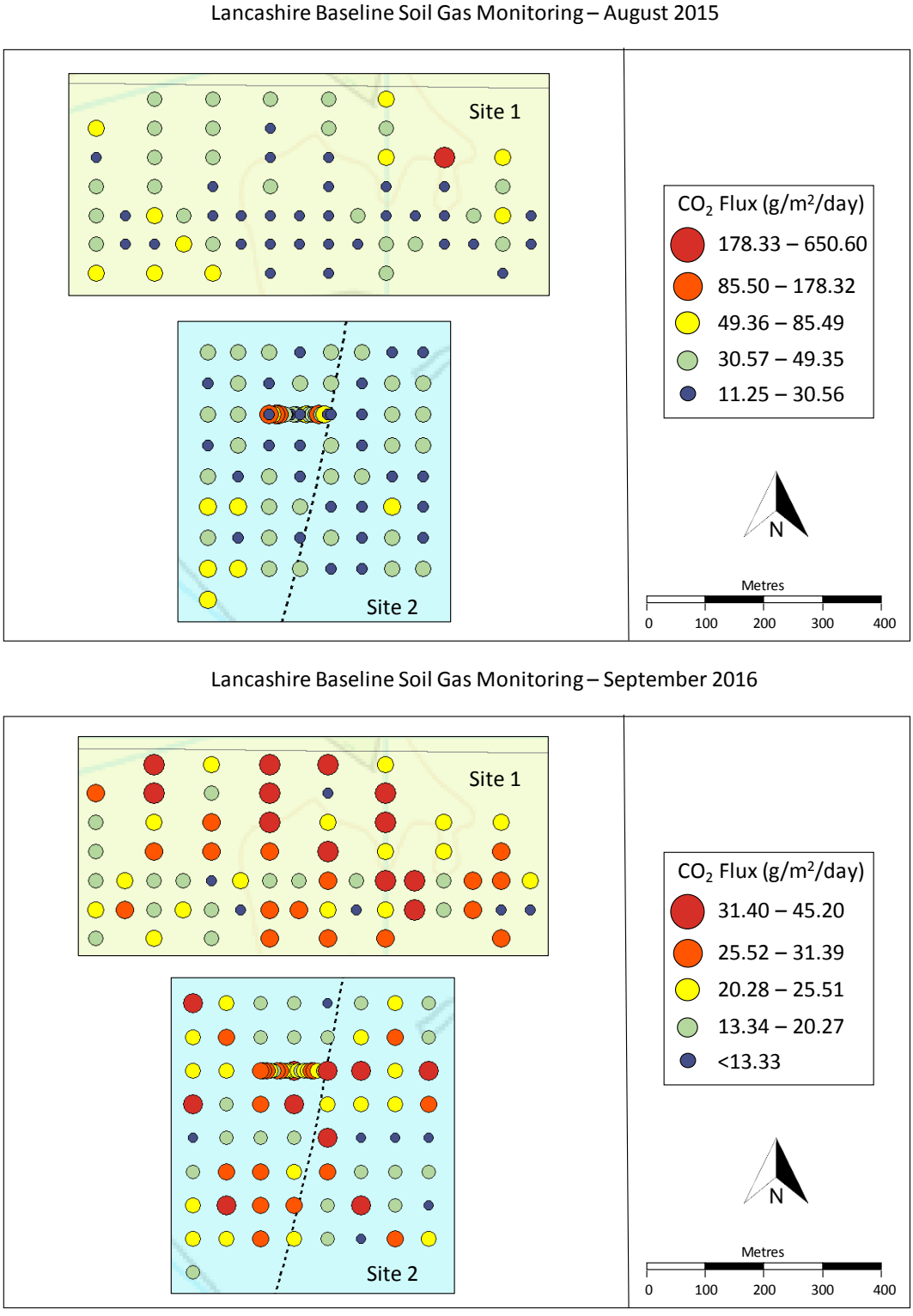

Figure 64. Spatial plots of CO_2 flux from the soil for the different surveys

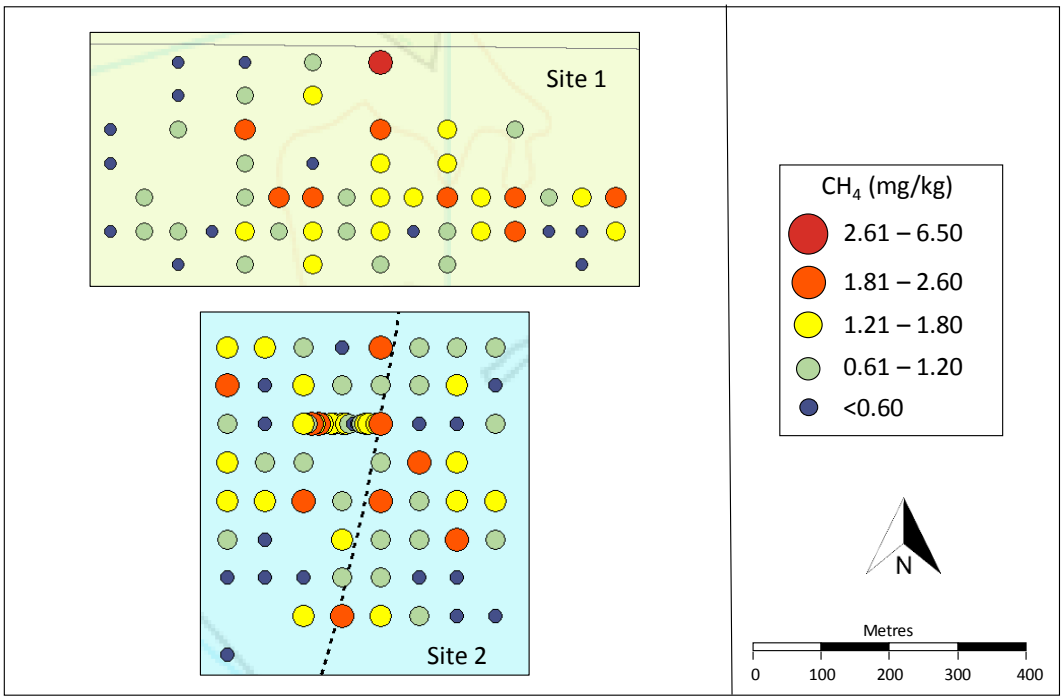

Figure 65. Methane concentrations in soil gas for September 2016

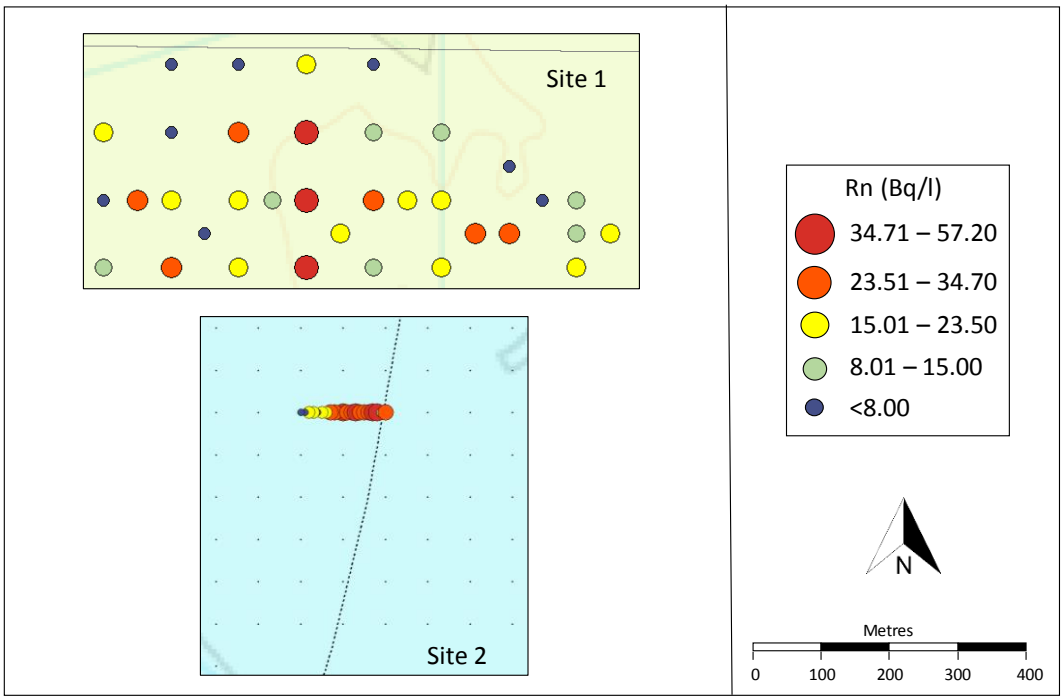

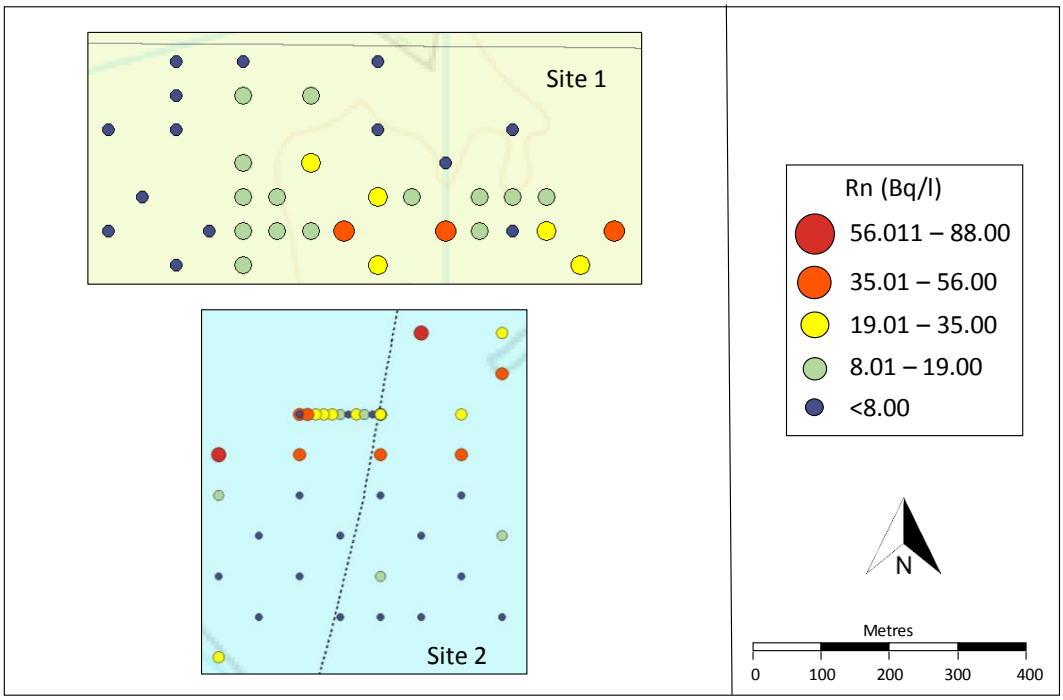

Figure 66. Radon in soil gas for August 2015 (top) and September 2016 (below)

The mobile laser data for CH_4 (Figure 67) generally have a similar range of values to the soil gas with an upper limit only marginally above the base atmospheric level of 1.9 mg/kg. The CO_2 laser data (Figure 68) also show a fairly restricted range with maxima around 530 mg/kg, only a little above the global atmospheric average of around 400 mg/kg. Apparent spatial variability probably reflects diurnal changes and is more likely temporally than spatially controlled. This is suggested by gradual changes as the traverses progressed from one end of a field to the other. Seepage of gas through the soil, of geological or anthropogenic origin, is typified by relatively rapid short-term changes in gas concentration over the scale of seconds to a few minutes, at particular locations, rather than such longer-period variations. No such features were seen in either of the datasets.

Gas ratios can be a useful tool in source attribution, especially CO_2/O_2 and CO_2/N_2 plots. These have been used successfully in a number of studies related to geological CO_2 storage (Beaubien et al., 2013; Jones et al., 2014; Romanak et al., 2012; Romanak et al., 2014; Schroder et al., 2016). Examples from the Fylde are shown in Figure 69. This shows points plotting close to the ideal biogenic CO_2 line (where one mole of O_2 is consumed for every mole of CO_2 produced) but with scatter, most likely caused by dissolution of a proportion of CO_2 into soil pore water, more apparent at Site 2. The Site 1 data show less scatter and define a trend somewhat to the leakage side of the biogenic line. The well-defined trend (r^2 of 0.8622) suggests a slight departure from perfect calibration of the instruments rather than a component of deep CO_2. The smaller number of data points from site 1 in 2015 that had reliable O_2 data (the O_2 sensor failed on one instrument) lay on the biogenic trend, supporting this conclusion.

Other possible methods of source attribution include the use of stable or radiogenic carbon isotopes in CO_2 and CH_4, or noble gas isotopes. These approaches have yet to be applied to our baseline soil gas studies in Lancashire.

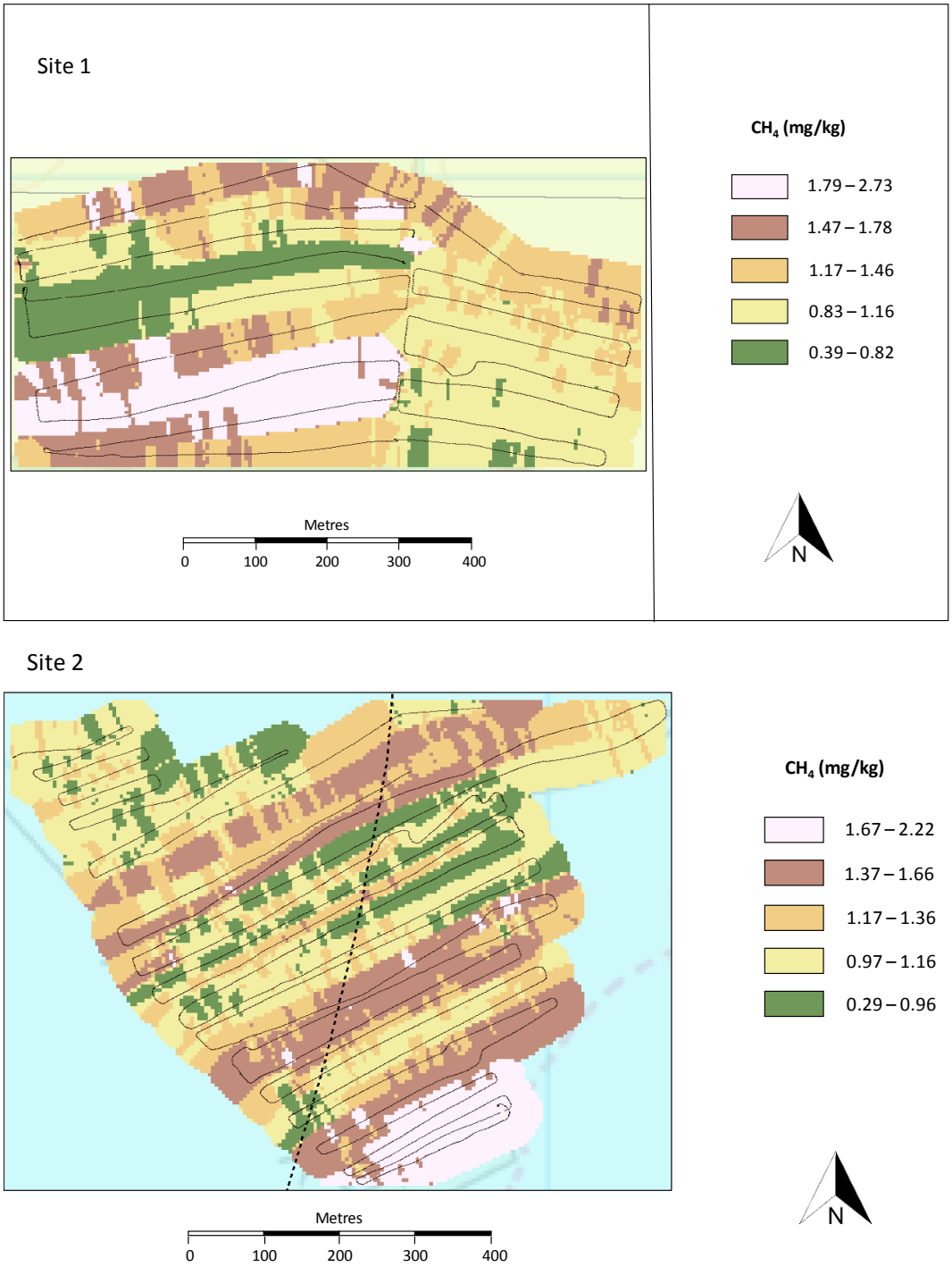

Figure 67. Mobile open-path laser data for CH_4 for Site 1 (top) and Site 2 (below) from September 2016

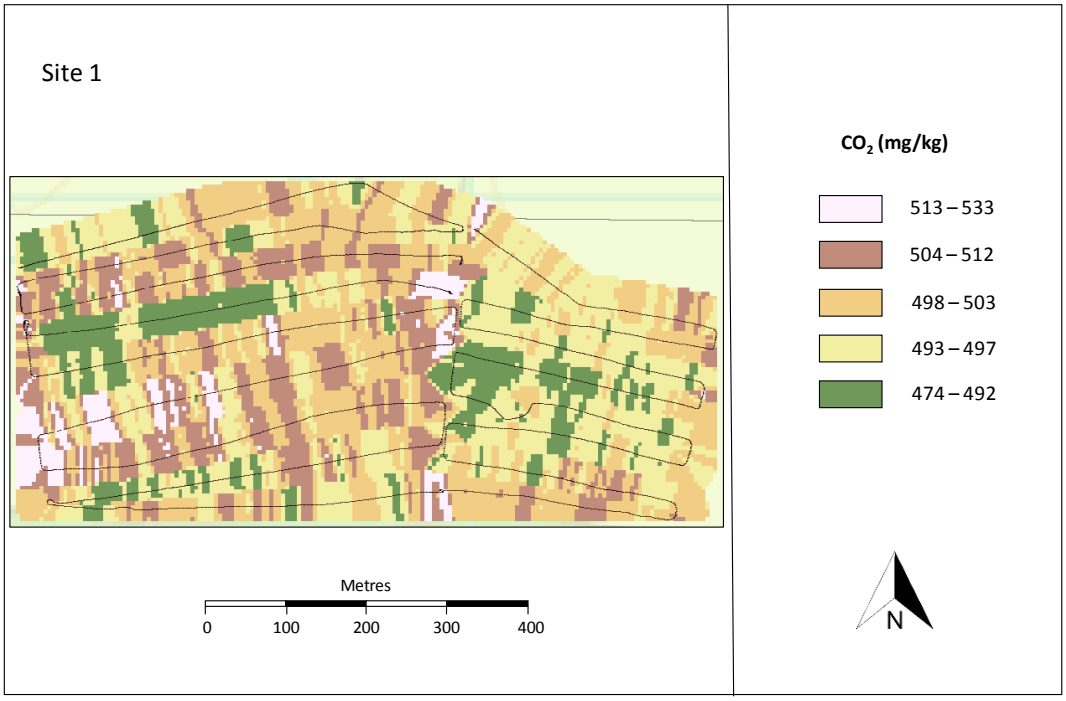

Lancashire Baseline Soil Gas Monitoring – September 2016

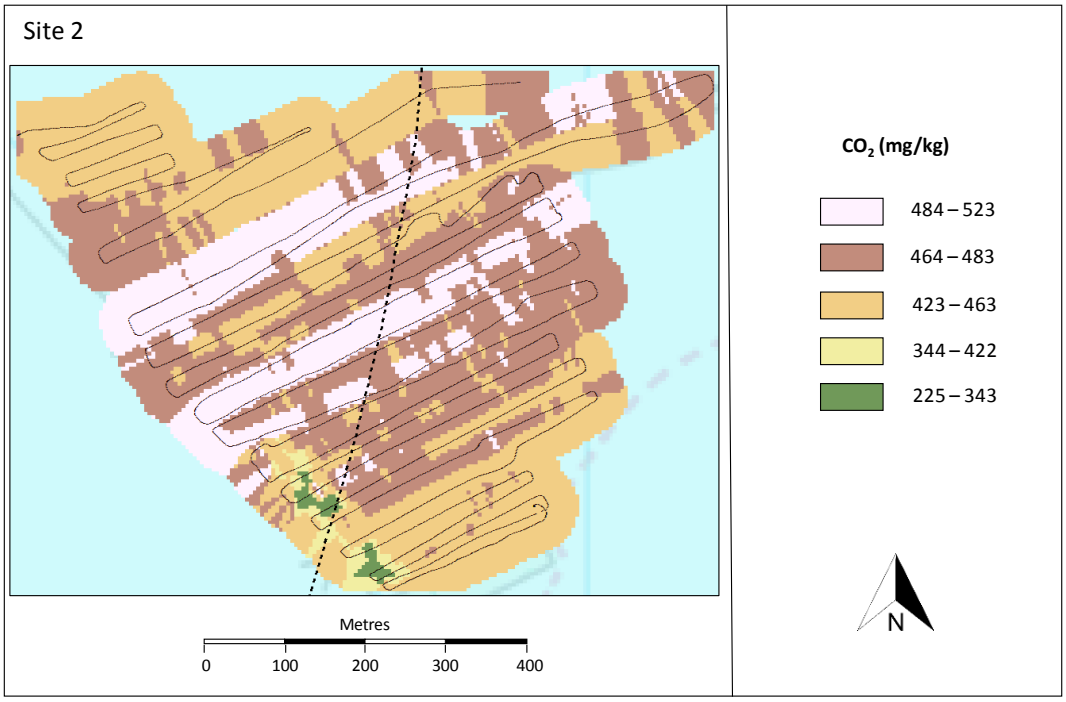

Figure 68. Mobile open-path laser data for CO_2 for Site 1 (top) and Site 2 (below) from September 2016

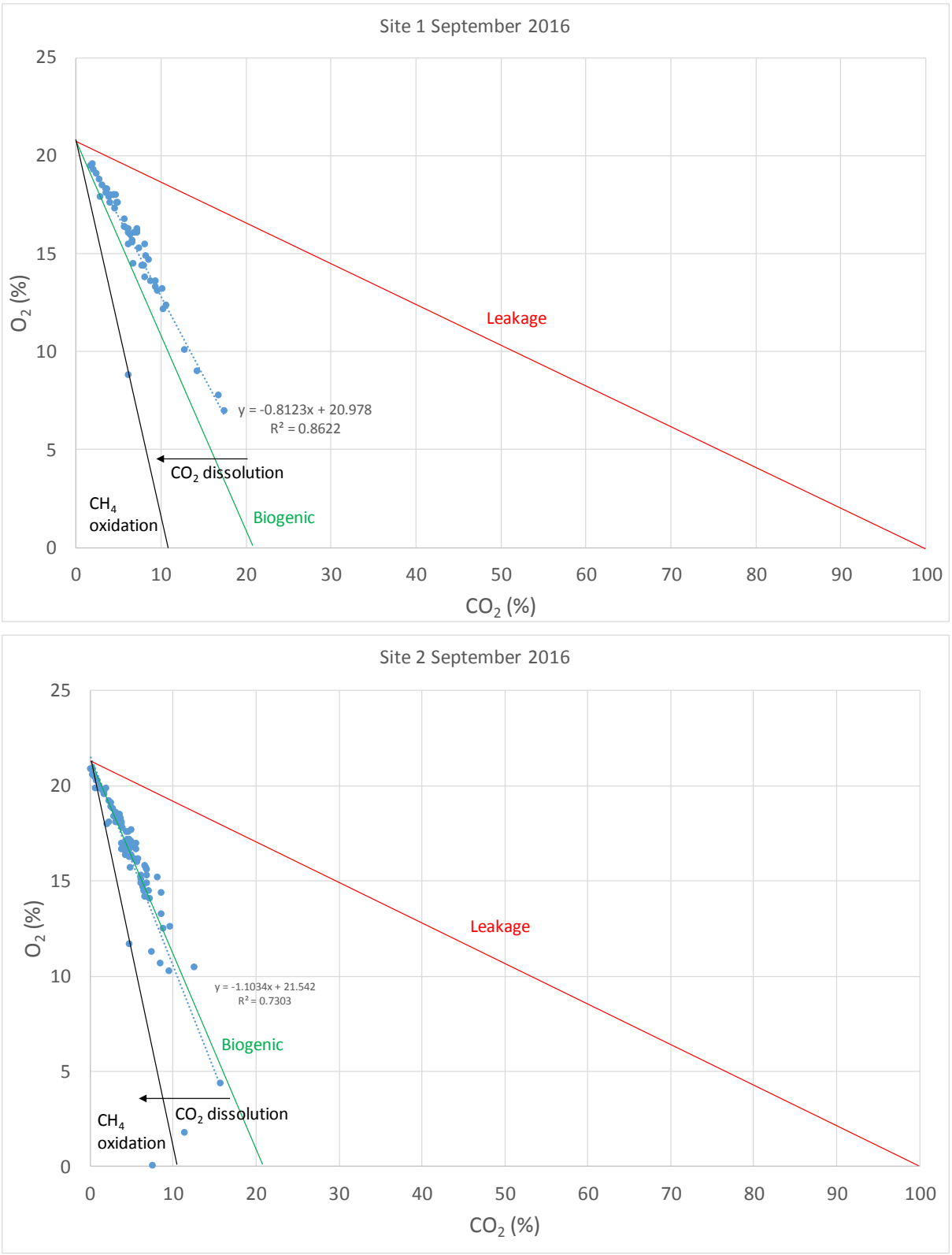

Figure 69. CO_2/O_2 ratio plot for soil gas data for Site 1 (top) and Site 2 (below) from September 2016.

7.4.2 Eddy covariance

A CO_2 eddy covariance system was installed at the Preston New Road atmospheric monitoring site in January 2016 and has recorded data continuously (with minor breaks) for over 18 months.

The Eddy Covariance (EC) system collects meteorological information and CO_2 observations. Post-processing allows CO_2 flux to be determined and the covariance of vertical and horizontal

wind statistics and CO_2 flux to be calculated. The system ran continuously from the 19th Jan 2016 to the present with a short down-period between 4th May 2016 and 19th May 2016.

From the data it appears that CO_2 concentration broadly mirrors temperature which in turn follows diurnal and seasonal trends (Figure 70, Figure 71). Biological controls on natural CO_2 production give rise to concentration ranges from 210 to over 600 mg/kg although the majority of readings fall between 350 and 450 mg/kg. It is likely that the extreme concentrations are generated from non-local natural and anthropogenic sources, transported to the EC by the wind. Although it is not possible to distinguish natural and anthropogenic sources using the EC, the fully mixed concentration (around 370 mg/kg) can be considered close to the natural background for the site (see Figure 72).

Using wind direction plotted against CO_2 concentration, there is a broad tendency for increased CO_2 concentrations when the wind is from the east and lower concentrations from the west (Figure 73). This is likely due to the proximity of the coast to the west of the Preston New Road site, where there are fewer potential biological or anthropogenic sources and relatively clean oceanic air reaches the instrument (see also atmospheric monitoring section). As with the CO_2 concentration, CO_2 flux shows clear diurnal and annual trends consistent with natural biological processes (Figure 74). CO_2 flux increases during the summer months, and during this period there is also the greatest spread in flux values.

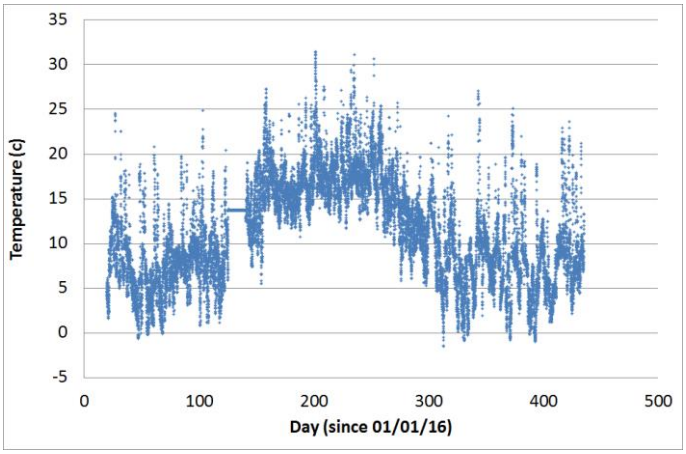

Figure 70. Atmospheric temperature at the Preston New Road site

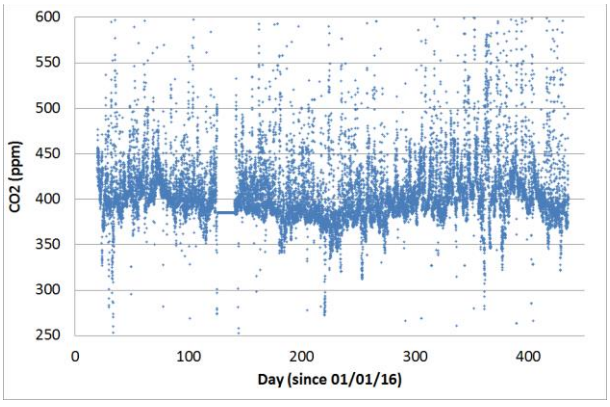

Figure 71. CO_2 concentration (ppm; mg/kg) from EC data at the Preston New Road site

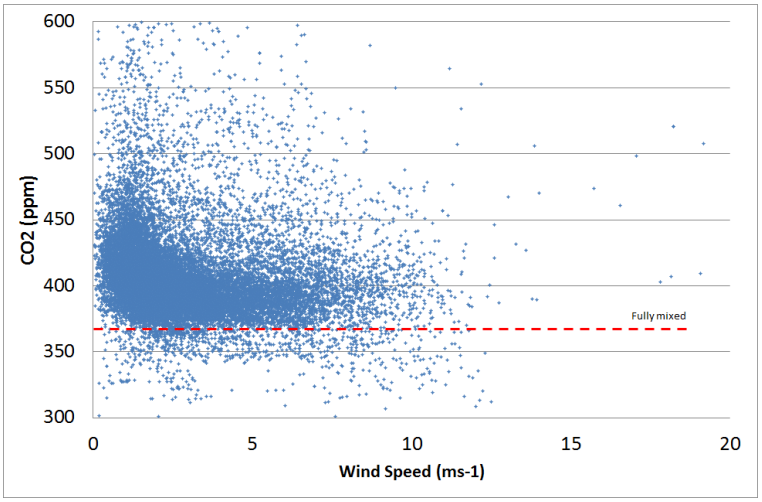

Figure 72. Fully mixed (background) atmospheric CO_2 concentration at the Preston New Road site, determined by plotting CO_2 concentration against wind speed from EC data.

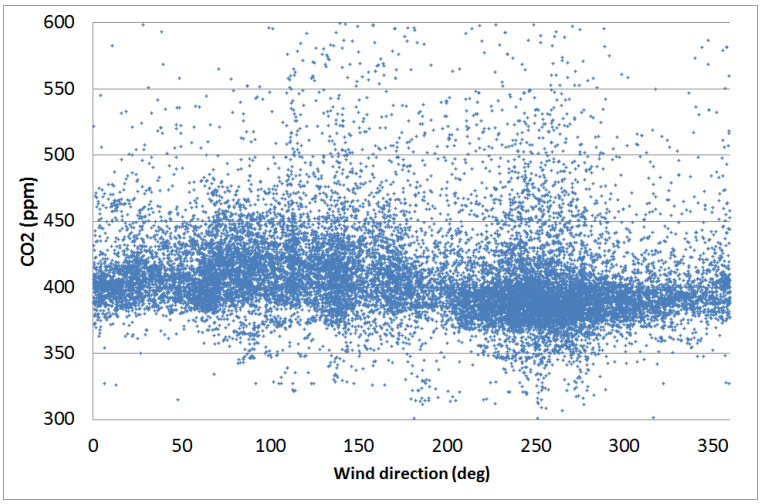

Figure 73. Atmospheric CO_2 concentrations from EC data related to wind direction. Easterly winds tend to give higher concentrations while westerly winds are associated with lower concentrations

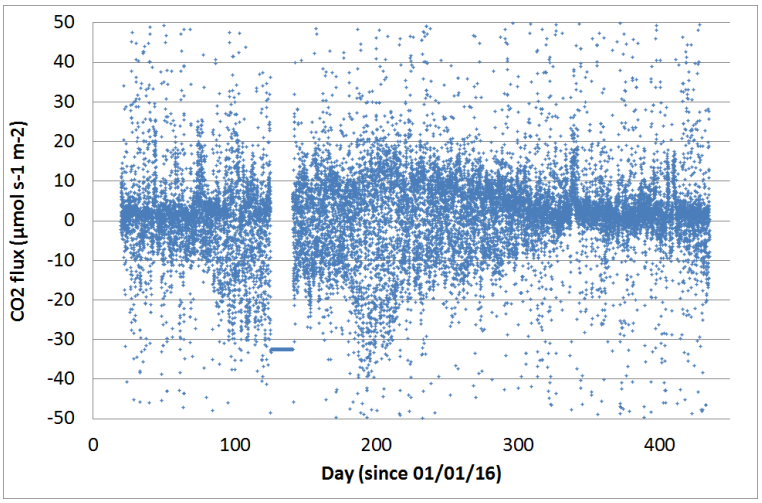

Figure 74. Atmospheric CO_2 flux calculated from EC data at the Preston New Road site

7.5 SUMMARY

Seasonal variability is evident in the soil gas and flux results from the Fylde. Meaningful data are best obtained under the relatively dry soil conditions from spring to autumn. Soil gas concentrations can be higher under wetter conditions, due to surface capping, making them more difficult to interpret. The optimal time for soil-gas surveys in the UK during shale gas operations would seem to be in the autumn, when biological activity (plant and microbial) is reduced but before the soil becomes saturated in the winter. In the autumn, gas concentrations and fluxes are more restricted in range, making any anomalous values easier to detect. Because there is still some plant growth, the effects (visually detectable or through remote sensing techniques) of any gas leakage on the vegetation should still be apparent. The lack of vegetation in harvested arable fields, or those ploughed prior to re-seeding, removes any visual clues of the impact of any gas. This is also true when there is frost or snow cover. Ideally a soil gas survey needs to be carried out under stable conditions with dry soil and no significant rainfall.

In the two Fylde surveys, soil CO_2 concentrations covered a wide range, up to almost 18%, although a high proportion was below 2% in August 2015. Soil conditions were inferred to be damper in September 2016 such that probable surface capping caused the majority of readings to be between 3 and 8%. CO_2 flux was generally below 40 $g/m^2/d$ in August 2015 and 30 $g/m^2/d$ in September 2016. There was a small number of much higher measurements in the August visit (up to around 180 $g/m^2/d$ at Site 2), whilst the maximum was around 50 $g/m^2/d$ in the September survey, consistent with reducing biological activity in the autumn.

Methane concentrations were low in September 2016, both in the soil gas and atmosphere, except for one low-lying wetter site. Radon was relatively variable spatially and temporally. In the autumn it should, therefore, be possible to detect relatively small additional gas emissions through the soil, particularly for CH_4, despite this being readily oxidised to CO_2 by soil microbes unless flux rates are relatively high.

Continuous eddy covariance monitoring data show clear diurnal and seasonal trends as well as the influence of meteorological events. Wind direction affects the CO_2 concentration with cleaner air from over the sea contrasting with more contaminated air from landward sources.

Once a reasonable body of soil gas baseline data have been collected, a fuller geostatistical analysis will be possible. This would allow optimization following the principles set out by Marchant and Lark (2007) (i) to support reliable characterization of space-time mean concentrations and fluxes and their spatio-temporal variation and (ii) to allow the development of a statistical model of the variability of the measurements which can be used to support decisions on sampling requirements for operational monitoring beyond the baseline phase of the project.

8 Radon monitoring

8.1 INTRODUCTION

In 2014, Public Health England (PHE) published a review of the potential public health impact of possible chemical and radiological pollutants resulting from shale-gas extraction (PHE-CRCE-009). Although it was concluded that any exposures from radon released were not expected to add significantly to existing radon exposures, it was recommended to determine initial radon concentrations in areas where shale-gas extraction is planned to take place.

A PHE-funded programme of indoor and outdoor monitoring in Lancashire is currently underway, based on the experience gained in the Vale of Pickering, N. Yorkshire, but reflecting the known differences in radon potential in the Fylde area.

The area of Fylde in Lancashire is not considered to be a Radon Affected Area (see Figure 75). This means that fewer local areas are needed for both indoor and outdoor radon monitoring compared with the Vale of Pickering programme. For Lancashire, outdoor monitoring focuses on two areas: around the Preston New Road (PNR) site where shale-gas extraction is planned, to about 2–3 km from the site; and a control site on the Fylde, at least 10 km from PNR and with similar characteristics in terms of overall housing density. The indoor radon monitoring includes also an area around Roseacre Wood, which is another site where shale-gas extraction is being considered.

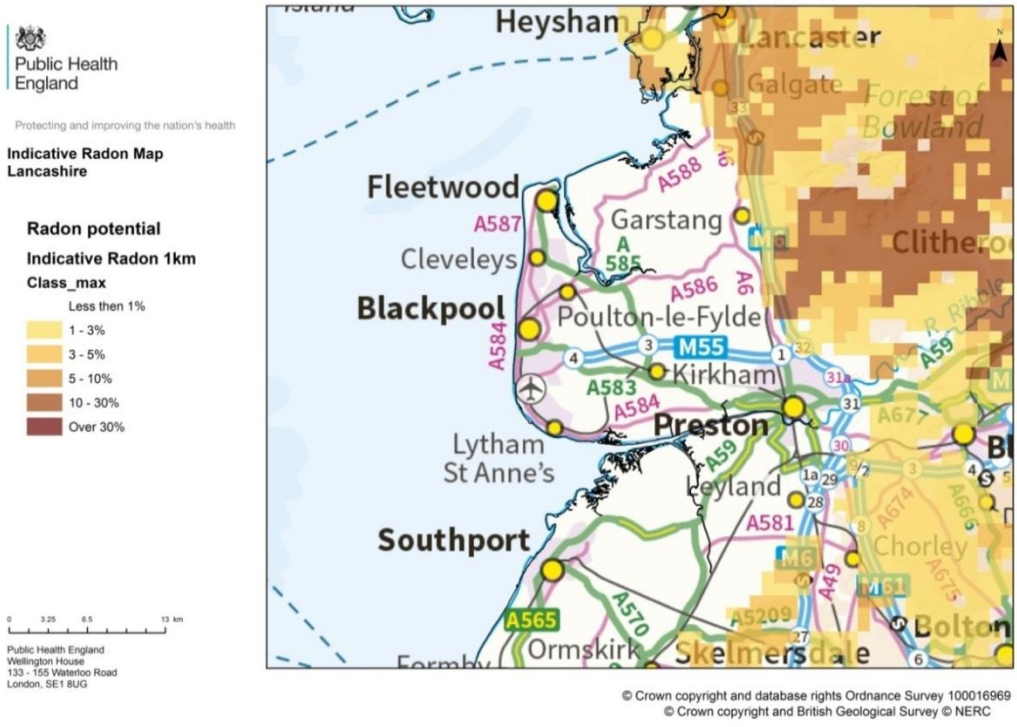

Figure 75. Radon potential in the Fylde. © Crown Copyright and/or database right 2018. Licence number 100021290 EUL

8.2 OUTDOOR RADON MONITORING

Two sites have been selected for outdoor radon monitoring in the Fylde:

- Area around Little Plumpton at about 2 km from the Preston New Road (PNR) site - 9 sampling points;
- Area around Woodplumpton at about 10 km from the PNR site, control site - 10 sampling points.

8.2.1 Results from the first 3- month period (March to May 2017)

There are two small aluminium-wrapped plastic pots at each sampling point, which contain four 3-month and four 1-year passive detectors to record radon concentration. The estimated average radon concentrations at each sampling point in the areas around Little Plumpton and Woodplumpton are presented in Figure 76a and b.

The analysis of the detectors for the first 3-month period indicates that the average radon levels were the same around the PNR and control sites:

- 4 ± 1 Bq/m^3 for the area around Little Plumpton;
- 4 ± 1 Bq/m^3 for the local control area around Woodplumpton.

The above results are similar to those measured in previous studies (Wrixon et al 1988). It should be noted that the 3-month results are close to the detection limit for the passive radon detection technique.

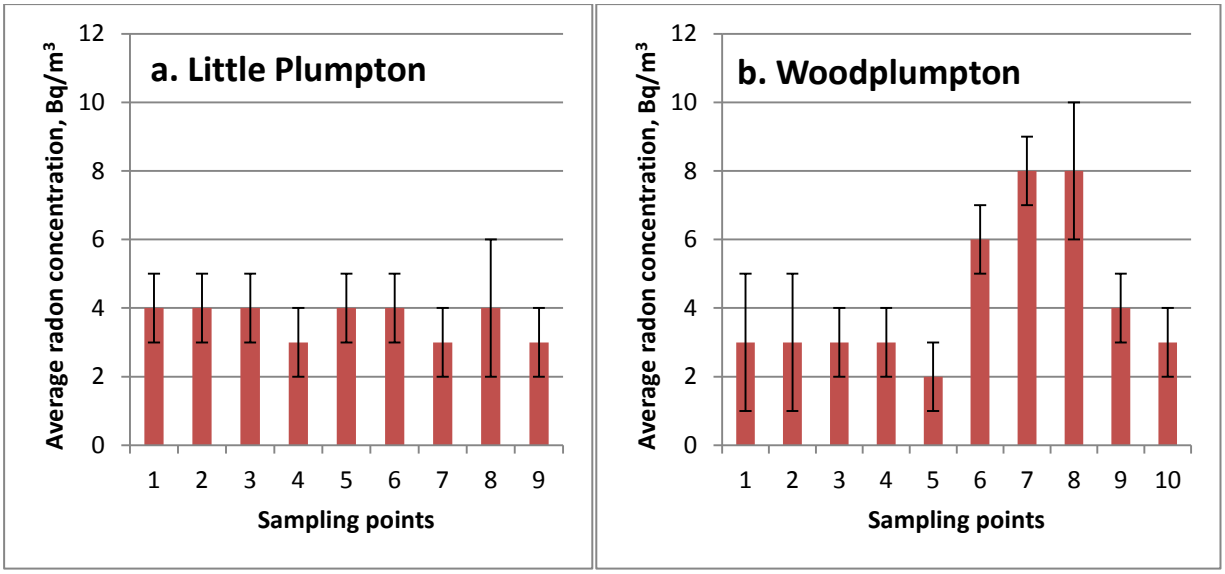

Figure 76. Average radon concentrations at the sampling points around Little Plumpton and Woodplumpton

8.3 INDOOR RADON MONITORING

8.3.1 Results from the first 3-month period (May to July 2017)

Three areas were selected for indoor radon monitoring in the Fylde: the area around Little Plumpton, (at about 2–3 km from the PNR extraction site), the area around Roseacre Wood and the area around Woodplumpton, a control site. The control site was chosen to be situated within a similar distance of both the PNR site and Roseacre Wood site. In early April 2017, 600 invitation letters were sent to householders in the areas around Little Plumpton, Woodplumpton and Roseacre Wood. There were 135 positive replies (23 % response rate).

In early May 2017, detectors were sent to householders who agreed to monitor radon in their homes in the target areas around Little Plumpton, (51 houses), Roseacre Wood (47 houses) and Woodplumpton (37 houses). Each participating householder was sent a pack containing 4 detectors, two for the living area and two for the bedroom. One set was to be placed for 3 months and one set for a year. By the end of August 2017, 111 householders had returned their three-month detectors. The analysis of the 110 results for the first 3-month monitoring period (May to July 2017) is included in this report. Reminder letters were sent to participants who had not

returned their detectors. The second set of back-to-back 3-month detectors was sent to 140 householders (5 joined later) at the beginning of August 2017.

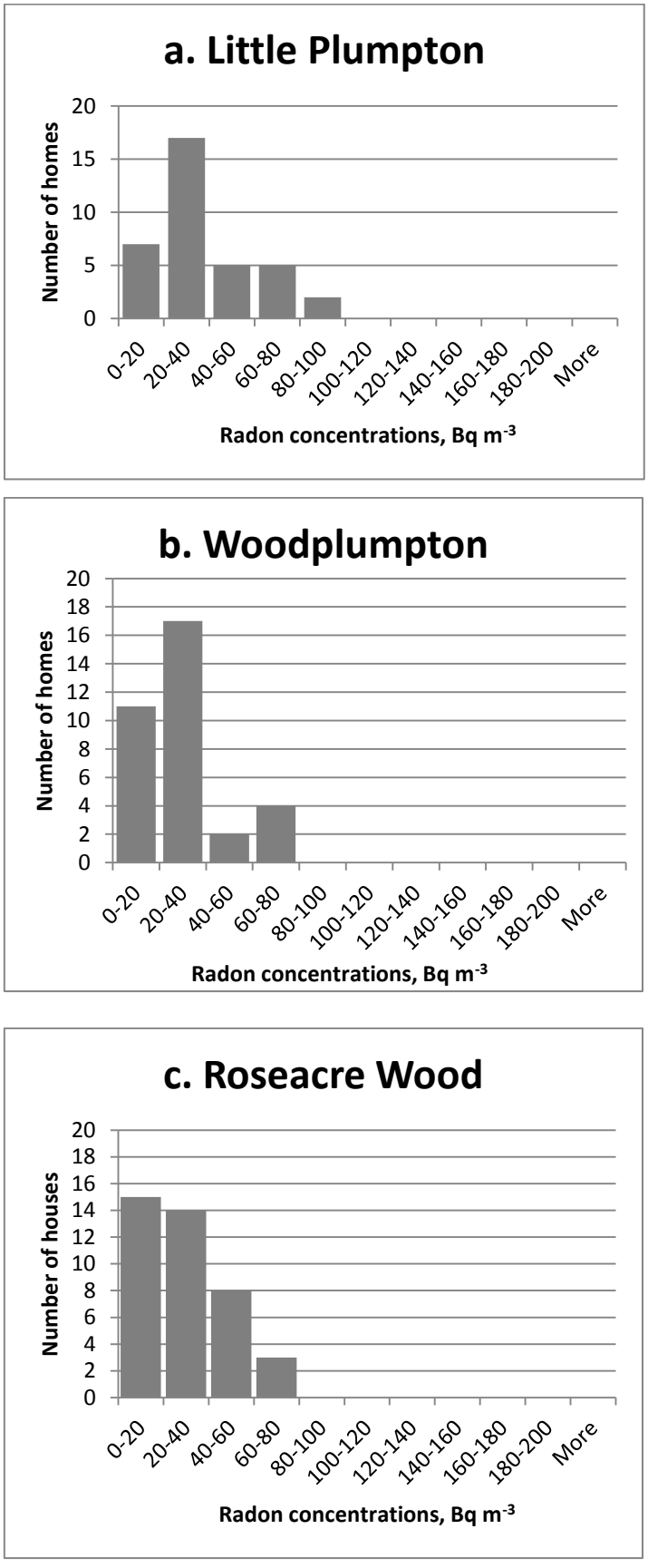

Figure 77. Reported indoor radon concentrations in the areas around Little Plumpton, Woodplumpton (control area) and Roseacre Wood

The annual average radon concentrations were calculated employing seasonal correction factors as outlined in the PHE Validation scheme (Howarth and Miles, 2008). Distribution parameters were calculated for each area, assuming log-normality. The results for the homes around Little Plumpton, Roseacre Wood and Woodplumpton are consistent with the expected low radon potential for this area.

Table 15. Range and distribution of reported annual average radon concentrations

Area (number of homes)	Range	**First 3-month results (May–July 17) (Bq/m^3)** Arithmetic mean(AM)	Geometric Mean(GM)	Geometric Standard Deviation (GSD)
Little Plumpton (36)	6-92	40	33	1.9
Woodplumpton (34)	8-92	29	25	1.7
Roseacre Wood (40)	10-77	30	26	1.7

Local radon distributions for the first 3-month test in homes in and around Little Plumpton, Woodplumpton (control area) and Roseacre Wood are given in Figure 77 a, b and c, respectively.

8.4 MONITORING AT PRESTON NEW ROAD SITE

Data from an AlphaGUARD radon detector, placed in an enclosure at the Preston New Road site for periods March–June 2017, are plotted in Figure 78. The background of the instrument was taken into account when the data were processed. The radon data, taken at 1-hour intervals, are log-normally distributed. The distribution parameters for the above monitoring period are given in Table 2. The average radon concentration measured with the passive detectors in the enclosure was 7 ± 2 Bq/m^3. The value is in good agreement with the arithmetic mean of the distribution, 6 Bq/m^3, in Table 16. Time series of the measured radon (without background correction) are given in Figure 79.

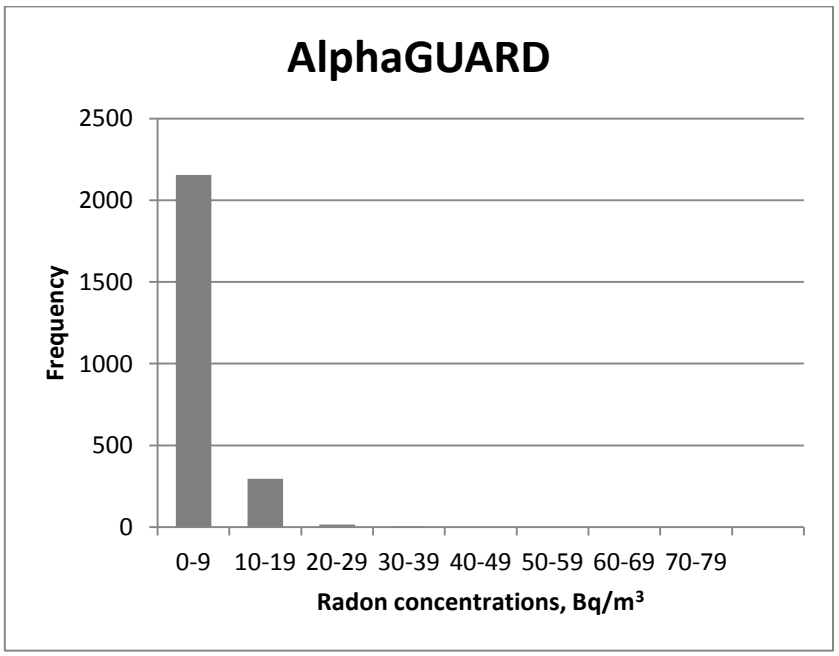

Figure 78. AlphaGUARD data from the enclosure of Preston New Road site

Table 16. Range and distribution of AlphaGUARD radon measurements. See Table 1 for key.

Period of monitoring	Bq/m^3			
	Range	AM	GM	GSD
March–June 2017	1–35	6	5	1.9

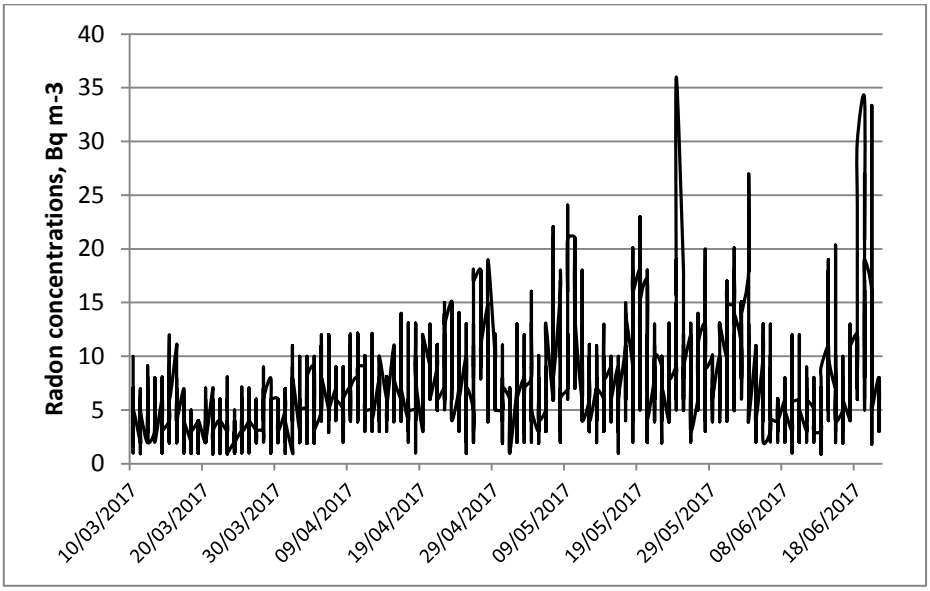

Figure 79. Time series of radon concentrations recorded by AlphaGUARD at Preston New Road between March and June 2017

9 Concluding remarks

This report details the activities being carried out by BGS and Partners to establish the baseline environmental conditions in the Fylde before any shale-gas exploration begins. The project activities are independent of operations at the Preston New Road site and of environmental regulation and regulators. The research is ongoing and the project team will continue in its remit to acquire and report data and evidence for the characterisation of baseline conditions. We are also committed to continuing environmental monitoring through any exploration stage, including during hydraulic fracturing, should this take place. Update reports will be provided as the project progresses, including through the BGS website: www.bgs.ac.uk/lancashire.

10 References

AITKENHEAD, N, BRIDGE, D M, RILEY, N J, AND KIMBELL, S F H, LONDON.) 1992. *Geology of the Country around Garstang. Memoir for 1:50,000 Geological Sheet 67 (England & Wales)*. (London: HMSO.)

ALLISON, M L. 2001. HUTCHINSON, KANSAS: A Geologic Detective Story. Geotimes, Vol. October 2001.

ANNUNZIATELLIS, A, BEAUBIEN, S E, BIGI, S, CIOTOLI, G, COLTELLA, M AND LOMBARDI, S. 2008. Gas migration along fault systems and through the vadose zone in the Latera caldera (central Italy): Implications for CO_2 geological storage. *International Journal of Greenhouse Gas Control*, Vol. 2, 353-372.

ARRICK, A, FORSTER, A., CLARK, D.F., STEWART, M., LAWRENCE, D.J.D. . 1995. A user's guide to Wigan's ground conditions. *A geological background for planning and development in Wigan*. FORSTER, A, ARRICK, A., CULSHAW, M. G., JOHNSTON, M. (editor). Vol 2. British Geological Survey Technical Report, No. WN/95/3. (British Geological Survey.)

BATESON, L, CIGNA, F, BOON, D, AND SOWTER, A. 2015. The application of the Intermittent SBAS (ISBAS) InSAR method to the South Wales Coalfield, UK. *International Journal of Applied Earth Observation and Geoinformation*, Vol. 34, 249-257. 10.1016/j.jag.2014.08.018

BEAUBIEN, S E, JONES, D G, GAL, F, BARKWITH, A K A P, BRAIBANT, G, BAUBRON, J C, CIOTOLI, G, GRAZIANI, S, LISTER, T R, LOMBARDI, S, MICHEL, K, QUATTROCCHI, F AND STRUTT, M H. 2013. Monitoring of near-surface gas geochemistry at the Weyburn, Canada, CO_2-EOR site, 2001–2011. *International Journal of Greenhouse Gas Control*, Vol. 16, Supplement 1, S236-S262.

CIGNA, F, JORDAN, H, BATESON, L, MCCORMACK, H, AND ROBERTS, C. 2015. Natural and Anthropogenic Geohazards in Greater London Observed from Geological and ERS-1/2 and ENVISAT Persistent Scatterers Ground Motion Data: Results from the EC FP7-SPACE PanGeo Project. *Pure and Applied Geophysics*, Vol. 172, 2965-2995. 10.1007/s00024-014-0927-3

CIGNA, F, AND SOWTER, A. 2017. The relationship between intermittent coherence and precision of ISBAS InSAR ground motion velocities: ERS-1/2 case studies in the UK. *Remote Sensing of Environment*, Vol. 202, 177-198. 10.1016/j.rse.2017.05.016

CRIPPS, C, BURKE, H F, LEE, J R, AND HOUGH, E. 2017. The Fylde, Lancashire: summary of the Quaternary geology. *British Geological Survey*, OR/16/013, (Keyworth, UK),

ENVIRONMENT AGENCY. 2010. Guidance on monitoring landfill gas surface emissions. *Environment Agency Report*, LFTGN 07.

EUROPEAN UNION. 2009a. Directive 2009/31/EC of the European Parliament and of the Council of 23 April 2009 on the geological storage of carbon dioxide and amending Council Directive 85/337/EEC, European Parliament and Council Directives 2000/60/EC, 2001/80/EC, 2004/35/EC, 2006/12/EC, 2008/1/EC and Regulation (EC) No 1013/2006 (Text with EEA relevance).

EUROPEAN UNION. 2009b. Directive 2009/29/EC of the European Parliament and of the Council of 23 April 2009 amending Directive 2003/87/EC so as to improve and extend the greenhouse gas emission allowance trading scheme of the Community.

GEERTSMA, J. 1973. Land subsidence above compacting oil and gas reservoirs. *Journal of Petroleum Technology*, Vol. 25, 734-744. 10.2118/3730-pa

HOWARTH C B AND MILES J C H (2008) Validation scheme for organisations making measurements of radon in dwellings: 2008 revision. Chilton, HPA-RPD-047.

JACKSON, R E, GORODY, A W, MAYER, B, ROY, J W, RYAN, M C, AND VAN STEMPVOORT, D R. 2013. Groundwater Protection and Unconventional Gas Extraction: The Critical Need for Field-Based Hydrogeological Research. *Ground Water*, Vol. 51, 488-510. 10.1111/gwat.12074

JOHNSON, G, HICKS, N, BOND, C E, GILFILLAN, S M V, JONES, D, KREMER, Y, LISTER, R, NKWANE, M, MAUPA, T, MUNYANGANE, P, ROBEY, K, SAUNDERS, I, PEARCE, J, SHIPTON, Z K AND HASZELDINE, R S. 2017. Detection and understanding of natural CO_2 releases in KwaZulu-Natal, South Africa. *Energy Procedia*, Vol. 114, 3757-3763.

JONES, D G, BARKWITH, A K A P, HANNIS, S, LISTER, T R, GAL, F, GRAZIANI, S, BEAUBIEN, S E AND WIDORY, D. 2014. Monitoring of near surface gas seepage from a shallow injection experiment at the CO_2 Field Lab, Norway. *International Journal of Greenhouse Gas Control*, Vol. 28, 300-317.

JORDAN, H, CIGNA, F, AND BATESON, L. 2017. Identifying natural and anthropogenically-induced geohazards from satellite ground motion and geospatial data: Stoke-on-Trent, UK. *International Journal of Applied Earth Observation and Geoinformation*, Vol. 63, 90-103. 10.1016/j.jag.2017.07.003

KIBBLE A, CABIANCA T, DARAKTCHIEVA Z, GOODING T, SMITHARD J, KOWALCZYK G, MCCOLL N P, SINGH M, MITCHEM L, LAMB P, VARDOULAKIS S AND KAMANYIRE R (2014) Review of the Potential Public Health Impacts of Exposures to Chemical and Radioactive Pollutants as a Result of the Shale Gas Extraction Process, Chilton, PHE-CRCE-009.

KLUSMAN, R W. 1993. *Soil gas and related methods for natural resource exploration*. (Chichester: J. Wiley & Sons.)

LLEWELLYN, G T, DORMAN, F, WESTLAND, J L, YOXTHEIMER, D, GRIEVE, P, SOWERS, T, HUMSTON-FULMER, E, AND BRANTLEY, S L. 2015. Evaluating a groundwater supply contamination incident attributed to Marcellus Shale gas development. *Proceedings of the National Academy of Sciences of the United States of America*, Vol. 112, 6325-6330. 10.1073/pnas.1420279112

MARCHANT, B.P., LARK, R.M. 2007. Optimized sampling schemes for geostatistical surveys. *Mathematical Geology*, **39**, 113–134.

MATHIESON, A, MIDGELY, J, WRIGHT, I, SAOULA, N, AND RINGROSE, P. 2011. In Salah CO2 Storage JIP: CO2 sequestration monitoring and verification technologies applied at Krechba, Algeria. 3596-3603 in *10th International Conference on Greenhouse Gas Control Technologies*. GALE, J, HENDRIKS, C, AND TURKENBERG, W (editors). *Energy Procedia*, 4.

MILES J C H AND ALGAR R A (1988) Variations in radon-222 concentrations. Journal of Radiological Protection, 8 (2), 103-106.

NEWELL, A J, BUTCHER, A S, AND WARD, R S. 2016. A 3D geological model of post Carboniferous strata in the south Fylde area of the West Lancashire Basin, Blackpool, UK. *British Geological Survey*, OR/16/007, SURVEY, B G (Keyworth, UK),

OSBORN, S G, VENGOSH, A, WARNER, N R, AND JACKSON, R B. 2011. Methane contamination of drinking water accompanying gas-well drilling and hydraulic fracturing. *Proceedings of the National Academy of Sciences of the United States of America*, Vol. 108, 8172-8176. 10.1073/pnas.1100682108

ROMANAK, K D, BENNETT, P C, YANG, C AND HOVORKA, S D. 2012. Process-based approach to CO_2 leakage detection by vadose zone gas monitoring at geologic CO_2 storage sites. *Geophysical Research Letters*, Vol. 39, L15405.

ROMANAK, K D, WOLAVER, B, YANG, C, SHERK, G W, DALE, J, DOBECK, L M AND SPANGLER, L H. 2014. Process-based soil gas leakage assessment at the Kerr Farm: Comparison of results to leakage proxies at ZERT and Mt. Etna. *International Journal of Greenhouse Gas Control,* Vol. 30, 42-57.

SAGE, R C, AND LLOYD, J W. 1978. Drift deposit influences on the Triassic Sandstone aquifer of NW Lancashire as inferred by hydrochemistry. *Quarterly Journal of Engineering Geology & Hydrogeology,* Vol. 11, 209-218.

SCHRODER, I F, ZHANG, H, ZHANG, C AND FEITZ, A J. 2016. The role of soil flux and soil gas monitoring in the characterisation of a CO_2 surface leak: A case study in Qinghai, China. *International Journal of Greenhouse Gas Control,* Vol. 54, Part 1, 84-95.

SEYMOUR, K J, INGRAM, J A, AND GEBBETT, S J. 2006. Structural controls on groundwater flow in the Permo-Triassic sandstones of NW England. 169-185 in *Fluid Flow and Solute Movement in Sandstones*. BARKER, R D A T, J.H. (editor). 263. (London: Geological Society.)

SHIRZAEI, M, ELLSWORTH, W L, TIAMPO, K F, GONZALEZ, P J, AND MANGA, M. 2016. Surface uplift and time-dependent seismic hazard due to fluid injection in eastern Texas. *Science,* Vol. 353, 1416-1419. 10.1126/science.aag0262

SMEDLEY, P L, WARD, R S, ALLEN, G, BAPTIE, B, DARAKTCHIEVA, Z, JONES, D G, JORDAN, C J, PURVIS, R M, AND CIGNA, F. 2015. Site selection strategy for environmental monitoring in connection with shale-gas exploration, Vale of Pickering, Yorkshire and Fylde, Lancashire. *British Geological Survey,* (Keyworth, UK),

WILSON, A A, AND EVANS, W B. 1990. *Geology of the country around Blackpool. Memoir of the British Geological Survey, Sheet 66 (England & Wales)*. (London: HMSO.)

WRIXON A D, GREEN B M R, LOMAS P R, MILES J C H, CLIFF K D, FRANCIS E A, DRISCOLL C M H, JAMES A C AND O'RIORDAN M C (1988) Natural Radiation Exposure in UK Dwellings. Chilton, NRPB-R190.

ZAZZERI, G, LOWRY, D, FISHER, R E, FRANCE, J L, LANOISELLÉ, M, AND NISBET, E G. 2015. Plume mapping and isotopic characterisation of anthropogenic methane sources. *Atmospheric Environment,* Vol. 110, 151-162.

ZIOGOU, F, GEMENI, V, KOUKOUZAS, N, DE ANGELIS, D, LIBERTINI, S, BEAUBIEN, S E, LOMBARDI, S, WEST, J M, JONES, D G, COOMBS, P, BARLOW, T S, GWOSDZ, S AND KRÜGER, M. 2013. Potential Environmental Impacts of CO_2 Leakage from the Study of Natural Analogue Sites in Europe. *Energy Procedia,* Vol. 37, 3521-3528.